GEOLOGICAL MAPPING IN KUALA KRAI AND LANDSLIDE SUSCEPTIBILITY ASSESSMENT USING GEOSPATIAL ANALYSIS OF REMOTE SENSING AND GIS

by

MUHAMMAD AFIQ BIN ABDUL KAHAR

A report submitted in fulfillment of the requirements for the degree of Bachelor of Applied Science (Geoscience) with Honors

FACULTY OF EARTH SCIENCE
UNIVERSITI MALAYSIA KELANTAN

2021

DECLARATION

I declare that this thesis entitled "**GEOLOGICAL MAPPING IN KUALA KRAI AND LANDSLIDE SUSCEPTIBILITY ASSESSMENT USING GEOSPATIAL ANALYSIS OF REMOTE SENSING AND GIS**" is the result of my own research except as cited in the references. The thesis has not been accepted for any degree and is not concurrently submitted in candidature of any other degree.

Signature : **……**
Name : MUHAMMAD AFIQ BIN ABDUL KAHAR
Date : **.....**

APPROVAL

"I/ We hereby declare that I/ we have read this thesis and in our opinion this thesis is sufficient in terms of scope and quality for the award of the degree of Bachelor of Applied Science (Geoscience) with Honors"

Signature	:	.....
Name of Supervisor	:	DR HAMZAH BIN HUSSIN
Date	:	.....

ACKNOWLEDGEMENT

My deepest gratitude goes to Allah the Almighty, for giving me health, knowledge, opportunity and time to complete writing this thesis with the help and support from fantastic peoples around me. First and foremost, a great appreciation to my research supervisor Dr Hamzah Bin Hussin that had guided and gave me from the start and lending me a book that is hard to find anywhere regarding the geological mapping techniques by Ibrahim Komoo in 1989. Where it is indirectly assisting myself in making research on the study area that needs to be focused on.

Besides, I would like to express my gratitude to my academic advisor Dr. Nor Shahida Binti Shafiee @ Ismail, for her advice and guidance in completing my FYP. I am deeply grateful to all lecturer from the Faculty of Earth Science for their encouragement and support in completing my research. Not forget to mention also for my examiners, Pak Arham Muchtar Achmad Bahar and Dr. Wani Sofia Binti Udin that had evaluate me during my poster presentation

Lastly, special thanks to my family members especially my father and mother also to all of my friends who support me to the successful completion of this project and also help me a lot through my 4 years study in Universiti Malaysia Kelantan.

This thesis results from a scientific discussion of the development of Geographical Information System technology which is expected to be useful in mapping today and the future. Hopefully, this article can be a part of science that can be useful for all of us. I realize that this thesis is far from perfect. Therefore constructive criticism and suggestions are expected to make this thesis better and useful.

GEOLOGICAL MAPPING IN KUALA KRAI AND LANDSLIDE SUSCEPTIBILITY ASSESSMENT USING GEOSPATIAL ANALYSIS OF REMOTE SENSING AND GIS

ABSTRACT

The research was conducted within Kampung Dusun Durian, Dabong, Kuala Krai, which was approximately 25 km^2 using the measurement dimension region of 5 km x 5 km from latitudes $05^0$17'0" N to $05^0$14'30" N and longitudes $101^0$59.7'30" E to $102^0$2.5'30" E. The purpose of this study is to determine the parameters that are potentially causing landslides and to update the geological map of the study area on the scale of 1:25, 000. Besides, it is conducted to analyze the impact of the landslide in the study area, and come out with landslide susceptibility analysis in the study area using the ArcGIS software. The study area comprises three main geomorphological units: plain geomorphology, sloping geomorphology, and steep geomorphology. Based on the AHP method in the ArcGIS software, landslide susceptibility in the study area was determined. Ten parameters have been chosen to determine the landslide susceptibility: slope, soil moisture, lithology, precipitation, distance to roads, distance to drainages, NDVI, LULC, distance to lineaments, and aspect. The weightage and score for each parameter had been assigned based on the references from the previous study. Ten maps from each of the parameters have been produced. In the end, the landslide susceptibility map of the study area was made by using "AHP ext 2.0" tools inside ArcGIS then evaluate the area under the curve (AUC) to know the accuracy. The calculated success percentage of AUC curve for prediction AHP model is 68.4%. The susceptibility zone was divided into five: the very low zone, low zone, moderate zone, high zone, and very high zone. It was later determined that slope is the most influenced to the landslide hazard because of the study area's location on the hilly areas.

Keywords: AHP, ArcGIS; Kampung Dusun Durian; Landslide susceptibility, AUC

PEMETAAN GEOLOGI DI KUALA KRAI DAN PENILAIAN KERENTANAN TANAH RUNTUH DENGAN MENGGUNAKAN ANALISIS GEOSPASIAL BAGI PENDERIAAN JAUH DAN GIS

ABSTRAK

Penyelidikan ini dilakukan di Kampung Dusun Durian, Dabong, Kuala Krai, yang kira-kira 25 km2 menggunakan wilayah ukuran dimensi 5 km x 5 km dari garis lintang $05^0$17'0 "N hingga $05^0$14'30" N dan garis bujur $101^0$59.7'30 "E hingga $102^0$2.5'30 "E. Tujuan kajian ini adalah untuk menentukan parameter yang berpotensi menyebabkan tanah runtuh dan mengemas kini peta geologi kawasan kajian pada skala 1:25, 000, Ianya juga bertujuan untuk menganalisis kesan tanah runtuh di kawasan kajian, dan juga untuk menganalisis analisis kerentanan tanah runtuh di kawasan kajian menggunakan perisian ArcGIS. Kawasan kajian merangkumi tiga unit geomorfologi utama: geomorfologi dataran, geomorfologi condong, dan geomorfologi curam. Berdasarkan kaedah AHP dalam perisian ArcGIS, kerentanan tanah runtuh di kawasan kajian ditentukan. Sepuluh parameter telah dipilih untuk menentukan kerentanan tanah runtuh: cerun, kelembapan tanah, litologi, taburan hujan, jarak ke jalan, jarak ke saliran, NDVI, LULC, jarak ke garis garis, dan aspek. Berat dan skor untuk setiap parameter telah ditentukan berdasarkan rujukan dari kajian sebelumnya. Sepuluh peta dari setiap parameter telah dihasilkan. Pada akhirnya, peta kerentanan tanah runtuh di kawasan kajian dibuat dengan menggunakan alat "AHP ext 2.0" di dalam ArcGIS kemudian menilai kawasan di bawah lengkung (AUC) untuk mengetahui ketepatannya. Peratusan kejayaan yang dikira AUC untuk ramalan model AHP adalah 68.4%. Zon kerentanan dibahagikan kepada lima: zon sangat rendah, zon rendah, zon sederhana, zon tinggi, dan zon sangat tinggi. Kemudian ditentukan bahawa lereng adalah yang paling berpengaruh terhadap bahaya tanah runtuh kerana lokasi kawasan kajian di kawasan berbukit tinggi.

Kata kunci: AHP, ArcGIS; Kampung Dusun Durian; Kerentanan tanah runtuh, AUC

LIST OF TABLES

LIST OF FIGURES

LIST OF ABBREVIATIONS

ALOS	Advanced Land Observing Satellite
ADEOS	Advanced Earth Observing Mission
AVNIR-2	Advanced Visible and Near Infrared Radiometer type-2
AHP	Analytical Hierarchy Process
AUC	Area Under Curve
CR	Consistency Ratio
CI	Consistency Index
DEM	Digital Elevation Model
ERTS-1	Earth Resources Technology Satellite
EROS	Earth Resources Observation and Science
ESA	European Space Agency
FPR	False Positive Rate
GIS	Geographic Information System
GUI	Graphical User Interface
HH	Horizontal Transmit and Horizontal Receive
HV	Horizontal Transmit and Horizontal Receive
JAXA	Japan Aerospace Exploration Agency
JAROS	Japan Resource Observation Systems Organization
JERS-1	Japanese Earth Resources Satellite 1
LIDAR	Light Detection and Ranging
LDCM	Landsat Data Continuity Mission
LULC	Land Use and Land Cover
LSI	Landslide Susceptibility Index
MSS	Multi-Spectral Scanner
MSI	Multispectral
MAD	Median Absolute Deviation
NASA	National Aeronautics and Space Administration
NDVI	Normalized Difference Vegetation Index
NIR	Near-Infrared
NNW-SSE	North-Northwest to South-Southeast

OLI	Operational Land Imager
PRISM	Panchromatic Remote Sensing Instrument for Stereo Mapping
PALSAR	Phased Array type L-band Synthetic Aperture Radar
RBV	Return Beam Vidicon
RS	Remote Sensing
RI	Random Index
ROC	Receiver operating characteristic
RMS	Root Mean Square Deviation
SWIR	Shortwave Infrared
TIRS	Thermal Infrared Sensor
TM	Thematic Mapper
TPR	True Positive Rate
USGS	United States Geological Survey
UTM	Universal Traverse Mercator
VV	Vertical Transmit and Vertical Receive
VH	Vertical Transmit and Horizontal Receive
WGS	World Geodetic System

LIST OF SYMBOLS

%	Percentage
D_d	Drainage density
L	Length
A	Channels per unit Area
λ_{max}	Maximum eigenvalue
n	Matrix size
$\leq$	Less than or equal
R_i	Groups of ratings, per layer
W_i	Weights of landslide conditioning factors
x	Multiply
$+$	Add

CHAPTER 1

INTRODUCTION

1.1 General Background

Dabong of Kuala Krai Signifies the next significant section in Kelantan Following the Gua Musang and among the eldest sections ever created by the British Authorities in 1909. The Malay Peninsula classification comprises three division: Eastern Belt, Central Belt, and Western Belt (Khoo & Tan, 1983). Therefore, the Dabong area is regarded as part of the Central Belt. The spatial analysis and satellite image interpretation employed here to recognize the landslide-prone area depend on the use of GIS and Remote Sensing. In Asian countries, mostly tropical rainforest-like Malaysia, it is inclined to be more vulnerable to landslide activity triggered by rain. By definition, landslides are a downward motion between compounds of Earth, rock, or a mix of the two, which may be seen and detected (Sharpe, 1938). Besides, a straightforward definition of the landslide from Cruden (1991) revealed the motion of a mass of stone debris or even soil in a downward slope direction. The measurements and landslide geometry are clarified with the model drawing, as shown in Figure 1.1.

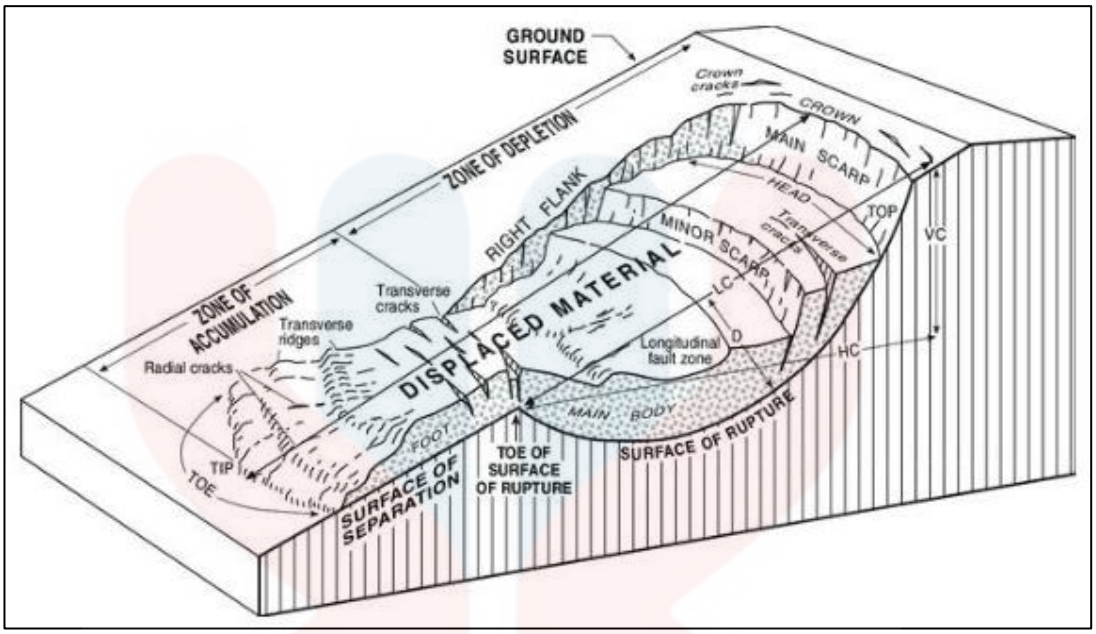

Figure 1.1: Terminology for describing landslide features (Cruden & Varnes, 1996).

1.2 Problem Statements

Landslides occurred due to a steep incline in a place, mainly in the hilly and mountainous terrain. Over time, the growth of the Earth processes could result particularly in alterations upon the field of interest, possibly regarding vulnerable places, most probably to possess landslides. The remote sensing data resources such as Landsat, Lidar, and aerial photography supply fundamental properties to categorize each landslide according to its attributes from very low, low, moderate, and high. Besides, the information concerning the geological and petrological study in Dabong was minimal to help the study outcomes. There are not many studies that were run by other researchers on landslides possible across the rural area of kampung Dusun Durian, Dabong. The demand for analysis upon the landslide dangers in Dabong, also thought of as a compelling aspect to suggest this study due to terrain area, includes a highly weathered rock mass. Nelson (2013) asserts that the existence of abundance fractures and joints toward the slope may have the ability to induce the landslide event where it ought to be highlighted to seek out details regarding the research region.

1.3 Research Objectives

i. To update the geological map with an area of 5km x 5km for the rural area in Kampung Dusun Durian, Dabong.

ii. To determine the parameters that are potentially causing landslides.

iii. To identify the region that is prone to landslide based on GIS and Remote Sensing, then develop a landslide susceptibility map of the rural area in Kampung Dusun Durian, Dabong.

1.4 Study Area

According to the Department of Town and Country Planning Peninsular Malaysia (2011), the local plan region of Kuala Krai has a total area of 227,670.01 hectares and represents the second largest region in Kelantan after the Gua Musang. Thus, it consists of three districts, namely Batu Mengkebang, Olak Jeram, and Dabong. The area of Dabong covers the whole of Olak Jeram and Dabong District, with about 145,173.25 hectares. As for the final year project, the study area will be focused on the rural area in Kampung Dusun Durian, Dabong (Figure 1.2).

The study area includes about 25 km^2 of 5km x 5km for the measurement dimension region with latitudes of $05^0$17'0" N to $05^0$14'30" N and longitudes $101^0$59.7'30" E to $102^0$2.5'30" E. In terms of residents, the Dabong district has the lowermost number of residents that is 12%, and it is noted that almost 40,659 of the total number population has in Dabong (Department of Statistics Malaysia, 2010).

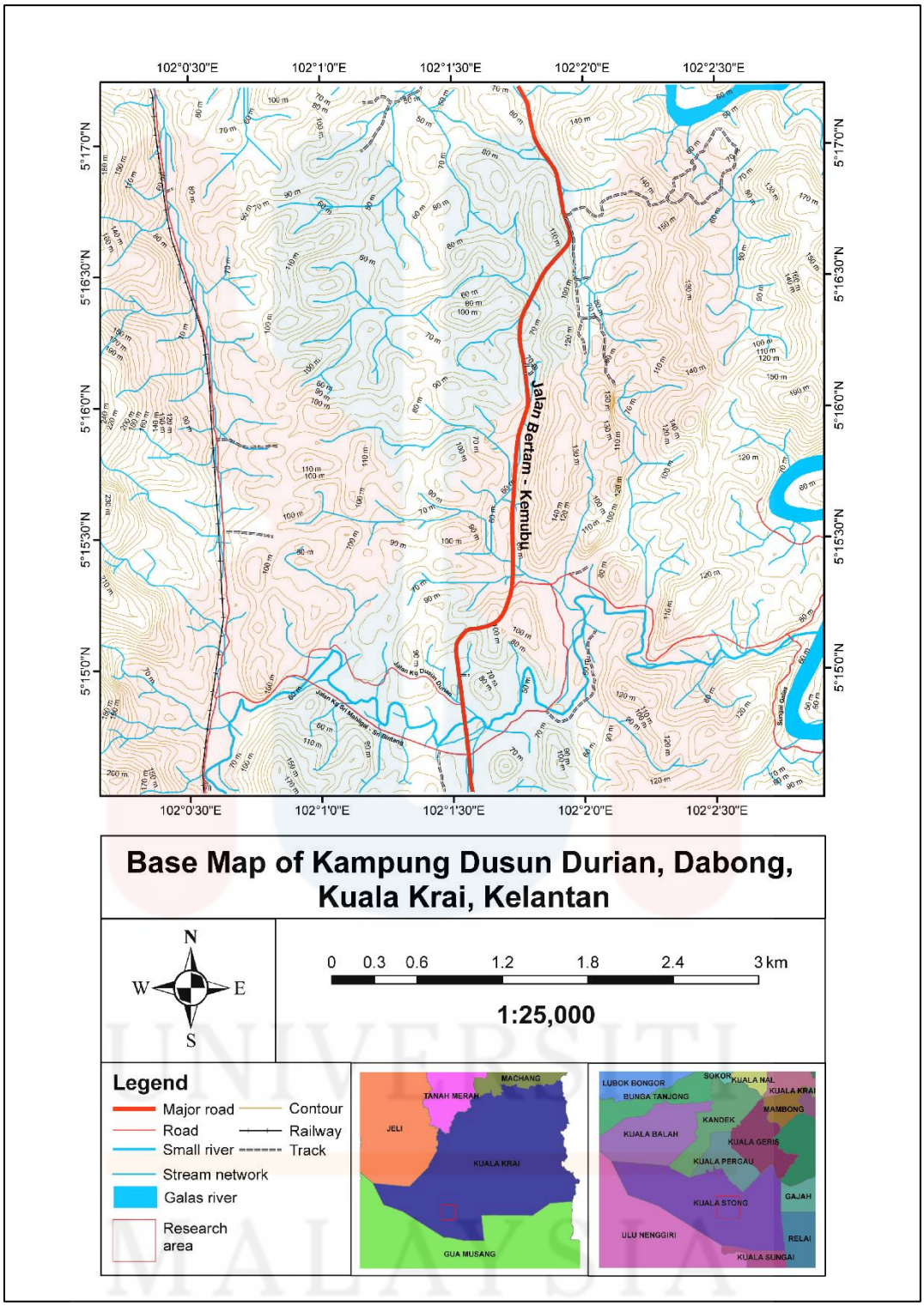

Figure 1.2: Base Map of Kampung Dusun Durian, Dabong, Kuala Krai, Kelantan.

1.5 Scope of the Study

The analysis region is composed of 25 km^2 using the measurement dimension region of 5 km x 5 km from latitudes of $05^0$17'0" N to $05^0$14'30" N and longitudes $101^0$59.7'30" E to $102^0$2.5'30" E (Figure 1.2). The research is utter regarding the geology and landslide investigation research. A geological catastrophe like landslide that may happen on account of the slope collapse, rain, debris flows, the impact of clear-cutting, tectonic motion, and many others could be observed mostly occurring all around the world. According to Cruden and Varnes (1996), rain, earthquakes, volcanic eruptions, groundwater changes, disturbances, and slope profile changes by construction activities could trigger the landslide event. The slope is an essential factor in the process of landslides. Hungr et al. (2014) presented within the original work updated and partly revised by Varnes (1978) the slope movement has been subdivided into six categories: falls, topples, slides, lateral spreads, flows, and composites. The division of the landslide susceptibility zone is very much related to the slope condition. Thus, it is essential to examine the landslide behaviour itself, and another method is advocated, for example, remote sensing reconnaissance, geological mapping, and area data collection to acquire a summary of an area of analysis.

1.6 Significant of Study

Within the spatial inquiry, the GIS, with its capabilities of data storage and multiple spatial analysis, can initiate an instance and easy landslide hazard evaluation towards the research region. The establishment of a landslide susceptibility map contributes to the landslide potential's scale and locality. Nowadays, GIS and Remote Sensing are widely applied in most landslide susceptibility analysis. Spatial data readiness for certain evolving countries makes remote sensing data such as satellite

imagery and Lidar are essential to be obtained. The application of GIS ensures that there is a possibility to acquire the qualitative as well as quantitative data and able to accumulate, analyze, alter, display and store the geographically referenced information, which is crucial for the landslide assessment. According to Mezughi (2012), the qualitative approaches are based on expert knowledge, and the exposure fields are defined explicitly in the field or by incorporating diverse index maps. Whereas quantitative methods calculate susceptibility probability based on mathematical expressions of the relationship among both causative factors and landslides

Besides, more detailed research is possible to be conducted by other researchers by referring to the current landslide susceptibility map produced and able to be a benchmark for any real estate contractor or city planner to develop the area in the future.

CHAPTER 2

LITERATURE REVIEW

2.1 Introduction

According to Amani Dahaman (2016), a literature review is an appraisal of information acquired from journals, books, and past research papers (thesis) for current research. A literature review is an assemblage of researcher information on the issues being studied. In revising a literature review, a researcher will ascertain what others have learned about the issues related to the ones studied. Other than the literature review is a systematic process that requires reading and thoughtfulness to detail. It involves written conclusions about articles in journals, books, and other documents that explain past and present information, compiling literature on specific topics, and documenting the need for the proposed study. The literature review is vital as it can give the researcher ideas and guidance on what to do.

2.2 Regional Geology and Tectonic Setting

Peninsular Malaysia's formation is classified into two tectonic blocks; Sibumasu blocks in the west and Sukhothai Arc/ Indochina blocks in the east, which occurred by the Late Triassic, and it is a part of the Southeast Asian continental core of Sundaland (Metcalfe, 2013). The state of Kelantan is situated in the northeast corner of the Malaysian Peninsula. Almost 85% of the State of Kelantan is covered by the river, which is about 248 km long and drains an area of 13,100 km^2 (Ibbitt et al. 2002).

The Kelantan river system is devised from a hydrological feature from the flat slope and moderately sloping areas. Both southern sides, as well as on the southwest, are high-level plains. The steep scraps and the high slopes in the southern part of the river basin can be attributed to the significant runoff zone to the Kelantan River (Pradhan et al., 2009). Thus, there are four types of landscape in Kelantan: mountainous areas, hilly areas, plain areas, and coastal areas (Unjah et al., 2001). According to Adriansyah Nazaruddin et al. (2017), the Department of Minerals and Geoscience Malaysia in 2003 discusses that the geology of the state of Kelantan stated as follows (from younger to older, and their percentages): Unconsolidated sediments (6%), Extrusive/volcanic rocks (10%), Sedimentary/ metasedimentary rocks (51%) and Granitic rocks (33%). Sedimentary/ metasedimentary rocks occupy the north-south central portion of the state. According to Zaiton Harun (2002), Kelantan's state is delimited within the west and east by the Main Range Granite and Boundary Range Granite, respectively, and is truncated to the north by unconsolidated sediments of the state's alluvial plain. The eastern part of the Kelantan state indicated the Lebir Fault Zone (Figure 2.1), one of the significant lineaments in Peninsular Malaysia and considered a post-Cretaceous and a sinistral strike-slip fault.

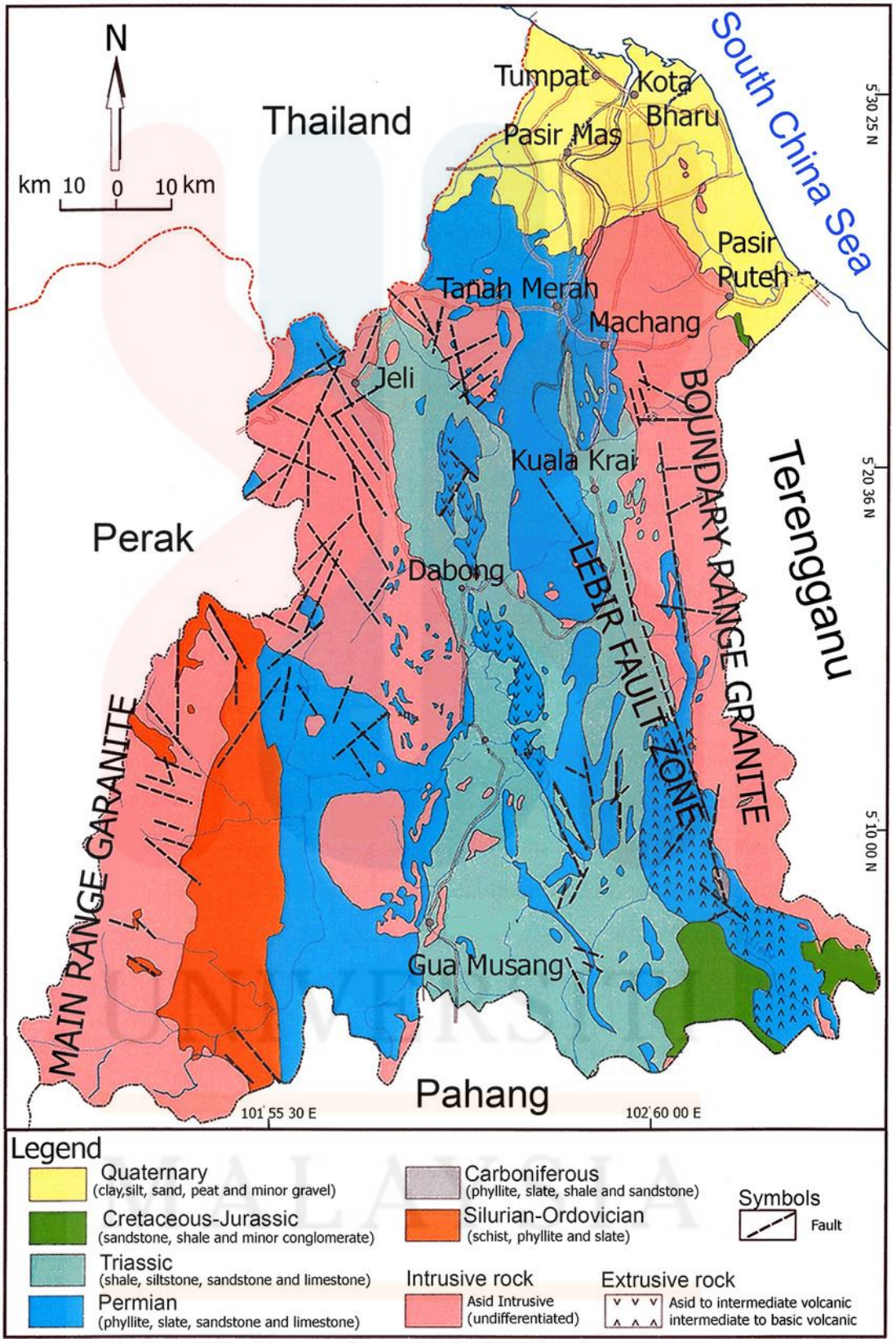

Figure 2.1: Map of Kelantan (Department of Minerals and Geoscience Malaysia, 2003).

2.2.1 Stratigraphy

Heng (2006) states that the Main Range Granite comprises of Stong Complex included the presence of Dabong region with intrusive igneous rocks, sedimentary rocks, and metamorphic rocks close to it. The Dabong region is situated in the southern part of Kelantan. The southern part of Kelantan is divided into three groups, which are lower Paleozoic rocks (west part of southern Kelantan), Permian-Triassic rocks (middle part of southern Kelantan), and Jurassic-Carbonaceous rocks (eastern part of southern Kelantan). The Stong Complex in the north of Dabong consists of three plutonic components (in a sequence of deteriorating age) from Berangkat Tonalite, Kenerong Micro-granite, and Noring Granite. The first, as well as second components of Berangkat Tonalite and Kenerong Micro-granite, are strongly foliated and highly deformed.

Meanwhile, the third component of Noring granite is unfoliated and undeformed. The Stong complex, dated from the Cretaceous and placed in metasedimentary rocks of sillimanite and Calc-silicate gneisses (Heng, 2003). The Noring granite is the largest part of the Stong Complex, which forms the oval pluton of Terang and Belimbing hornblende bearing facies. The Noring granite is undeformed and characterized by distinctive pink K-feldspar.

2.2.2 Structural Geology

The Stong Complex was the key structure that was created in these regions. In the north section, the Stong Complex consists of three types of components: Berengkat tonalite, Kenerong microgranite and Noring granite (In a deceased age order).

The Lebir Fault Zone was developed and tracked by the RADARSAT images as a curvilinear line along Sungai Lebir near Manek Urai in Kelantan bordering by

areas of NNW-SSE trending curvilinear line. The line was traced continuously to the south. It moves along the granite batholiths east of the Sungai Lebir and west of the Gagau Formation, as well as the Koh Formation's eastern margin. The fault zone, between Sungai Lebir and Taku Schist's margin near Kuala Krai, is at least 10 km wide.

In the region of Sungai Aring, the motion of sinistral slip around the faulting zoning can be found. This fault is referred to as the Lebir fault zone, as it passes through the Jurassic-Cretaceous basins containing the formation of Koh, Tembeling and Gagau. The current Triassic to Jurassic-Cretaceous basin has been affected by the faulting occurrence. Due to the movement of strike-slip at the faulting area, it went through the deformation phase. The new Jurassic-Cretaceous basin was created and deformed by strike-slip movements along the fault zone and deformed by strike-slip motions in the fault zone (Mustaffa Kamal Shuib, 2000).

2.2.2 Lithology

Lithology in geology often refers to the study and description of a rock's characteristics physically, especially on the scale of outcrops and hand specimens. By other definitions, it refers to characteristics such as the type of rock, the colour that is owned either fresh or weathered, mineral composition, and grain size, which is different in every rock. The types of rocks can be classified into three classes: igneous, sedimentary, and metamorphic rocks. The igneous rocks are rocks resulting from the cooling of magma; the sedimentary rocks are layered rocks resulting from the process of deposition of various mineral particles originating from pre-existing rocks, while the metamorphic rocks are rocks originating from igneous rocks or sedimentary rocks that have undergone physical and chemical changes due to heat and high pressure.

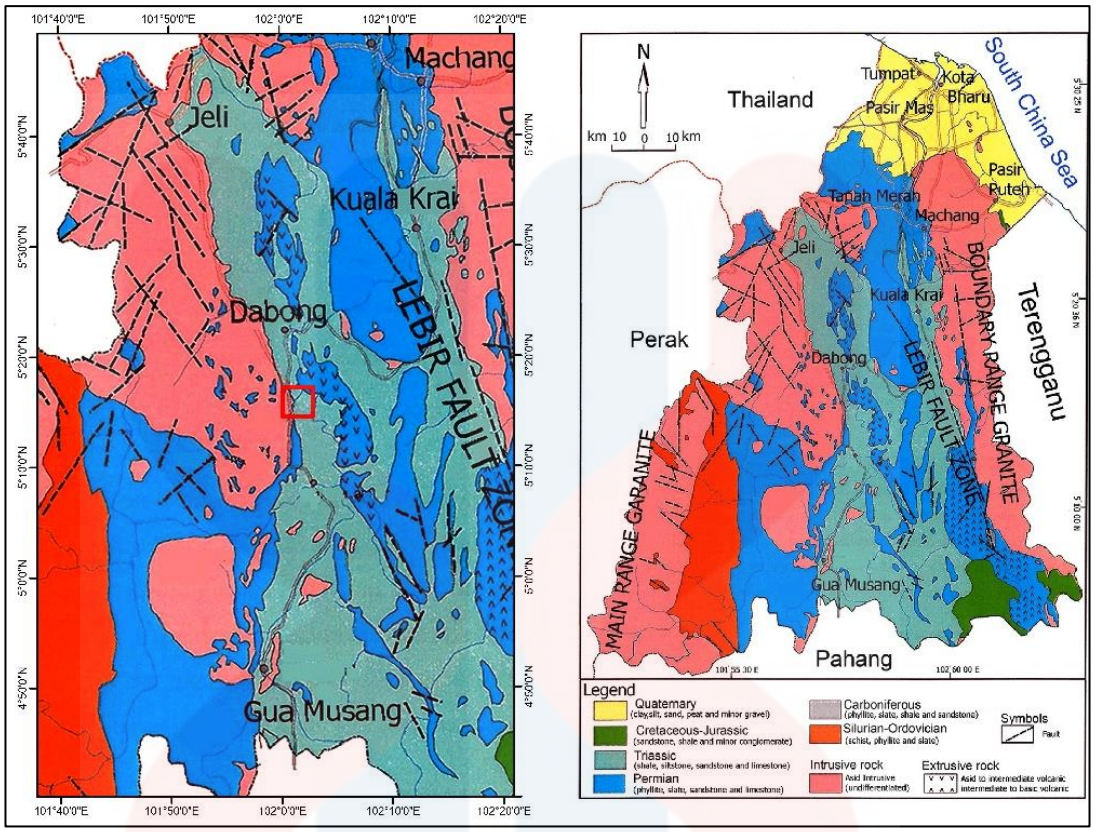

Figure 2.2: Rural region of Kampung Dusun Durian, Dabong (red outline colour of the square symbol) is marked on the Map of Kelantan using polygon tool and georeferencing tool in ArcMap

Based on the Map of Kelantan as illustrated in Figure 2.1, the study area's lithology focuses on the rural region of Kampung Dusun Durian; Dabong is marked with a polygon tool in ArcGIS depicted the red outline colour of the square symbol. The lithology included periods from Triassic (shale, siltstone, sandstone, limestone) and Permian (phyllite, slate, sandstone, limestone) while the red colour indicates the intrusive rock.

2.2.2 Hydrology

The Drainage system in the research region portrayed only one major river, which is Sungai Galas. The others are rivers situated outside the local study area, namely Sungai Jelawang, Sungai Serong, and Sungai Kenerong (Figure 2.3).

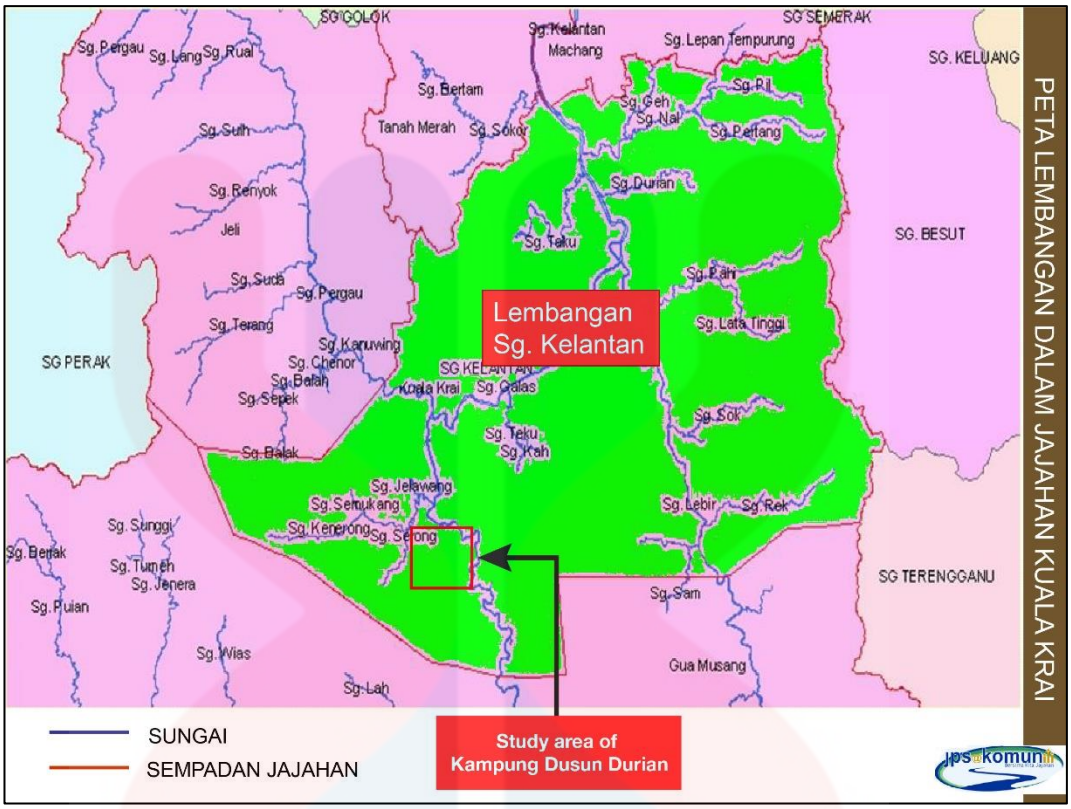

Figure 2.3: River Basin of Kelantan Map (JPS Jajahan Kuala Krai, n.d.).

2.2.3 Historical Geology

For the most part, Permian sedimentary rocks take place largely on the east of Kelantan where the Lower Paleozoic sequence of southwest Kelantan is placed. The Gua Musang Formation name is chosen from a broad limestone hill in South Kelantan and spreads southward to central Pahang, northward (about 32km) from Gua Musang. This rock unit becomes more metamorphic towards the Stong Migmatite Complex.

According to Hutchison (2009), it appears to the east and north of Gunung Stong as Phyllite and meta-volcanic rock near Dabong. The Gua Musang Formation is primarily argillaceous. However, the argillaceous rocks are poorly defined because their weathering presence is very low compared to that of the cliff-forming limestones. The formation consists of argillaceous bedding with calcareous, pyroclastic rocks and Taku Schist.

Richardson (1950) described that the Gua Musang formation's volcanic rocks are predominantly tuff of trachytic, trachyandesitic and andesitic structure. Ichikawa and Yin (1966) remarked on the strong deformation of the Lower Triassic strata near Gua Musang, where the metamorphic grade rises northwards, and 32km north of Gua Musang, the Stong Complex intrudes on the rocks. The formations of limestone were mainly recrystallized into marble. With occasional biomicrite presence, the limestone formations are mainly calcium-rich. The limestone is generally white, pink, light grey to black, depending on the number of carbonaceous materials.

There are three forms of sedimentary facies from the Gua Musang Formation.: limestone/calcareous facies, shale facies, and sandstone facies. Limestone constitutes up to 80% of the Gua Musang Formation. The Lower Palaeozoic series in southwest Kelantan is excessively unconformable. The calcareous bedding produces an extensive limestone formation consisting of thin or thick beds or even massive calcareous beds, typically compact and massively jointed. The limestone was mostly recrystallized to marble, and with the occasional existence of biomicrite, it is primarily calcium-rich. The limestone deposition environment of the formation of Gua Musang is perceived as a shallow water environment. (Richardson, 1939).

A mountainous region centred on Gunung Stong and Gunung Ayam, situated about 8 km west of Kemubu and Dabong railway towns occupies the Stong Complex. The whole complex migmatitic to varying degrees. Stong Complex is an injection complex combining Paleozoic rocks with a primary granite intrusion (Macdonald, 1967). According to Hutchison (2009), the Stong Complex's metamorphic parts are schist and gneiss rich in biotite, hornblende and garnet.

The Stong Complex consists of three granitic bodies located in metamorphic, metasedimentary and meta-volcanic low-grade rocks of the Permian period.

Concerning overlying rocks, the belt of greenschist facies phyllite, marble and metavolcanic rocks separate Taku Schist's formation. Because of the metamorphism, The fossils found in these rocks may be destroyed. However, Gua Musang Formation's greenschist facies, which has almost similar lithology to that of Stong Complex, suggest that the period is Permian to Lower Triassic period. The occurrence of significant marble formation in the series indicates a correlation with the Gua Musang Formation that occurs immediately to the south. In Dabong, about 10km away, there are hills of limestone which are part of the Limestone Aggregates of Gua Musang.

2.3 Research Specification

2.3.1 Landslide

A landslide is a geological event in which land movements occur, such as falling rocks or large lumps of soil from a higher place to a lower place due to the push of water, wind, or gravity. The landslides occurred when the propulsive force on a slope greater than the retaining force. Retaining forces are generally influenced by soil density and rock strength. While the propulsive force is influenced by the magnitude of the load, slope angle, and rock density. The occurrence of landslides can be described as follows; the water seeped into the soil will add weight to the ground. If the water penetrates to an impermeable soil that acts as a sliding plane, the ground becomes slippery, and soil weathering will move to follow the slope and off the slopes. The process goes through three stages, namely detachment, transportation or movement, and deposition.

Landslides can have several causes, including geological, morphological, physical, and human (Cruden & Varnes, 1996). However, Varnes (1978) argues that only one trigger it to occur. Hence, the external stimulus which is vulnerable as a

triggering booster of landslides can be earthquake shaking, storm waves, heavy rainfall, volcanic eruption, and rapid stream erosion by enhancing the stress or reducing the strength of slope materials. In some cases, the landslide might be happened due to numerous causes, like the weathering processes of materials, by time able to bring the slope to failure.

2.3.2 Landslide Classification

The most common classification of slope failure was applied by Varnes (1978). The slope's movement can be classified into six aspects: falls, topples, slides (rotational and translational), lateral spreads, flows, and composites in terms of a combination of types.

According to Varnes (1978), again, there are two terms included for the landslide classification; the first term describes the material type, and the second term to describe the type of movement (Figure 2.4). In Malaysia, two types of landslide classification have been introduced by local scientists, namely Ibrahim Komoo and Tajul Anuar Jamaluddin (Hamzah Hussin et al., 2015). Furthermore, Ibrahim Komoo (1985) generally used the landslide classification as it takes into account local factors, due to the highly weathering and heavy rainfall often cause failure in the form of erosion (Tajul Anuar Jamaluddin, 1990).

In most cases in Malaysia, prolonged heavy rainfall frequently leads to landslide failure. Indeed, most of the slope failures occur every year during the monsoon seasons between November and February. Landslides have also occurred in other months. However, the occurrence of landslides is also closely related to the occurrence of heavy rainfall at the time of the event or a few days before the slope failure incident. Most researchers acknowledge that among the essential factors that

cause slope failure is geological material forming the slope, the influence of surface water runoff, groundwater, weathering, discontinuity of geological structure, weaknesses in slope design, slope leg cutting, the occurrence of sudden tremors such as an earthquake may trigger slope instability and there is a load on the slope (Tajul Anuar Jamaluddin, 2006). The following indicates the characteristics of slope forming mass movements by Varnes (1978), where it can be divided into five types:

1) Falls

Fallout is falling movement slope forming material (soil or rock) in the air, with no interaction between the parts of the slide material. Rockfall can occur on all rock types and generally occurs due to weathering, changes in temperature, water pressure, or excavation/scouring at the bottom of the slope. Fallout can occur along the stocky, the base plane, or a local fault zone. It generally occurs on steep slopes to hang, especially in coastal areas.

2) Topples

Topples are the movement of collapsed material and usually occur on slopes of very steep to erect rocks under gravity's actions. The type of movement is almost the same as the fall, only the movement of rock avalanche is rolling over until it collapses, which results in loose rocks from the slope's surface.

3) Slides

Slides are the movement of slope-forming material caused by shear failure, along with one or more landslide areas. Based on the geometry of the sliding plane, slides can be divided into two types, namely:

a) Translational

Translational avalanches are movements along discontinuities or weak fields parallel to the slope surface so that the ground motion is translational.

b) Rotational

Rotational avalanches are the movement of masses of soil and rock in the form of a sliding plane. It has curved upward planes and often occurs in landmasses that move in a single unit. Slump occur in a homogeneous material such as dykes

4) Spreads

Spreads, including translational avalanches, also called lateral spreading, is a combination of a vast landmass and downs of the rock mass is fragmented into soft material underneath.

5) Flows

Flow is the motion of crushed material down a slope and flows like a viscous liquid. This flow can occur when a moving landmass is driven by water. The motions occur along the valley and can reach hundreds of meters away.

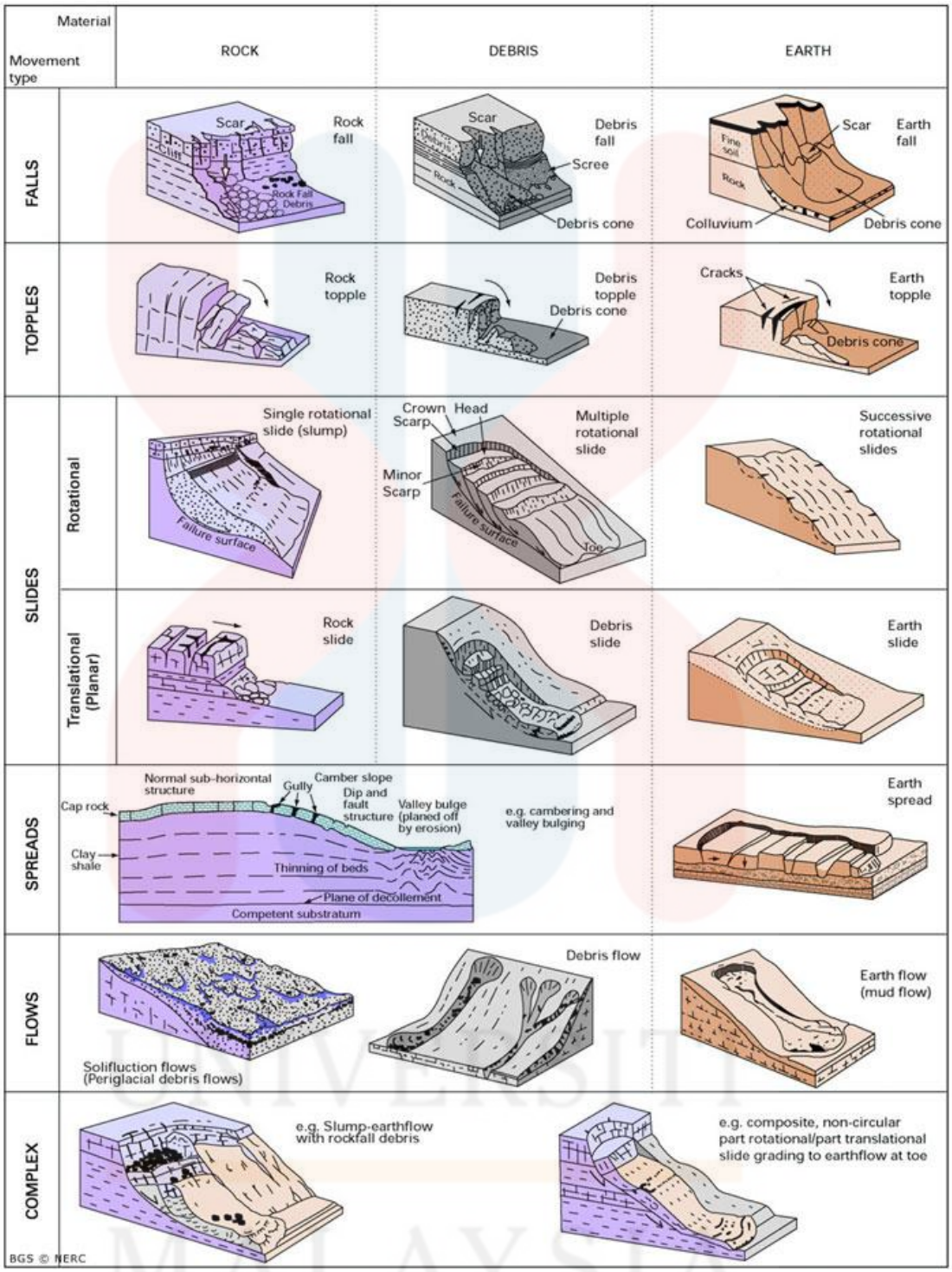

Figure 2.4: Examples of landslide occurrences (Novotný, 2013).

New Landslides	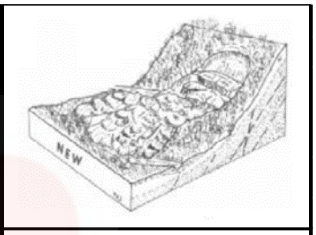
The shape and geometry of the landslide are clear	
Features associated with landslides such as main escarpment, heads, tension cracks, rock/soil blocks, can still be distinguished	
The riverbed is blocked due to a temporary dam by the collapse	
Latent Landslides - Young	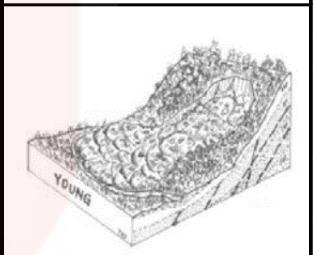
The shape, geometry, and key features associated with it are still clearly visible	
Parts of the rubble's body is still clear but have been gradually smoothed by erosion and sediment deposition. the action of runoff begins to form erosion of gullies and rills	
Grass and secondary plants begin to grow, covering part of the surface of the rubbles	
The river begins to form a diversion groove according to the lobe or foot of the rubble	
Latent Landslides - Mature	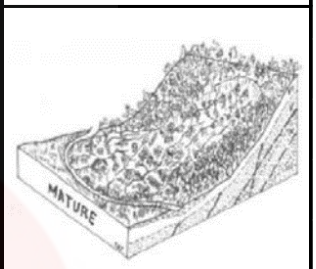
The shape, geometry, and key features associated with it are increasingly blurred and unclear	
The body part of the rubble is declining, but the topography at the bottom of the rubble remains undulating	
New drainage has just begun to form due to deep erosion of the gullies on the surface of the rubble and branched upstream in the form of a 'Y'	
The accumulation of colluvium is seen more clearly in the tail and legs of the rubble	
Latent Landslides - Old	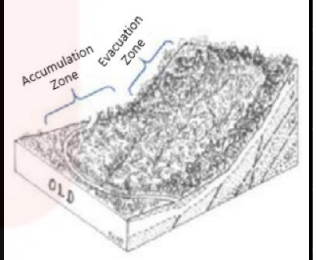
The rubble is increasingly blurred due to erosion, weathering, and vegetation cover	
The presence of landslides is detected by the contrast of the cover and the density of the plants	
The vegetation cover is thicker in the accumulation zone due to the loose soil texture and high water content	
Evacuation zones forming concave morphology can still be detected on slopes, while accumulation zones form sloping convex morphology to almost horizontal	

Figure 2.5: The evolution and geomorphic cycle of natural slope landslides in humid tropical hills and highlands (Tajul Anuar Jamaluddin, 2020)

2.3.3 Causes of Landslides

According to Highland et al. (2008), factors contributing to landslides can be divided into natural and human factors. Natural factors are related to material type and thickness, geomorphology, precipitation, and slope cut-off. Human factors include slope modification, peak slope overloading, drainage modification, and vegetation removal. Landslides are caused by soil or rock material failure that cannot withstand its original position due to certain factors. Thus, the process of soil mass depletion

occurs on the surface of the Earth. Commonly, In Malaysia, the cause of landslides can be attributed to several factors, such as:

1) Erosion occurs by rivers, glaciers, or ocean currents that produce cliffs or slopes exposed to weathering surfaces.
2) Hills cut-off and deforestation by human activities also pose a risk of worse erosion on slopes. As a result, there are no more plants to bind with the soil.
3) High water content causes the soil to become saturated and lose its cohesive properties. The soil will be loose, which is easy to move and will flow elsewhere. Groundwater pressure acts to make the slope becomes unstable
4) Earthquakes that produce tremors and tensions can cause existing slope structures to collapse or cause discontinuity to become more active.
5) Shocks from machinery, explosives, and even thunder may also cause a weak slope to collapse. Uncontrolled mining and uncontrolled quarrying activities can also cause landslides.
6) Extreme weight arising from the accumulation of rain, piles of rocks or ore, piles of rubbish, or human-made structures that pressure the slope to collapse
7) Continuous heavy rainfall can also cause the slope to be saturated and loose and most likely to collapse.

The landslide, which is often reported in Malaysia, is not much different from other countries in the world. The only difference is just the location and the current situation, in particular climate change. It is common in Malaysia to experience hot and humid climates throughout the year. Rainfall is also high, especially in the monsoon season. Thus the occurrence of landslides is one of the characteristics of slope failure. Various factors contribute to slope failure in Malaysia. Among them are high rainfall

distribution rates. Other factors include changes in the geomorphological properties of a place, rock plane conditions, and the nature of surface runoff that change soil properties due to rainfall action.

According to Bujang et al. (2008), he argues that most of the landslides that occurred in Malaysia occurred from September to January as the number and occurrences recorded in most of these rural areas were high and frequent during that period. Besides, other factors contributing to slope failure in Malaysia include:

1) Gravity

Gravity is a force acting anywhere on the surface of the Earth. Therefore, the force of gravity acts by pulling the object toward the centre of the Earth. Thus, on a flat surface, its gravitational force acts downward. The material on a flat surface will not move due to the gravitational attraction. However, on the sloping surface, the gravitational force can be solved using two components, one that acts perpendicular to the slope and the component acting parallel to the slope surface.

2) Influence of soil type

Generally, the main material characteristics that determine the soil type are distribution (grading), particle size, and plasticity. Therefore, particle size distribution and complexity can be determined either by doing laboratory tests or by simple human observation. The secondary properties of a material are the colour, shape of the soil, texture, and the particles' content. The distinction between description and classification of soil is essential to know. The description of the soil includes details on the properties of the material and the mass. It is, therefore, impossible for two soils to have the same description. According to the description from BS 5930 (1981), in accordance with the

necessary soil type standards are boulders, cobbles, gravel, sand, silt, and clay. Therefore, all of these types of soil are defined based on their range size of particles.

3) Geometry of slope

The geometry of the slope is where the shape of the slope depends. Dahal et al. (2008) and Avanzi et al. (2004) categorized slope gradients into four groups: 30 - 35, 35 - 40, 40 - 45, and over 45. From the results of the analysis, it is shown that the slope angle between 40 - 45 has a high frequency of landslides. Meanwhile, Van Zuidam (1985) suggested the relationship between slope class, process properties, and land conditions, along with colour symbols (Table 2.1). The slope geometry includes the slope's height, the width of each slope, and a number of slopes located in the region. Therefore, every aspect of the geometry of the slope will influence the stability of the slope. The slope angle should also be known and identified. Consequently, a very steep slope is more vulnerable to slope failure, such as landslides.

Table 2.1: Relationship between slope class, process properties, and land conditions accompanied by suggested colour symbols.

Slope Class		**Process, Characteristics and Land Condition**	**Symbol colours suggested.**
0 - 2°	0 - 2%	Flat or almost flat, no erosion big one can be processed easily in dry conditions.	Dark green
2 - 4 °	2 - 7%	The land has a gentle slope. If a landslide moves at a low speed, erosion will leave very deep marks.	Light green
4 - 8 °	7 - 15%	The land has a gentle slope to steep slope. If a landslide moves at a low speed, it is very prone to erosion.	Light yellow
8 - 16 °	15 - 30%	The land has a steep slope, prone to landslides, surface erosion and channel erosion.	Dark yellow

16 - 35 ^{o}	30 - 70%	The land has a steep to a steep slope, erosion and soil movement often occur with a slow speed. Areas prone to erosion and landslides	Light red
35 - 55 ^{o}	70 - 140%	The land has a steep slope, often found outcrops of rock, prone to erosion.	Dark red
> 55^{o}	> 140%	The land has a steep slope, rock outcrops appear on the surface, prone to rock slides.	Dark purple

(Van Zuidam, 1985)

4) Crops on slopes

Generally, the vegetation in the slope also affects the occurrence of landslides. In this case, the crop on slopes is a covering layer that can control erosion on the slope surface and strengthen the slope's soil structure. The plants on the slope also act to bind the subsurface layer by creating a branching structure between the plant roots and the subsurface layer. The plant roots will act by growing deep into the soil and acting as retention that prevents the soil surface from sliding. It also absorbs the momentum of rainfall from falling directly into the ground and controlling the quantity of water surface flow as the water is absorbed by the vegetation in the slope allowing the effect of erosion on the slope surface to be minimized.

5) The effects of nature

In general, the natural processes impression is very influential and has a connection with the instability of the slope, such as changes in weather and seasons in Malaysia itself. In this case, continuous hot and dry weather conditions may cause cracking in the land surface.

The surface of soils and rocks that are cracked will be more exposed to the weathering agents and erosion that act by entering each of these fissures. The annual rainfall level is also one of the crucial criteria for ensuring the stable

slope surfaces at the hills, where each hill receives a different amount of rainfall. The slope surface region that receives high rainfall distribution is an area of high risk for slope failure compared to the region that receives a low rainfall distribution.

The phenomenon of an earthquake may also affect the stability of a slope. In this case, if an earthquake strikes when it rains, the safety factor will become decrease, and the slope will become more unstable. Indeed, a strong ground shake will also increase the shear stress in the soil. Besides, the impression from the frequency and Earthquake magnitudes may overcome the soil's adhesion force and its retaining structure.

The movement of soil particles will be more likely to move downward. As for Malaysia's country, it is one of the few countries that survived the Pacific ring of fire.

Therefore, the Earthquake was not a significant factor in the failure of the slope of the country.

6) Drainage system

The design of a drainage network is one of the most significant facets of stabilizing the slope. A good drainage system can supply water better towards surface runoff and subsurface. Therefore, the role of drainage systems for slope surfaces is crucial, especially during the rainy season. The effects of surface water flow can create erosion on slopes by bringing soil down the slope. Despite the heavy rainfall, not all the water will go down the slope. The soil will absorb part of the surface water flow, which will further increase the amount of water content in the soil. However, the water diffusion will cause an increase in pore water pressure and subsequently add the shear stress in the

ground. As a result, it can weaken the force of soil particles on the slopes. Consequently, the effects of an unsystematic drainage system will contribute to slope failure in an area of hills.

2.3.4 Remote Sensing

Remote sensing technology is the development of aerial photography technology introduced in the late 19th century. At the beginning of its development, remote sensing was only a technique developed to obtain and analyze information from the Earth's distance. The benefits of aerial photography are considered very large in the first and second world wars, just before this method is widely utilized in space exploration. Since then, the application of remote sensing becomes known and popular in the world of mapping. However, along with the development of science and technology, it turns out that remote sensing often functions as a powerful scientific tool to conduct observations and reconnaissance upon the spatial elements of the Earth's surface. The information extracted is in the form of electromagnetic radiation transmitted or absorbed from the Earth's surface by the sensor tools developed. The sensor functions to track, detect, and record an Earth object within a specific coverage area. Sensors can be in the form of a camera, scanner, and radiometer. In general, the sensor is mounted on a platform in an airplane, satellite, or shuttle. Data acquisition from the Sentinel satellite program platform for Sentinel-2 satellite data and ALOS satellite data is taken into account for this research.

2.3.5 Sentinel Satellite Program

European Space Agency (ESA), under The European Union's Copernicus Program, is developing a series of seven Earth Recognition Missions for each of the two satellites, which will provide free data to monitor Earth's resources at a global

level. The ESA has launched four satellites so far (in early 2017). These are Sentinel-1A (April, 2014), Sentinel-1B (April, 2016), Sentinel-2A (June, 2015) and Sentinel-3A (February, 2016) and Sentinel-2B (March, 2017). For this research, Sentinel-2 satellite types comprised of Sentinel-2A and Sentinel-2B are used to observe the Earth's landform. Sentinel-2 will carry an optical instrument charge that will sample 13 spectral bands: four bands with 10 m spatial resolution, six bands with 20 m spatial resolution, and three bands with 60 m spatial resolution (Earth Observing System, 2015).

Table 2.2: Sentinel-2 band designations.

Sensor	Band number	Band name	Sentinel-2A		Sentinel-2B		Resolution (meters)
			Central wavelength (nm)	Bandwidth (nm)	Central wavelength (nm)	Bandwidth (nm)	
MSI	1	Coastal aerosol	443.9	20	442.3	20	60
MSI	2	Blue	496.6	65	492.1	65	10
MSI	3	Green	560.0	35	559	35	10
MSI	4	Red	664.5	30	665	30	10
MSI	5	Vegetation Red Edge	703.9	15	703.8	15	20
MSI	6	Vegetation Red Edge	740.2	15	739.1	15	20
MSI	7	Vegetation Red Edge	782.5	20	779.7	20	20
MSI	8	NIR	835.1	115	833	115	10
MSI	8b	Narrow NIR	864.8	20	864	20	20
MSI	9	Water vapour	945.0	20	943.2	20	60
MSI	10	SWIR-Cirrus	1373.5	30	1376.9	30	60
MSI	11	SWIR	1613.7	90	1610.4	90	20
MSI	12	SWIR	2202.4	180	2185.7	180	20

(Earth Observing System, 2015)

2.3.6 ALOS

ALOS is a multi-mission Japanese-owned satellite, a cutting-edge generation of JERS-1 and ADEOS satellites equipped with more advanced technology. The ALOS satellite was successfully launched on January 24, 2006, with an H-IIA rocket launcher, from the Tanegashima Space Center's launch site, southern Japan. This satellite ceased operation in April 2011. During operation, the satellite has five primary missions: cartography, regional observations, natural disaster monitoring, natural resource research, and technology development. In order to achieve this primary mission, the ALOS satellite is equipped with three remote sensing sensors with side view capability. The three sensors consist of two optical sensors: the PRISM used for digital elevation mapping and the AVNIR-2 sensor for accurate observation of land coverage, and a microwave or radar sensor called PALSAR for surface observations day and night and in all weather conditions.

PALSAR is an active microwave sensor or L-band (centre frequency 1270 MHz, 23.6 cm) developed by JAXA in collaboration with JAROS. This sensor functions for day/night observations, free of clouds and weather observations. The following indicates three main modes of operation of PALSAR:

1) Fine mode is a high-resolution mode with a spatial resolution of 10m and a common operating mode for interferometric observation with 70km wide unit image coverage in a single HH or VV polarisation.
2) ScanSAR mode is a mode that allows obtaining images with an image unit coverage width up to 350km with a single polarisation of HH or VV and a spatial resolution of 100m
3) Polarimetric mode is a mode that is operated on an experimental basis in the HH + VV + HV + VH polarisation.

Table 2.3: Characteristic of PALSAR

Mode	Fine		ScanSAR	Polarimetric (Experimental mode)*1
Center Frequency	1270 MHz(L-band)			
Chirp Bandwidth	28MHz	14MHz	14MHz,28MHz	14MHz
Polarization	HH or VV	HH+HV or VV+VH	HH or VV	HH+HV+VH+VV
Incident angle	8 to 60deg.	8 to 60deg.	18 to 43deg.	8 to 30deg.
Range Resolution	7 to 44m	14 to 88m	100m (multi look)	24 to 89m
Observation Swath	40 to 70km	40 to 70km	250 to 350km	20 to 65km
Bit Length	5 bits	5 bits	5 bits	3 or 5bits
Data rate	240Mbps	240Mbps	120Mbps,240Mbps	240Mbps
NE sigma zero *2	< -23dB (Swath Width 70km) < -25dB (Swath Width 60km)		< -25dB	< -29dB
S/A *2,*3	> 16dB (Swath Width 70km) > 21dB (Swath Width 60km)		> 21dB	> 19dB
Radiometric accuracy	scene: 1dB / orbit: 1.5 dB			

(JAXA, 2006)

Palsar can be used to eliminate cloud effects on optical data and can be used at 1: 30,000 or smaller. Besides eliminating the cloud effects, Palsar can be used to create Digital Elevation Models (DEM).

2.3.7 Geographic Information System (GIS)

GIS is a set of computer-based tools that allow for processing spatial and non-spatial data into related information about the Earth and is used to collect, store, manipulate, analyze, and display data that is then used as material to make decisions. Geographic Information Systems consists of five basic components: data, software, hardware, human resources, and GIS users. Data is the main component that will be processed using GIS. Software is a component to integrate various kinds of input data,

which will be processed in GIS hardware in the form of a computer, digitizer, scanner, plotter, monitor, and printer. Human resources are system users, operate software and hardware, and analyze data as needed.

In GIS, it consists of data dimensions: geographical data (spatial dimensions) and data attributes (non-spatial dimensions). Besides, the geographic data in GIS is relatively complex. Therefore, it must contain topology information elements (the relationship between geographic elements) and the data attributes. The GIS is also a combination of spatial data and attributes data displayed together, thus providing convenience in conducting an analysis.

2.3.8 Data from GIS

GIS systems can integrate a range of geographic technologies, such as remote sensing data and global positioning systems; thus, it has become crucial for landslide susceptibility mapping. It may range from simple methods using minimal data to sophisticated computational formulas using functional numerical methods in the computer-oriented Geographical Information System (GIS) using complex databases. In this study, the landslide susceptibility regions are analyzed and mapped using the landslide accident factors by the AHP approach according to the GIS-based AHP system implemented in previous studies by Mezughi (2012). GIS data has two essential components that make it diverse from other data, namely locality information and attribute information, which can be defined as follows.

1) Firstly, is the locality information or spatial information. Typical examples are latitude and longitude information, as well as datum and projection information. An additional example of spatial information that can be used to identify locations is Zip Codes. It can usually be obtained

through a spaceborne platform of the satellite, aerial photograph, analogue map (a traditional form of spatial data, where data is displayed on paper or film), tabular data, and Survey Data (Observation or measurement in the field).

2) Next is the descriptive information (attributes) or non-spatial information. A location usually has several attributes or properties associated with it; for example, an oil well has attributes/properties into a well, oil production per day, the start of production, and the date of drilling.

Locality information is determined based on a coordinate system, which includes datum and map projections. Datum is an assemblage of parameters and control points whose geometric interactions are known, either through calculation or measurement, whereas the map projection coordination is a system designed to signify the surface of a curved or spheroid plane (such as the Earth) on a flat plane. This representation process causes distortions that need to be taken into account to acquire the precision of several classes of properties, such as distance, area, or angle. In GIS, spatial data can be represented in two formats: Vector Format and Raster Format (Humboldt State University, 2017, Conversion between Data Model).

1) Vector Format

In vector format data, our Earth is signified as a mosaic of strokes (arc/line), polygons (areas surrounded by lines that start and end at a similar point), points (nodes that have labels), and nodes (are the point of intersection between two lines). The main advantage of vector data formats is the accuracy in representing points, constraints, and straight lines. It is very advantageous for analyses that require position accuracy. Another example of usage is to delineate the spatial relationships of several features. The main weakness of

vector data is its incapability to put up the gradual change. The file extension is in the forms of SVG and pdf.

2) Raster Format

Raster data (also called grid cells) is data created from the remote sensing system. In raster data, geographic objects are symbolized as grid cell structures called pixels (photo elements). In raster data, the resolution (visual definition) depends on the pixel size. In other words, pixel resolution designates the actual size on the Earth's surface signified by each pixel in the image. The smaller the dimensions of the Earth's surface signified by one cell, the higher the resolution. Raster data is very decent for indicating boundaries that change gradually, such as soil type, soil temperature, vegetation, and soil moisture. The primary constraint of raster data is the large file size; the higher the grid resolution, the larger the file size. The file extension is in the forms of tiff, gif, jpg, and bmp.

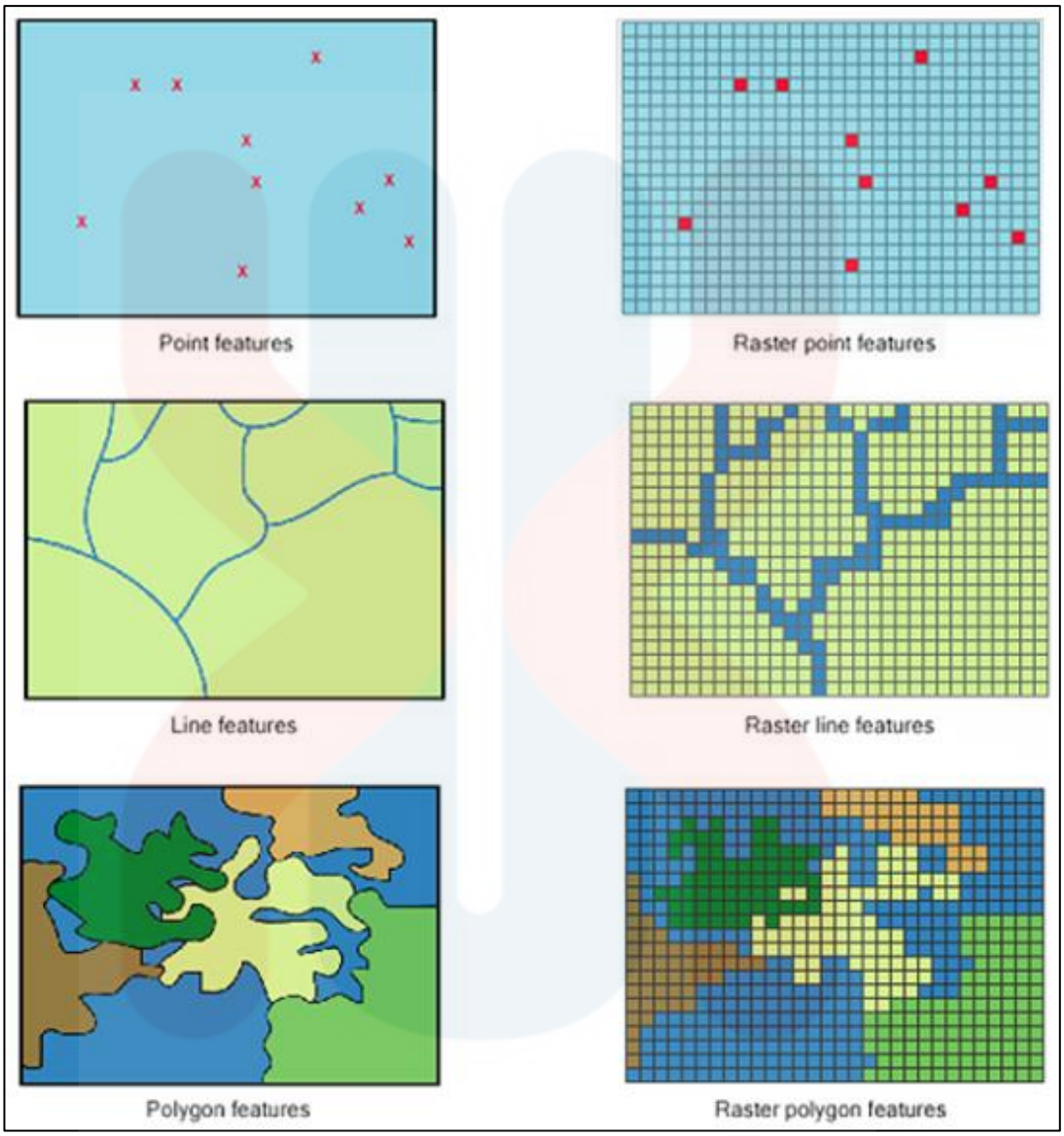

Figure 2.6: Spatial data of vector format and raster format (Humboldt State University, 2017).

Each data format has advantages and disadvantages. The choice of the data format used depends on the proposed use, accessible data and volume of data produced, the preferred accuracy, and the ease of inquiry. Vector data is somewhat more economical in terms of file size and precision in position, but it is very challenging to use in mathematical computing. In contrast, raster data usually require larger file storage space and lower location precision but is easier to use mathematically.

2.3.9 Analytical Hierarchy Process (AHP)

AHP is a judgement support model developed by Saaty (1980); this decision support model will breakdown complex multi-factor or multi-criteria difficulties into a hierarchy. According to Saaty (1980), hierarchy is defined as representing a complex problem into a multi-level structure where the first level is the goal, followed by the level of factors, criteria, and sub-criteria. With hierarchy, a complex problem can be broken down into groups, which are then arranged into a hierarchical form so that the problem will appear more structured and systematic.

CHAPTER 3

MATERIALS AND METHOD

3.1 Introduction

Material and technique are imperative to direct the exploration, where some methodology needs to follow to guarantee the research accomplishments and satisfy the standards provided. All the strategies and mechanisms must first make sense of whether it is reasonable or not. For sure, it is vital to make the research led easily and comply with the goal executed. This research includes the quality outcome based on the research area, positioned in the rural region of Dabong, Kuala Krai, and Kelantan. The application of data from GIS and Remote Sensing are taking into account. The following are the research materials and several stages of methods involved:

3.2 Materials

The equipment included in this research is classified into Hardware and Software for the GIS and Remote Sensing application.

1) Hardware

The hardware used to operate GIS can be classified into three primary groups, namely:

a) Input Data: the input data can use a data reader for digital data from previous work stored on video, hard disk, flash drive, and other storage devices; also, the data is inputted by transforming the data format from

hard copy into digital data, for example by digitizing tables, scanners, or by typing through the keyboard. Examples of input data: table data, report data, digital data, map data, satellite data, aerial photo data, and others.

b) Data management and analysis: GIS computer work's primary ability can do data management and analysis. There are two necessary forms of GIS work: a desktop computer (PC) and a laptop that is used alone or in the form of a computer server that operates the network.

c) Output: GIS can produce a variety of products. Data can be displayed on a monitor or presented in hard copy using a printer or plotter. GIS output can also be in digital format stored on disk, which can be used in other GIS applications. Example of output: map, report, and others.

2) Software

The software included as a cutting-edge tool for processing GIS and Remote Sensing data consists of ArcMap 10.7, Google Earth Pro, PCI Geomatics 2016, SASPlanet, Global Mapper, and ENVI 5.3. This software provides functions and tools capable of storing data, analyzing, and displaying geographic information. Thus, the element that must be contained in the GIS software component included:

a) Tool for performing geographic data input and transformation

b) Tools that backing geographic queries, analysis, and visualization

c) Graphical User interface (GUI) for easy access to geographic tools.

As the core of the GIS system is software from GIS itself that provides functions for storing, managing, linking, querying, and analyzing geographic data. GIS

software is an application software package that contains various computer programs to map, manage, and analyze geographic data.

The main characteristic of GIS software is the availability to process and analyze spatial data and attributes. GIS software requirements: Graphic data processing, Database processing, Analysis and presentation of data, Cartographic Operations, and Special application and development. The acquisition of satellite data and parameters used for the creation of landslide susceptibility Map and geological Map are depicted from the following Table 3.1.

Table 3.1: Source of data used for research

Data Type	Data Structure	Source
Sentinel - 2	Raster	USGS GloVis (https://glovis.usgs.gov/app?fullscreen=1)
ALOS PALSAR DEM (5-10 meters resolution)	Raster	Alaska Satellite Facility (https://search .asf.alaska.edu/#/)
Normalized Difference Vegetation Index (NDVI)	Raster	Sentinel - 2 NDVI = (Band 8 - Band 4) / (Band 8 + Band 4)
Land Use and Land Cover (LULC)	Raster, Vector	Sentinel - 2, Google Earth Pro
• Aspect • Slope • Distance to roads • Distance to drainage	Shapefile, Raster, Vector	ArcGIS

• Distance to lineaments		
Lineament	Raster, Shapefile	PCI Geomatics 2016
Aerial Photographs	Vector	Google Earth Pro, SASPlanet
Precipitation	Raster	Matomo Webanalysis (https://climatecharts.net/) CHRS Data Portal (https://chrsdata.eng.uci.edu/)
Soil moisture	Raster	EARTHDATA (https://nsidc.org/data/SPL2SMAP_S/versions/3)
Lithology	Vector	Department of Minerals and Geoscience Malaysia in 2003 • Geologic map of the Kelantan state (scale 1:250,000) Previous researcher namely Zakiah Ainul Kamal in 2013 • Lithology map of Batu Ban Chuan (scale 1:25,000)

3.3 Research Methodologies

The inquiry or investigation plan is classified into four segments based on the following specified:

1) Data collection
2) Spatial data processing
3) Spatial data analysis
4) Analysis of landslide susceptibility regions

3.3.1 Data collection

Sufficient preparations before undertaking the research must be accomplished to ease work later on. Numerous studies need to be done to guarantee that the data can be useful when encountering a problem that will happen in the future. In this manner, perusing many journals, articles, and books identified with the research of interest gained from the library and the site like Researchgate, Google Scholar, Academia, and OpenAthens must be done. Installing any applications, for example, Google Earth Pro, ArcMap 10.7, PCI Geomatics 2016, SASPlanet, Global Mapper, and ENVI 5.3 also essential in aiding to construct any other maps or the base map of the study area, as per the contour, requested either 5 meters, 10 meters, or otherwise. References from previous research of other researchers regarding the lithology or locality of Dabong and a region close to it are included to assist the study.

3.3.2 Spatial data processing

Spatial data in GIS is presented in two formats, namely vector format and raster format. Data that has been collected before for vector format is in the form of analogue maps, namely Map of Kelantan and raster format of remote sensing data from the Sentinel-2 satellite and ALOS satellite. The analogue map is then converted into a digital map through the digitization process on screen, then a geometry or georeferencing correction is performed. Besides, Sentinel-2 satellite data is obtained from the sources of the USGS GloVis website. The acquisition of remote sensing data is taken from 2016 until 2020, and the comparison is conducted to investigate the changes detection for Land Use and Land Cover (LULC). As for the ALOS Satellite, the data is acquired from the Alaska Satellite Facility Website. Due to the limited data year from 2010 until 2011, decisions are made by choosing the 2011 PALSAR dataset

to create the DEM of the research area. It is essential to have an ALOS satellite dataset as the PALSAR sensor is equipped with its capability to penetrate the cloud with a clear projection of satellite images above the Earth. The process of entering remote sensing data and analogue maps is done through computers with ArcMap 10.7 software.

Geometric correction or georeferencing is the process of projecting maps into a particular map projection system. Uniforming the data into the same coordinate and projection system needs to be done to facilitate the process of integrating the data. The projections used in this study are UTM (Universal Transverse Mercator) datum WGS 1984 and zone 47N, using ArcMap software version 10.7 with the Projection and Transformation extension. After the correction process for both vector and raster format dataset is complete, then proceed with cropping the dataset according to the research area.

Different wavelengths can decipher some features than others or observe features such as clouds/smoke. For example, The SWIR bands could potentially be useful for discerning differences in bare Earth and telling what is wet and what is dry in a scene. The wavelength that is usually applied on multispectral sensors like NIR band potentially to discern vegetation reflects proven useful in terms of vegetation analysis. From the Sentinel-2, the LULC and NDVI are produced by ArcMap 10.7 software. In other to evaluate the accuracy of LULC, the comparison approach is used to one another based on the extraction of High Resolution of Satellite Imagery from Google Earth Pro created by SASPlanet software and LULC from Sentinel-2. The image processing that emphasizes lineament extraction and edge enhancement is conducted through the PCI Geomatics software. Lineaments, also known as linear features, probably can be faults line, joints, or any kind of boundaries. There are two

common ways of lineament extraction, which are through the visual process by experience or expert persons and the software's digital process. The digital process is chosen for this research where the lineament can be generated automatically from ALOS PALSAR satellite data by PCI Geomatics 2016 software.

To some extent, the edge enhancement delineates linear trends in the satellite image by using a filtering technique. Edge enhancement processes (directional and non-directional filtering) are performed in ENVI 5.3 software, and lineament was extracted with the LINE module of PCI Geomatics 2016. By referring to Salui (2018), the LINE module extracts a linear feature in vector form by using six parameters (RADI, GTHR, LTHR, FTHR, ATHR, and DTHR). The following indicates an explanation of each parameter by Sarp (2005),

RADI (Filter radius): This parameter specifies the edge detection filter (in pixels). Thoroughly determines the smallest detail level in the input image is detected. The data range for this parameter is between 0 and 8192.

GTHR (Gradient threshold): This parameter specifies the minimum gradient level threshold for an edge pixel to obtain a binary image. The data range for this parameter s between 0 and 255.

LTHR (Length threshold): This parameter specifies the minimum length of a curve (in pixels) to be considered as lineament or for further consideration (e.g., linking with other curves). The data range for this parameter s between 0 and 8192.

FTHR (Line fitting error threshold): This parameter specifies the maximum error (in pixels) allowed n fitting a polyline to a pixel curve. Low FTHR values give better fitting but also shorter segments n a polyline. The data range for this parameter is between 0 and 8192.

ATHR (Angular difference threshold): This parameter specifies the maximum angle (in degrees) between segments of a polyline. Otherwise, it is segmented into two or more vectors. It is also the maximum angle between two vectors for them to be linked and the data range for this parameter s between 0 and 90.

DTHR (Linking distance threshold): This parameter specifies the minimum distance (in pixels) between the endpoints of two vectors for them to be linked. The data range for this parameter s between 0 and 8192.

3.3.3 Spatial data analysis

The parameters used to determine the susceptibility level are Aspect, Slope, Curvature, Lithology, LULC, NDVI, distance to the road, distance to drainage, distance to lineament, and Drainage density.

1) Aspect

According to Esri (2016), aspect identifies the downslope direction of the maximum rate of change in value from each cell to its neighbours. Aspect can be thought of as the slope direction. The values of the output raster will be the compass direction of the aspect. Usually, the aspect is often utilized upon the Digital Elevation Model (DEM)

2) Slope

In landslides, the slope is a very influential factor; the higher and more upright slopes, the possibility of avalanches to occur is higher. This is related to the stability of the slope; the steep slope of the slope will experience a greater load pressure until resulting to more unstable in other to withstand the load on it from the influence of gravity. The slope degree also can be related closely to the elevation as classified by Van Zuidam (1985).

Table 3.2: Classification of reliefs based on the slope angle and elevation difference

No	Relief	Slope (%)	Elevation difference (m)	Colour
1	Plain topography	0-2	<5	Green
2	Weak wavy - Strong topography	3-7	5-50	Light green
3	Weak wavy - Hills topography	8-13	25-75	Yellow
4	Strong wavy - Hills topography	0-2	50-200	Orange
5	Hilly - Strong cut topography	14-20	200-500	Light red
6	Strong cut – Highlands topography	21-55	500-1000	Dark red
7	Mountainous/ Highlands topography	>140	>1000	Purple

(Van Zuidam, 1985).

3) Precipitation

The precipitation data is obtained by IDW (Inverse Distance Weight) interpolation technique by interpolating a raster surface of mean rainfall (mm) data from CHRS Data Portal by using point feature of each rainfall station situated in Kelantan (Appendix A). The year of rainfall data from 2014 until 2019 observed from six rainfall observation stations within Kuala Krai region. The observation stations are located at Station Keretapi Kemubu, Station Pertanian Dabong, Station Keretapi Bukit Abu, Ladang Kuala Pergau, Dabong and Ladang Kuala Gris, where it is situated nearby the research region.

4) Lithology

Lithology data were obtained based on the Map of Kelantan (Figure 2.1) and Kelantan geological data in 2003 (scale 1:250,000) from the Department of Minerals and Geoscience Malaysia as well as lithology map of Batu Ban Chuan (scale 1:25,000) from the previous researcher namely Zakiah Ainul Kamal in 2013. Lithology can be a crucial parameter conditioning for landslide occurrences as the different lithological units have various vulnerability to landslides.

5) Land Use & Land Cover (LULC)

The LULC is generated from the comparison between Sentinel-2 satellites within the years 2016 to 2019. It is also considered important as the observation through the satellite for remote sensing data of previous years capable of analyzing the Earth's landform and able to detect changes based on the past and present framework.

6) Normalized Difference Vegetation Index (NDVI)

NDVI is used to obtain land cover data from Sentinel-2 imagery. This method is based on the research conducted on USGS EarthExplorer websites of bands combination.

NDVI values are obtained by comparing the difference between the infrared band and the red band. The satellite image band used band 8 for Sentinel-2, which states the condition of biomass and delineation of water bodies, and band 4, which describes the level of chlorophyll absorption in vegetation.

The resulting attribute is called the NDVI attribute, which describes the condition of land cover. This attribute is then processed using the supervised

classification method with a comparison in observation of vegetation conditions in the field.

Sentinel-2

$$NDVI = \frac{(Band\ 8 - Band\ 4)}{(Band\ 8 + Band\ 4)} \quad (3.2)$$

7) Distance to the roads, distance to drainage, and distance to lineaments

The Euclidean distance tools are used to give an idea of each cell's relationship from a raster format dataset based on the straight-line distance (Table 3.3)

Table 3.3: Application of Euclidean tools from ArcMap 10.7 software.

Euclidean tools	**Description**
Euclidean distance	Distance from each cell in the raster to the closest source. Example of usage: What is the distance to the closest town?
Euclidean Direction	Direction from each cell to the closest source. Example of usage: What is the direction of the closest town?
Euclidean Allocation	Identifies the cells that are to be allocated to a source based on closest proximity Example of usage: What is the closest town?

(Esri, 2016)

8) Soil moisture

The soil map was extracted from SMAP/Sentinel-1 L2 Radiometer/Radar 30-Second Scene 3 km EASE-Grid Soil Moisture, Version 3. This satellite image is processed with parameters of brightness temperature, sigma naught and surface soil moisture. The spatial resolution is 3km x 3km

with data format in HDF5, then converted into raster (.tiff) through the ArcGIS software extension tools.

3.3.4 Analysis of landslide susceptibility regions

1) Susceptibility Mapping

In the AHP method, the following steps are taken (Suryadi, 1998):

I. Defining Problems

In this stage, the problem is determined and will be solved explicitly, in detail, and understood. From the existing problem, the solution is determined that might be suitable for the problem. There can be more than one solution to the problem. These solutions will be solved later in the next stage.

II. Create a Hierarchical Structure

After compiling the main objective as the top level, the hierarchy level below it will be arranged, the criteria suitable for considering or assessing the alternatives were provided, and determining those alternatives. Each criterion has a diverse intensity. The hierarchy continues with sub-criteria (if needed).

III. Make Pairwise Comparison Matrix

The advantage of the AHP method is its ability to combine qualitative and quantitative elements. Quantification of qualitative matters is carried out by providing a pairwise comparison scale. Someone who will give these perceptions must thoroughly understand the elements being compared and their relevance to the intended purpose. According to Saaty (1977), rating scales 1 to 9 are the best based on RMS (Root Mean Square

Deviation) and MAD (Median Absolute Deviation). The values and definitions of qualitative opinions can be seen in Table 3.4.

Table 3.4: Comparative scale in AHP Ratings.

Value	Definition	Explanation
1	Equally important	Two decision elements equally influence the parent decision element
3	Moderately more important	One decision element is moderately more influential than the other
5	Much more important	One decision element has more influence than the other
7	Very much more important	One decision element has significantly more influence over the other
9	Extremely more important	The difference between influences of the two decision elements is extremely significant
2,4, 6, 8	Intermediate judgement values	Judgement values between equally, moderately, much, very much and extremely

(Saaty, 1977)

IV. Calculation of Elemental Weight

The mathematical calculation process in the AHP method is carried out using a matrix. If in an operating subsystem, there are operating elements, namely $\mathbf{A_1, A_2 ... A_n}$, then the results of the comparison of these operating elements form a matrix **A** size n x n, as shown in Table 2.5. Filling in the value of a_{12} uses the following rules:

a) If $\mathbf{a_{12} = \alpha}$, then $\mathbf{a_{21} = 1 / \alpha}$.

b) If between the elements of operations A_1 and A_2 have the same importance, the value $\mathbf{a_{12} = a_{21} = 1.}$

c) Value of $\mathbf{a_{12} = 1}$ for **1 = 2** (diagonal matrix has a value of 1).

Table 3.5: Preference Comparison Matrix

	A_1	A_2	…	A_n
A_1	1	a_{12}	…	a_{1n}
A_2	$1/a_{12}$	1	…	a_{2n}
…	…	…	1	…
A_n	$1/a_{1n}$	$1/a_{2n}$	…	1

V. Calculation of Consistency and Priority Vector

The principle of transitivity or 100% consistency is not a requirement in AHP because the calculation of elements according to decision-makers sometimes changes. In matrix theory, it is known that a small error in the coefficient will cause a small deviation in the eigenvalue. By combining what has been described previously, if the main diagonal of the matrix A is one and if it is consistent, then a small deviation from a_{ij} will still indicate the largest eigenvalue, λ_{max}, the value will approach n, and the remaining eigenvalue will be zero. Deviations from consistency are expressed by the Consistency Index (CI), with the following Equation 3.2:

$$CI = \frac{\lambda_{max} - n}{n - 1} \tag{3.2}$$

Where:

λ_{max} = maximum eigenvalue

n = matrix size

Table 3.6: Random Index (RI) values are based on matrix size

Matrix Size (n)	Random Index (RI)
2	0.00
3	0.58
4	0.90
5	1.12
6	1.24
7	1.32
8	1.41
9	1.45
10	1.49

The CI from the above equation is a matrix of nine scales (1 to 9) and the RI. RI has the values set out in Table 2.6, depending on the matrix's size being compared. The comparison between CI and RI for a matrix is defined as the Consistency Ratio (CR) as seen in the following Equation 3.3:

$$CR = \frac{CI}{RI} \quad (3.3)$$

For the Analytical Hierarchy model, the comparison matrix can be accepted if the value of the CR ≤ 0, 1. Finally, the acquisitive weights were integrated the various causative classes in a single LSI using Equation 3.4 below

$$LSI = \sum_{i=1}^{n} R_i \, x \, W_i \quad (3.4)$$

R_i = groups of ratings, per layer. W_i = weights of landslide conditioning factors. In the resulting LSI map, the landslide susceptibility map's class intervals were categorized into five classes (very low, low, moderate, high and very high) based on the Jenks natural break classification algorithm.

2) Natural Breaks Algorithm for Classification of Landslide Susceptibility

Jenks natural breaks classification is an information order strategy intended to decide the best arrangement of various class values. Computations finish this to limit each class's average deviation from the class average while maximizing deviations between classes. In other words, the natural breaks method seeks to reduce the deviation in the classroom and to maximize the variation between classes (Esri, 1996). In applying this classification method, it requires subjectivity and visual logic. "An important objective by using this method is to minimize the difference in data values in one class. In conducting a semi-qualitative analysis for natural risk mapping, natural breaks classification methods provide satisfying results (Aditya, 2010)." The individual avalanches are commonly small and situated in explicit areas of a slant. Avalanches or landslides happen in an enormous assortment, contingent upon the kind of movement, for example, (slide, topple, flow, fall, spread), the

speed of movement (mm/year-m/sec), the material involved (rock, debris, and soil), and the activating instrument (seismic tremor known as Earthquake, precipitation, human activity).

Overview strategies ordinarily incorporate ground study, aerial or space-borne survey, or a mix. Hands-on work evaluation can be profoundly accurate, however moderate. When hazards or pandemic take place, accessibility is low and cannot be acquired. Therefore, it is impossible to conduct the geological fieldwork in near real-time or complete coverage, especially when confronting the global world crisis like Coronavirus pandemic or any geological hazards.

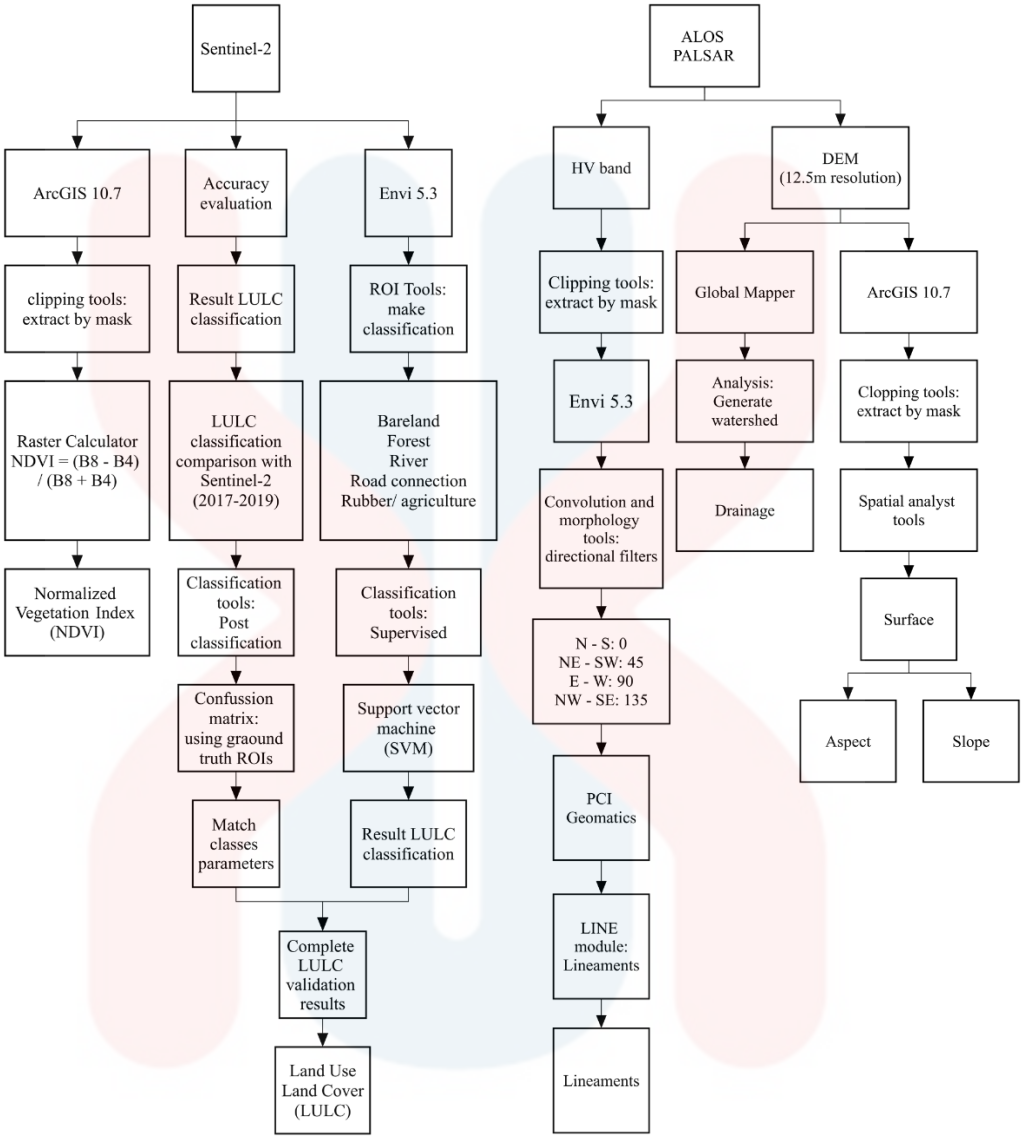

Figure 3.1: Flow chart of Sentinel-2 and ALOS PALSAR

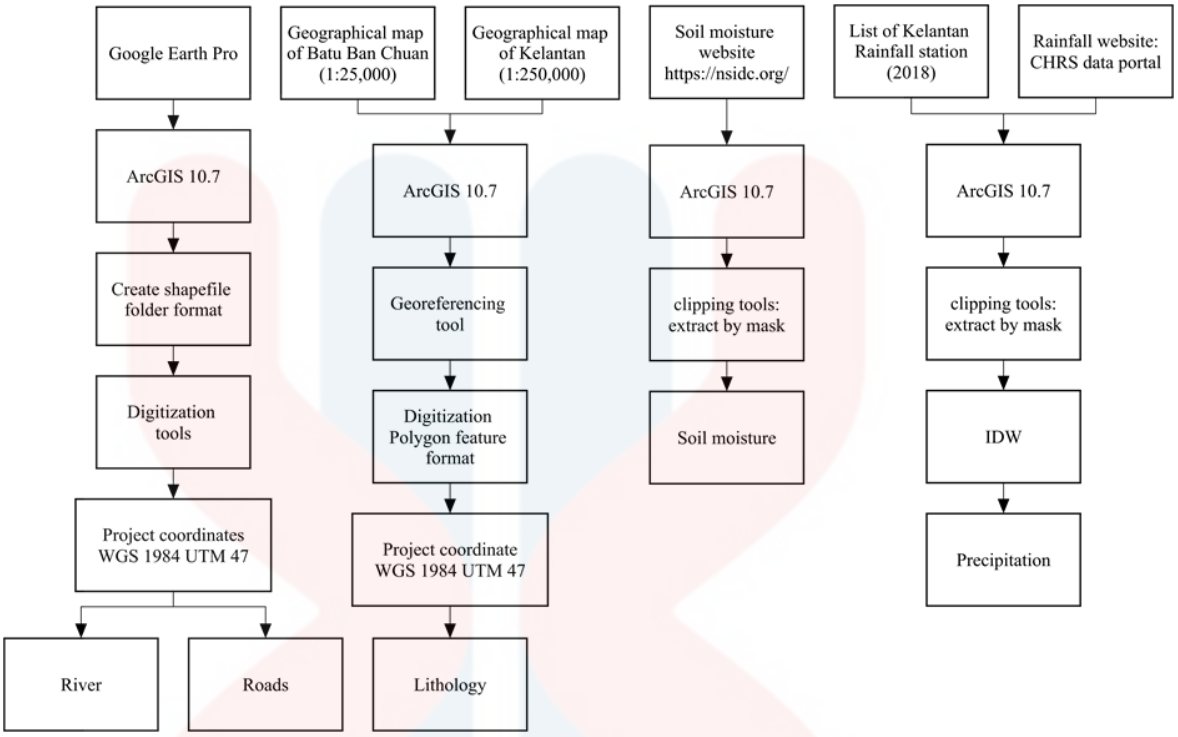

Figure 3.2: Flow chart for the production each of the parameters map

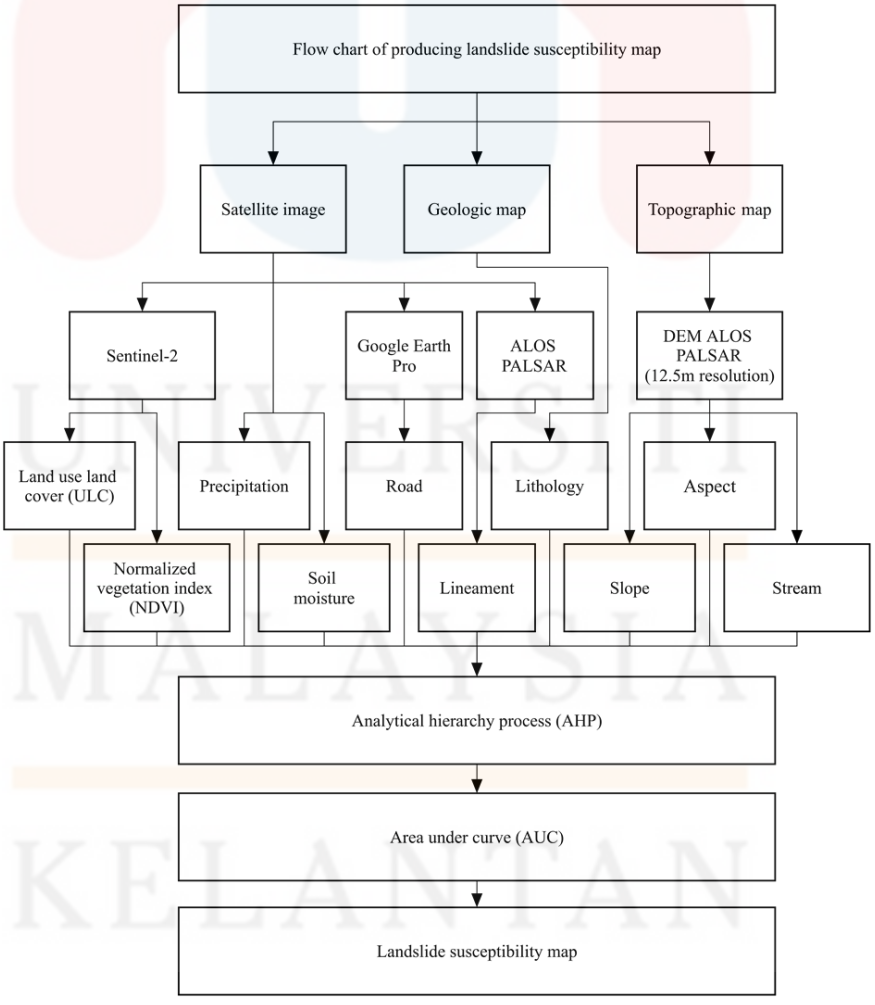

Figure 3.3: Flow chart for the production of landslide susceptibility map

CHAPTER 4

GENERAL GEOLOGY

4.1 Introduction

General geology refers to the chapter that emphasizes research and discussion results comprising geomorphology, stratigraphy, structural geology, and the research area's historical geology. The data discussed in this chapter comprises the previous research study, reconnaissance of remote sensing data, and the application of geographic information systems.

In essence, geomorphology is defined as the science of the Earth's features and the aspects that influence it, including description, classification, and development of the Earth's surface. It includes the study of changes in the shape of the landform, topography, drainage pattern, and weathering process.

Stratigraphy is the study of history, composition, relative age, and distribution of rock layers and the interpretation of rock layers to explain the Earth's history. Based on the results correlations between different layers, studies of lithology (lithostratigraphy), fossil content (biostratigraphy), their relative and absolute age (chronostratigraphy) able to further developed.

The geological structure indicates the architecture of the Earth's crust and the geological phenomena that cause changes in shape (deformation) in the rocks. Usually, it includes the individual structure such as anticlines, thrusts, faults, lineament, and others in a tectonic unit. Structural geology also includes primary and secondary

structures. The geological formation can identify historical geology and the lithology found in the study area.

The four aspects mentioned above are related to each other to conclude the Kampung Dusun Durian geological condition and its surroundings.

4.2 Geomorphology

4.2.1 Landform

Based on Van Zuidam (1985) classification, the research area is categorized as having lowland to hills with an altitude between 50 - 249 meters. The hills spread out within east and west, and plains depicted in the middle from northwest to east and southeast. The research area encompasses the fluvial landform origin and denudational landform origin.

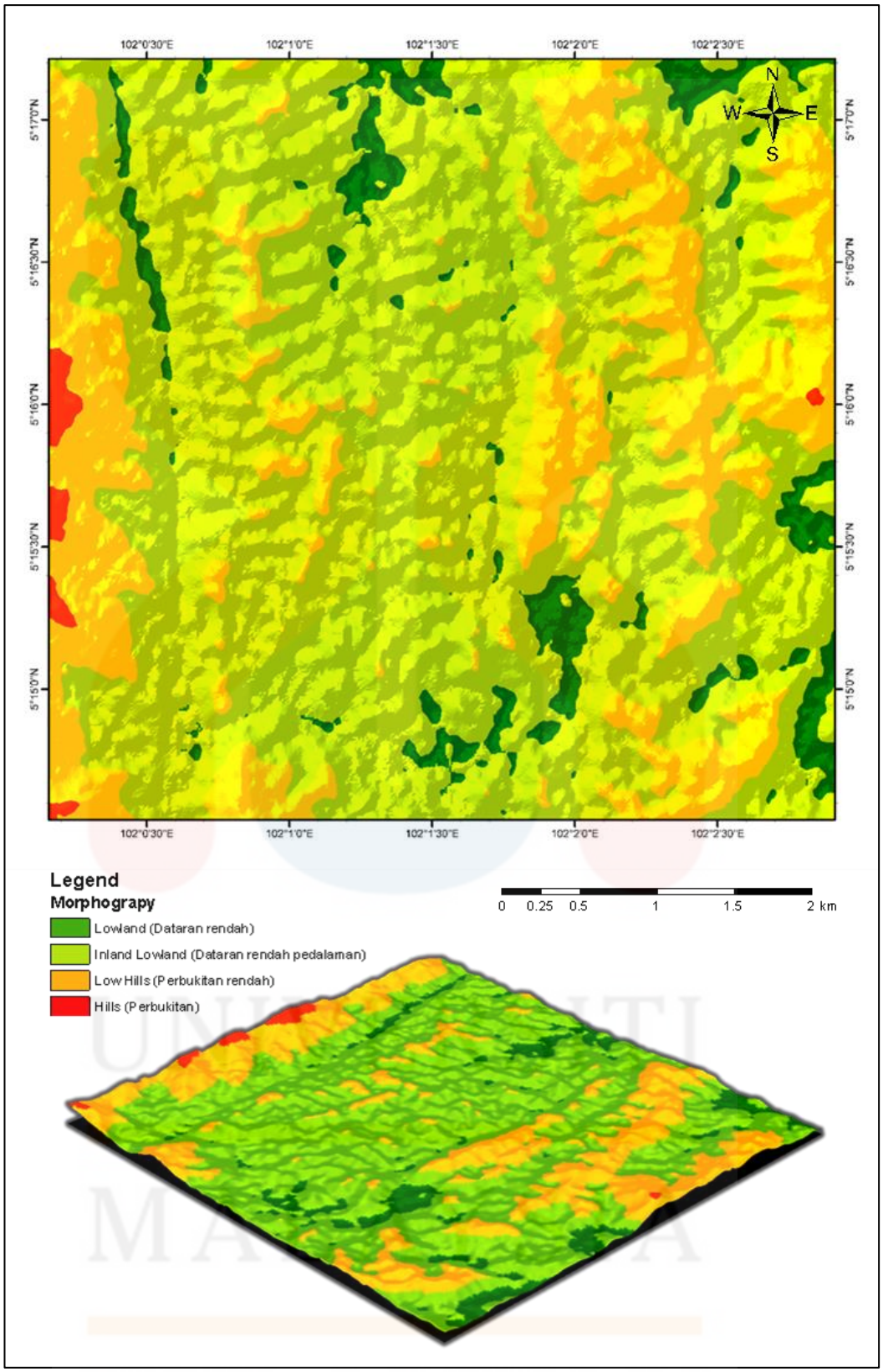

Figure 4.1: Landform map of the study area

Table 4.1: Morphography of research region

Elevation	Morphography	Area (m^2)	Area (%)	Colour
< 50 m	Lowland (Dataran rendah)	1593612.76	6.30	
50 – 100 m	Inland Lowland (Dataran rendah pedalaman	17180217.07	67.87	
100 – 200 m	Low Hills (Perbukitan Rendah)	6348717.61	25.08	
200 – 249 m	Hills (Perbukitan)	190861.52	0.75	

Interpretation of visual images assisted by geological maps, reconnaissance of remote sensing data, and slope maps derived from DEM, the terrain in this area is the result of the fluvial process as well as denudation process. A fluvial landform origin is a geomorphological unit whose formation is closely related to the fluviatile process. Fluviatile process is all processes that occur in nature, both physical and chemical, which result in changes in the shape of the Earth's surface, caused by the river action. Landform formed may occur because of the erosion process and sedimentation process carried by the water surface. Usually, it is composed of fine-grained materials such as clay and silt. The materials that make up the fluvial plain are called alluvium deposits, and if they were compressed, they are called conglomerates.

According to Van Zuidam (1985), the fluvial landform origin can be classified into three classes based on the following given:

1. Flood plain landforms
2. Natural levee landforms
3. Terrace Landforms

As for the research area, it is an active floodplain region found in the Galas River due to both erosion and deposition as well as formed by the action of water that redistributes sediment evenly during repeated flooding. Erosion eliminates any spurs that are interlocked, creating a broad, flat area on the northeast and southeast of the

research region. During a flood season, it deposits the material carried by the river. (as the river loses its speed and energy to transport material). Over time, the height of the floodplain increases as the material is deposited on either side of the river. Floodplains are often agricultural land, as the area is very fertile because it is made up of alluvium (deposited silt from a river flood). The floodplain is often a wide, flat area caused by meanders shifting along the valley. Floodplain Landforms Have 3 Main Characteristics:

1. A generally flat area of land
2. Borders a river
3. Floods when the river is exceptionally high

The denudational landform origin resulted from weathering, erosion, rock, and soil downslope movement under the influence of gravity (mass wasting) and deposition processes. Typically, it occurs because of aggradation or degradation. The degradation process tends to cause a deterioration in the Earth's surface, while aggradation causes an increase in the Earth's surface. The research region's weathering process is identified through aerial photography, and remote sensing data then classified according to the following factors.

1. Type of rock (mineral content, fracture, bedding plane, and fault). Resistant rocks are slowly exposed to external processes, so they are not easily weathered, while rocks that are not resistant are the opposite. Examples;
    a. limestone is more resistant to dry climates but not resistant to wet climates
    b. Granite is more resistant to wet climates but not resistant to dry climates.

2. Climate, especially temperature and rainfall, are significantly affect weathering. Examples:
    a. Arid climate, the type of weathering is physical
    b. Humid climate; the type of weathering is chemical
    c. Cold climate, the type of weathering is mechanical
3. Vegetation, or plants, have a significant role in the weathering of rocks.
    a. The roots of the plants penetrate the rock, increasing in length and enlarge, causing the rock to break.
    b. Chemically, plants, through their roots, release chemical substances that can accelerate the weathering of the rocks. The decomposing roots, stems, and leaves contribute to the weathering process due to the rotting parts of the plant able to release chemicals that further break down the rocks' chemical composition.
4. The topography with a large slope facing the direction of the sun or rainfall able to accelerate the weathering process.

Mass wasting is the displacement or movement of rock or soil masses on a slope by the influence of gravity or saturation of water masses. Some consider mass wasting as part of erosion, and some are separating it. It is easy to comprehend because it is easy difficult to separate clearly because, in erosion, the rock's gravity also works. In rocks containing water, mass wasting is smoother than in dry rock. The difference is that in mass wasting, water is only a small amount and its function is not as a carrier, but only to help smooth the movement. Meanwhile, in erosion, it is necessary to have transport power. The Earth's gravity causes the movement of rock masses.

Erosion is a geomorphological process, namely the process of releasing and transporting Earth's material by geomorphological forces as well as forces of water,

wind, or gravity. Factors that influence soil erosion include the nature of rain, the slope of the drainage pattern, land cover crops, and the soil's ability to withstand dispersion even to absorb and then seep water into deeper layers.

There are denudational hills in the research area with hilly and undulating topography with slopes ranging from 15 to <55%, with a height difference (local relief) between 50 to < 249 m. Generally, it is eroded moderately to small, depending on the conditions of lithology, climate, land cover vegetation, and land use. Besides, there is the presence of pediment and piedmont around the study area.

In geology, the pediment is defined as the relatively flat surface of bedrock (exposed or veneered with alluvial soil or gravel) that occurs at the base of a mountain or as a plain having no associated mountain. Though features characteristic of pediments attains their fullest development in arid regions, bevelled bedrock surfaces also occur in humid areas. For example, in the tropics, the surfaces tend to be mantled with soils and obscured by vegetation. Many tropical towns sited on pediments (which offer more specific building sites than the steep hillsides above or the river marshes below) show severe gullying where the water flow has been concentrated between walls and buildings. Besides, the piedmont is a gentle slope leading from the foot of mountains to a region of flat land.

4.2.2 Drainage Pattern

The drainage flowing in the study area comprises the Galas River's tributaries, which are located in the northeast and southeast research region. A river that meets another river can form a particular drainage pattern based on the surrounding area's geological conditions. Water flowing from the north-south of the study area, the Galas

River has several drainage patterns consisting of the Sub-Dendritic, Dendritic, and Trellis.

The Sub-Dendritic drainage pattern is characterized by the shape of a river that forms spreading branches like shady trees. The sub-Dendritic pattern is a modification of the dendritic pattern, and the angle between the tributaries was smaller than the dendritic drainage pattern in general. This drainage pattern characterizes landforms that are influenced by the structure and affected by changes in topography. It consists of sloping topography, and the lithology is classified within resistant to moderate. This drainage pattern develops in the middle and occupies about 9.57% of the study area. As a whole, it is composed of Interbedded sandstone, siltstone, and shale

The Dendritic pattern usually indicates patterns of a river where tributaries tend to align with the main river. Tributaries lead to the main river with an acute angle. The dendritic pattern model is like a tree with branches and twigs as branches and tributaries. This pattern is usually found in areas with a plain landform or similar rock areas (uniform, homogeneous) with a wide distribution. Usually, it reflects the resistance of the rock, which is not hard. Interpreted as areas that have low relief, horizontal layer, and areas control by faults are not developed. The drainage pattern covering 66.09% of the study area is dominated by Interbedded sandstone, siltstone, and shale. In the other part of the research area, phyllite and schist can be found in the northwest and southwest, granite in the west part, and limestone in the east part.

The drainage pattern of Trellis is characterized by a river that is shaped like a ladder with relatively equal angles between tributaries and the main river. This flow pattern indicates an elongated and parallel landform. It is found in the active area of the structure and consisting lithology within resistant to moderate. The drainage

pattern covers 28.8% of the study area, and the majority comprised of granite, as well as minor in limestone and interbedded sandstone, siltstone, and shale.

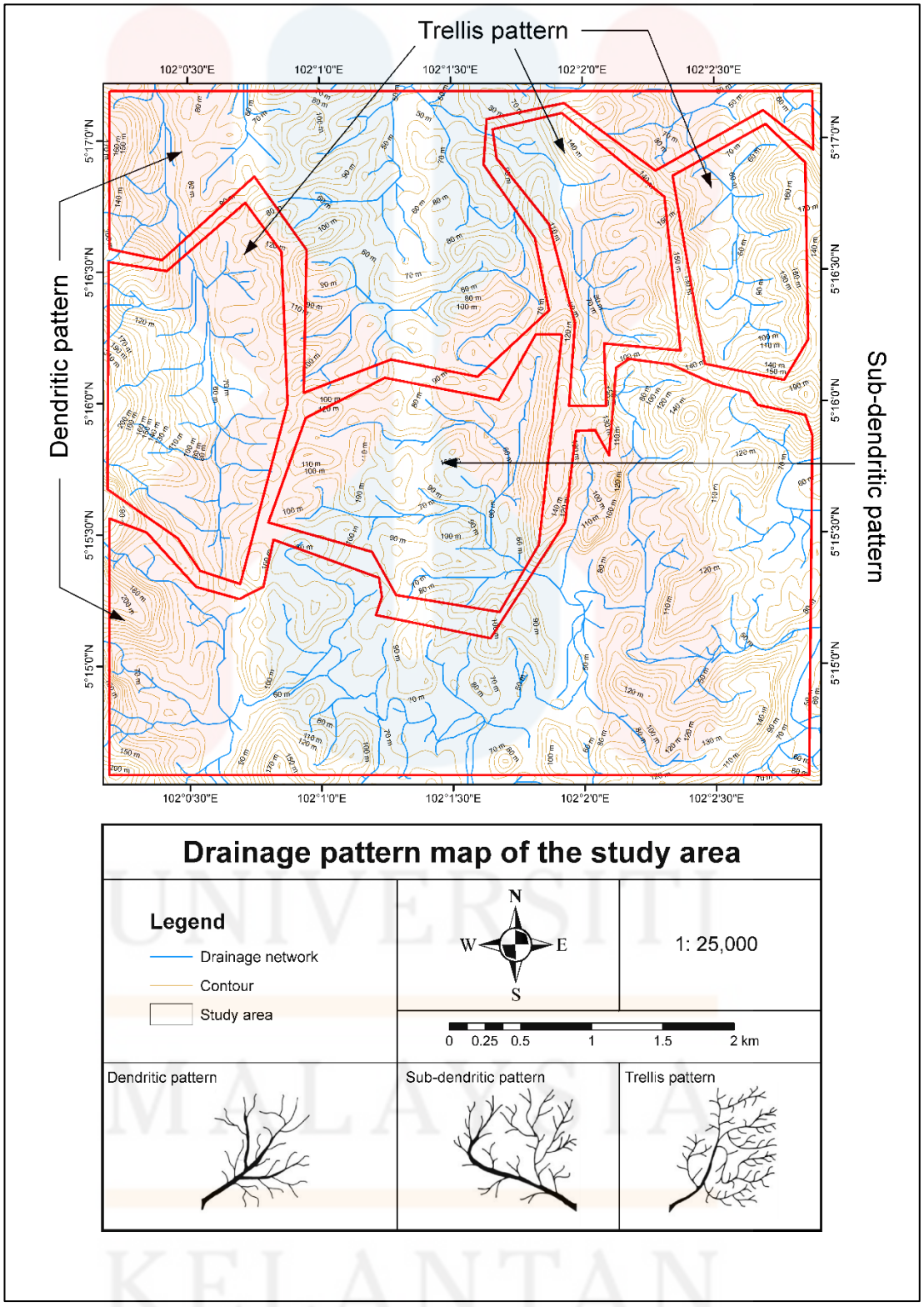

Figure 4.2: Drainage pattern map of the study area

HUMID	
TOPOGRAPHY	DRAINAGE
Uniform slopes	Dendritic: medium
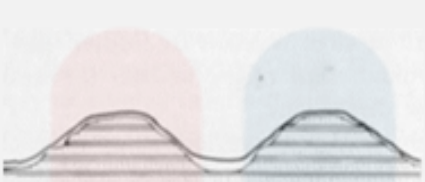	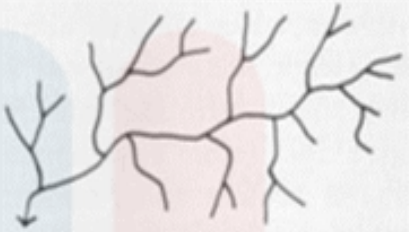
Thin, interbedded sedimentary materials do not have terraced slopes, although faint banding may be observed. Sandstones have steeper slopes than shale or limestone masses. Hilltops throughout such regions have approximately the same elevations.	The drainage pattern in thin, interbedded sedimentary rocks is dendritic and of medium texture, similar to shale drainage in humid climates. The presence of shale in the interbedding, however, increases surface runoff, resulting in a more dissected topography.
TONE	VEGETATION AND LAND USE
Medium grey	Cultivation and forested
Since the beds are thin usually covered with residual soil which masks their tonal differences, an overall medium grey tone results.	Gentle slopes, hilltops, and valley are cultivated, while steeper slopes facing the drainage system are in forest cover. The beds are too thin for differences in vegetation preference to be easily observed. Highways tend to follow major valleys and ridgelines, to be curvilinear, and are controlled by the drainage system.
GULLIES	
Sag and swale	
Gullies found in these regions are of the sag-and-swale type, indicating cohesive soils.	

Figure 4.3: Sedimentary rocks: thin interbedded in humid and arid (Van Zuidam, 1985).

HUMID	
TOPOGRAPHY	DRAINAGE
Parallel ridges	Trellis and dendritic
	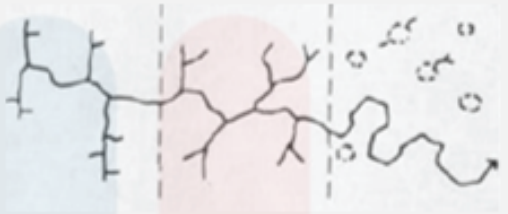
In sandstone- shale combination sandstone forms resistant, sharp, parallel ridges, shale forms soft, rounded hills in the lowlands. Limestone-shale forms low, rounded hills in shale formations, and karst topography with rounded or oval sinkholes in limestone areas. Thin beds give the ridge topography a sawtoothed appearance.	In mos situations a trellis drainage pattern of medium to fine texture exists, controlled by the tilted rock structure. Interbedded limestone and shale may have a dendritic pattern and solution topography with internal drainage. Stream courses are generally located in shale lowlands; if they are located in limestone lowlands, some angularity should occur as a result of jointing influence.
TONE	VEGETATION AND LAND USE
Faint banding	Forested and cultivated
Faint bands of total difference relate to the tones of the different rock materials. These tones may be masked by the residual soil.	Vegetation and land use relates to the types of interbedded rock materials. Sandstones are very rugged, with steep slopes, and have forest cover; shale, with softer hills, has forest cover and or cultivation; limestone is typically cultivated. Roads and major development patterns are concentrated in the valleys.
GULLIES	
Vary	
Gully cross sections relate to the surrounding residual soils. Generally, sag-and-swale gullies are found in shale and limestone. Gullies with steeper sides may indicate sandstone.	

Figure 4.4: Sedimentary rocks: Tilted, interbedded in humid and arid (Van Zuidam, 1985).

<table>
<tr><td colspan="2">HUMID</td></tr>
<tr><td>TOPOGRAPHY</td><td>DRAINAGE</td></tr>
<tr><td>Bold, domelike hills</td><td>Dendritic: medium</td></tr>
<tr><td>  </td><td> 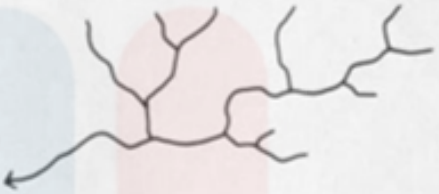 </td></tr>
<tr><td>The topographic relied of granitic intrusions typically shows as massive, rounded, domelike hills. The tops of the hills are softly rounded, the side-slopes are steeper. The weathering processes of presure-release and exfoliation tend to maintain the domelike appearance. Debris and large boulders weathered into rounded shapes accumulate in drainage courses and depressions.</td><td>A dendritic drainage pattern of medium texture is common in humid climates and indicates the uniform materials of which the forms are made. The domelike hills cause curvilinear alignments to develop, and these are important evidence in the identification of granite. Intersections of tributaries occur at right angles or may be slightly acute upstream.</td></tr>
<tr><td>TONE</td><td>VEGETATION AND LAND USE</td></tr>
<tr><td>Uniform dull grey</td><td>Cultivated and forested</td></tr>
<tr><td>The uniform composition of granite is reflected in its overall uniform soil tne which varies in colout from dull to light grey. Fracture zones may be identified by linear, dark-toned areas.</td><td rowspan="3">Nonglaciated regions are characterised by cultivation on the gently rolling hilltops and forests on the steeper slopes. Settlement patterns occur either on hilltops or in the major valleys. Glaciated regions typically have thin soil profiles over bedrock; their rugged topography is too severe for traditional, intense land uses. These areas are generally forest-covered.</td></tr>
<tr><td>GULLIES</td></tr>
<tr><td>U-shaped</td></tr>
<tr><td>The residual soils developed from granite in humid climates show a U-shaped gully cross section, indicating a moderately cohesive, sandy-clay soil</td><td></td></tr>
</table>

Figure 4.5: Intrusive igneous rocks: Granitic forms (Van Zuidam, 1985).

<table>
<tr><td colspan="2">HUMID</td></tr>
<tr><td>TOPOGRAPHY</td><td>DRAINAGE</td></tr>
<tr><td>Rounded crests, steeps sideslopes</td><td></td></tr>
<tr><td>  </td><td> 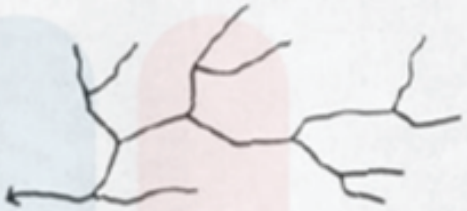 </td></tr>
<tr><td>In humid climates schist formation develop deep redual soils reflected by rounded hills with steep sideslopes. The overall appearance of the topography is that of smooth, undulating hills.</td><td>A rectangular, dendritic drainage system of medium to fine texture, having many long, deep, parallel gullies, develops in humid climates. The drainage pattern is developed and controlled by the parallel foliation structure of the parent material, whose weaker materials are more easily eroded to form valleys and whose more resistant materials form ridges.</td></tr>
<tr><td>TONE</td><td rowspan="5">VEGETATION AND LAND USE
Cultivated and forested
In humid climates schist formations may occur entirely in forest cover or in a combination of cultivation and forest cove, depending upon the degree of dissection of the topography. Typically, the rolling hilltops are cultivated and the steeper slopes facing the drainage system are forested. Contour farming may be practiced, indicating highly erosive residual soils.</td></tr>
<tr><td>Uniform light greys</td></tr>
<tr><td>In humid climates uniform light greys are observed unless obscured by vegetation cover.</td></tr>
<tr><td>GULLIES
Parallel, U-shaped</td></tr>
<tr><td>Many parallel, U-shaped gullies occur, indicating sandy or mica fragments within the residual soil. Gullies are dark, contrasting with tones in surrounding fields.</td></tr>
</table>

Figure 4.6: Metamorphic rocks: Schist of humid (Van Zuidam, 1985).

4.2.2 Valley Types

The surface of the Earth, which has an area of surface water runoff, will form valleys. At first, surface water runoff erosion in the form of sheet erosion becomes real erosion, gully erosion, valleys, and valleys as a reservoir for water flow to become rivers. Surface water runoff that enters the valley always carries the sediment load resulting from the water's erosion, and then the river carries the sediment load to be deposited in a particular area (basin) into the sediment. The types of valleys divided based on the following:

1. U blunt valley type
2. U sharp valley type
3. V blunt valley type
4. V sharp valley type.

The blunt U-valley type occurs in relatively flat areas; the ongoing erosion tends to be lateral (side), and vertical erosion (river bed) is relatively non-existent. Erosion to the vertical has stopped because it has reached the river bedrock, which is relatively hard compared to the rocks that are on the river bank. The sharp U valley type occurs in areas that have a gentle slope, lateral erosion (sideways) is more significant than vertical erosion (towards the river bed), sediment collection (accumulation) takes place from the slopes of the valley.

The blunt V valley type occurs in areas with gentle to slightly steep slopes, vertical erosion (towards the river bed) is more potent than lateral erosion (towards the side), which is accompanied by erosion from the top of the valley slope and accumulation (accumulation). Sediment (sediment) occurs at the bottom of the valley. The shape of the blunt valley V is asymmetrically due to the differences in rock types or structures on one side of the valley. The sharp V valley type occurs in areas that

have steep slopes. Vertical erosion (towards the river bed) is very strong due to the tectonics influence. Rock and climatic conditions greatly influence the formation of the sharp V valley type.

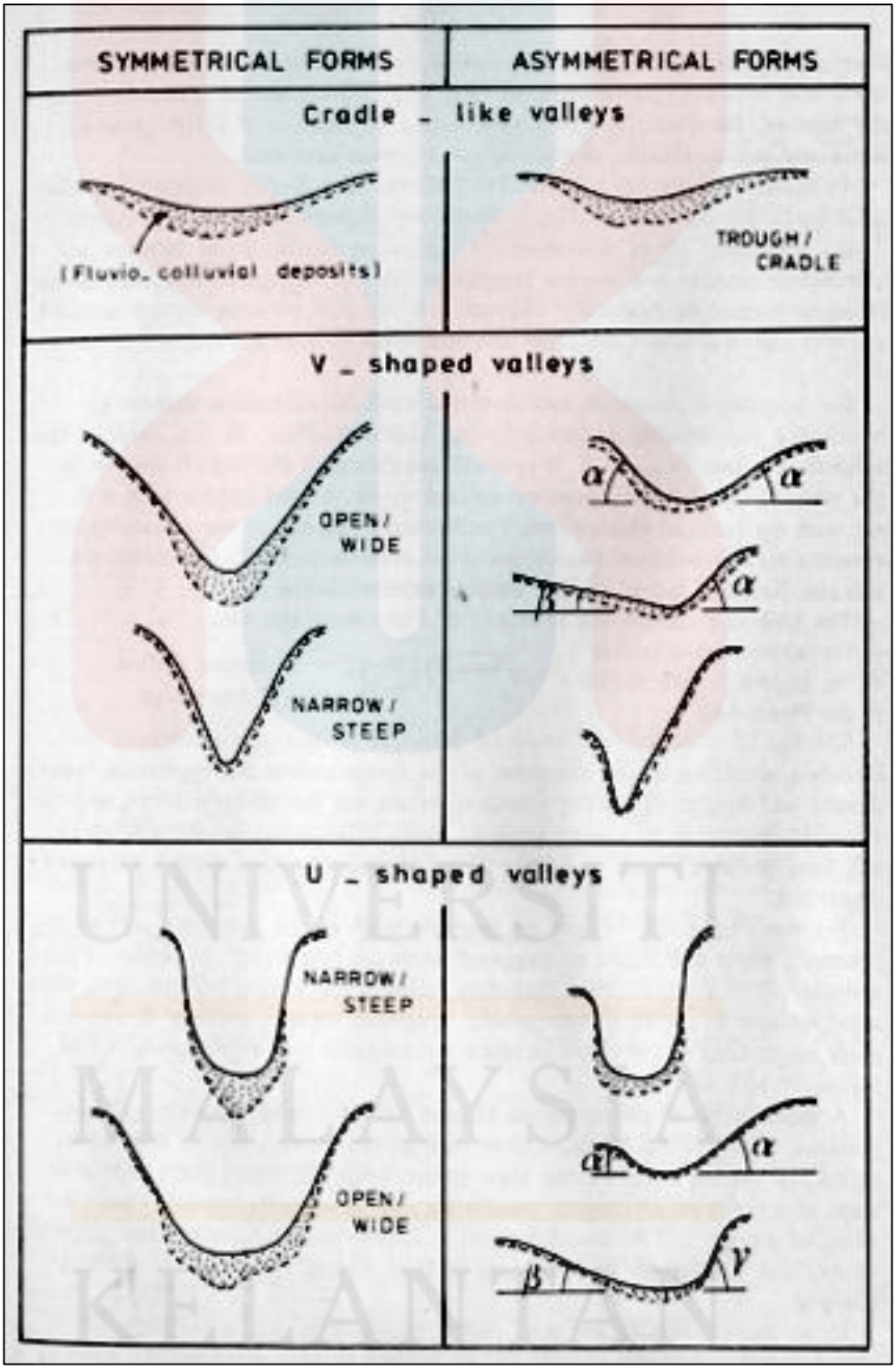

Figure 4.7: Valley types (Van Zuidam, 1985).

4.2.3 Geomorphological Unit of Research Area

The study area is divided into three geomorphological units, namely:

1. Plain Geomorphological Unit
2. Sloping Geomorphological Unit
3. Steep Geomorphological Unit

The plain geomorphological unit has an area that covers 6.3% of the entire study area. This geomorphological unit is marked with colour from dark green to light green based on the study area's relief classification. The flow pattern in this geomorphological unit is dendritic, and the elevation ranges from 0 - 50 meters, and the slope is (2-7%). The shape of the river valley in the geomorphology unit is U-shaped, indicating that the erosion stage that develops relatively mature tends to be trending laterally. The lithology that composes the morphology of the plain is sandstone, siltstone, and shale.

The sloping geomorphological unit has an area that covers 36.03% of the entire research area, which is marked with yellow colour based on the relief classification of the study area. The flow pattern in this geomorphological unit is dendritic and Trellis. Elevations range from 50 - 75 meters, and the slope is (7-15%). The lithology that makes up the sloping morphology comprises igneous rocks, sedimentary rocks like (limestone, marble) and interbedded sandstone, siltstone, and shale. The shape of the river valley in this unit is U-shaped, indicating that the erosion stage that develops is relatively mature and tends to be lateral in this unit.

The steep geomorphological unit has an area that covers 57.67% of the study area. This geomorphological unit is marked with colour from light red to dark red based on the study area's relief classification. The elevation is around 75 – 249 meters, and the slope is around (15 - 30%), with dendritic flow patterns and U-V valley forms.

The lithology that makes up this geomorphological unit is igneous rocks and metamorphic rocks (Phyllite, slate, shale).

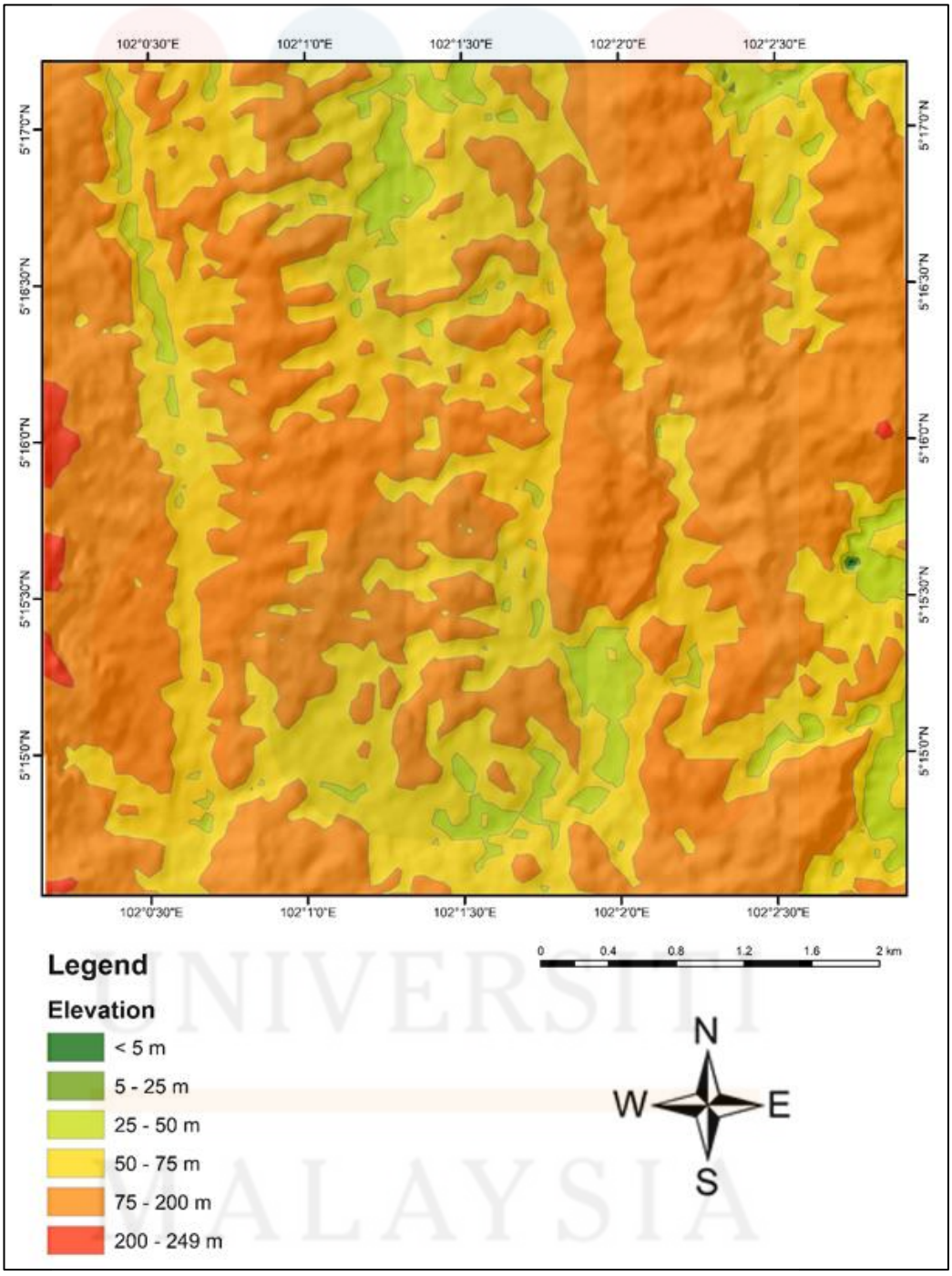

Figure 4.8: Relief classification map of the study area

Table 4.2: Elevation concerning relief classification of the study area

No	Elevation	Area (m^2)	Area (%)
1	< 5 m	1888.86	0.01%
2	5 – 25 m	6689.45	0.03%
3	25 – 50 m	1585034.45	6.26%
4	50 – 75 m	9119719.23	36.03%
5	75 – 200 m	14409018.46	56.92%
6	200 – 249 m	190861.52	0.75%

Table 4.3: Classification of reliefs based on the slope angle and elevation difference

No	Relief	Slope (%)	Elevation Difference (m)	Colour
1	Plain Topography	0 – 2	< 5	Green
2	Weak Wavy Topography	3 – 7	5 – 50	Light Green
3	Weak Wavy – Strong Topography	8 – 13	25 – 75	Yellow
4	Strong Wavy - Hills Topography	14 – 20	50 – 200	Orange
5	Hilly - Strong Cut Topography	21 – 55	200 – 500	Light Red
6	Strong Cut - Highlands Topography	56 – 140	500 – 1000	Dark Red
7	Mountainous/ Highlands Topography	> 140	> 1000	Purple

(Van Zuidam, 1985)

4.3 Stratigraphy

Stratigraphy is one of the branches of science in geology, especially to explain the rock formation cycle and the relationship between one rock segment/layer with other layers. Stratigraphy makes it easy for researchers to determine the geological conditions of an area concisely. It encourages to reveal more other geological information, such as structures, geological age, depositional environment, and the area's chronology and evolution. Lithostratigraphy is one of the sub-disciplines of stratigraphy, where it involves the analysis of the rock layer and explains the relationship between them.

4.3.1 Lithology

There are six main lithologies found in the study area. The following depicted the types of lithology found in the research region.

1. Alluvium

   The alluvium is a substance that rivers have deposited. It typically occurs most widely in the lower part of the river's course, Floodplains and deltas forming. But it can be deposited at any stage where the river flows over its banks or where a river's speed is examined. The alluvium is made up of silt, sand, mud, and gravel, also possessing a large deal of organic matter.

2. Granite

   Granite is found to be a common form of intrusive, felsic, phaneritic textured igneous rock. Granite consists predominantly of minerals such as quartz, mica, feldspar and ferromagnesium. Granite situated on the west below the Stong Complex is found in the study area.

3. Interbedded sandstone, siltstone and shale

From the study area map, interbedded sandstone, siltstone, and shale extended from the middle of the study area to the east. This is listed under sedimentary rock

4. Limestone

The higher percentage of lithology contained in the area comprises interbedded sandstone, siltstone and shale. The limestone is a sedimentary layer, primarily consisting of calcite ($CaCO_3$). Via precipitation, limestone forms in soft, shallow seas and sometimes contains marine fossils. Limestone outcrop of the Batu Ban Chuan cave is unique as it takes place as a single outcrop, separated from other limestone hills such as Gua Musang.

5. Phyllite and Slate

The parent rock that undergoes the process of metamorphism to form phyllite and slate is shale. Phyllite, on the other hand, typically develops from slate. Shale consists of minerals of clay, and ideal temperature and pressure are metamorphosed into slate over time.

6. Acid to intermediate volcanic (pyroclastic, rhyolitic to dacitic composition)

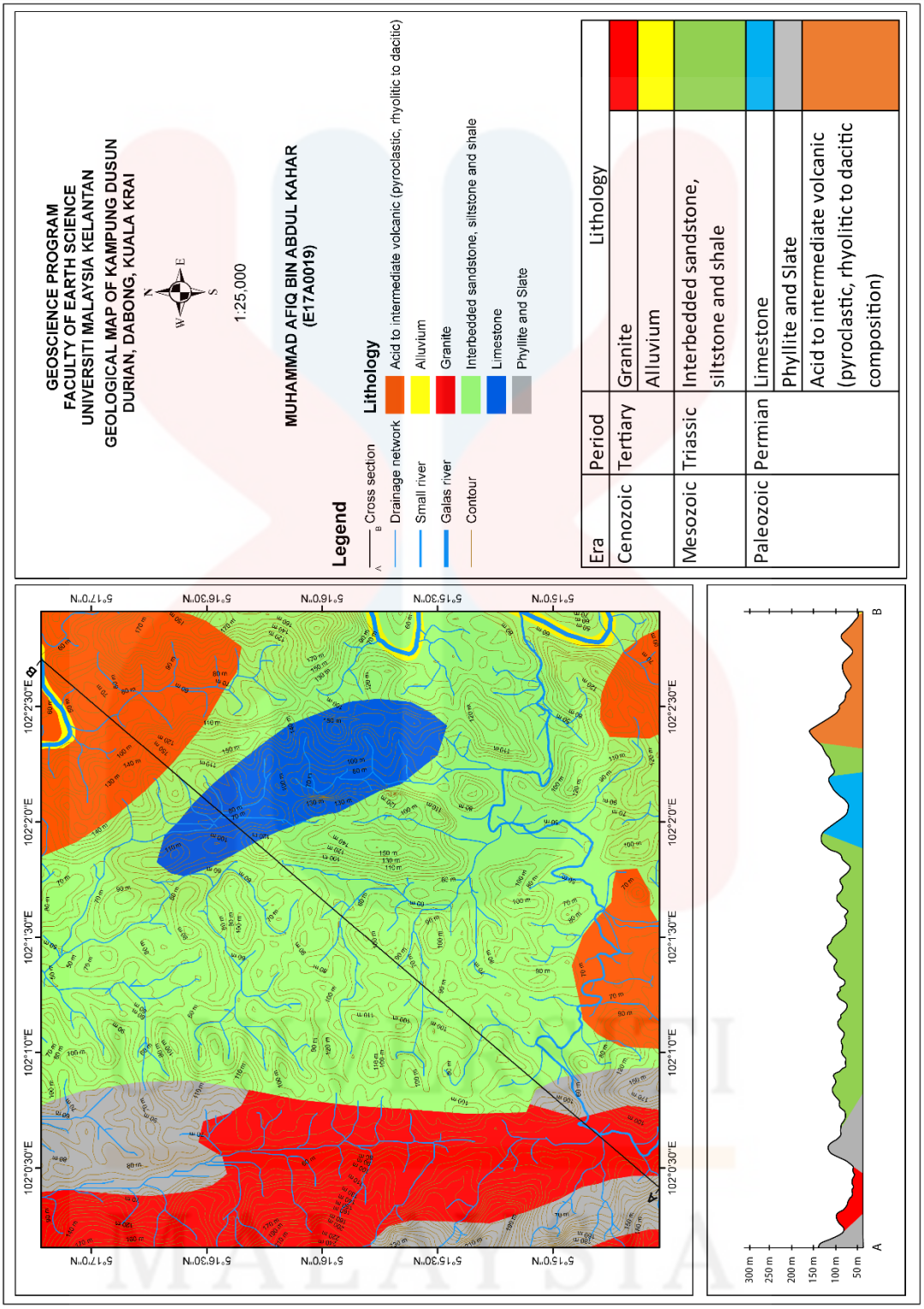

Figure 4.9: Geological map of the study area

4.4 Structural Geology

4.4.1 Lineament extraction

The lineaments are produced based on the PALSAR imagery, where the unstable terrestrial surfaces were identified on the PALSAR image, and the length of the lineament is variable, depending on the slope and aspect of the ground surface. In this study, directional filters were used to enhance specific linear trends based on four principal directional filters; N–S: 0°, E–W: 90°, NE–SW: 45° and NW–SE: 135° with 7 x 7 kernel size. The algorithm produces the image input's first difference in the horizontal, vertical, and diagonal directions. The HV polarization is more suitable for lineament extraction and edge enhancement in tropical environments than other polarization channels because cross-polarization is more sensitive to lineaments and enhances penetration. The 7 x 7 kernel matrix was applied to fine and Polarimetric scenes for enhancing semi-smooth and smooth/rough features. Figure 4.4 illustrated ways of lineament extraction: digital and visual processes (Khanh, 2009).

Visual process	Digital process
Depends on the quality of the image	Depends on the quality of the image
Depends on the complexity of the research area	Totally depends on the complexity of
Strongly depends on human experience	Totally depends on the function of the software
Takes a lot of time	Very quickly
Strongly effected by human subjectiveness	Little effected by human subjectiveness
Easy to distinguish the kind of lineament (tectonic	Can not recognize the kind of lineament, so the result
Simple but subjective	Complex but objective

Table 4.4: The characteristic of an image from the visual and digital perspective (Khanh, 2009).

4.4.2 Edge detection

The edges are characterized by small variations in brightness that can be difficult to identify. Typically, the linear features are created by the edges. Digital filters have been developed primarily to improve images' edges, which fall into two categories: non-directional and directional filters. Both of them can be found from convolutions and morphology extension tools inside Envi software. As for the research

analysis, the directional filters are selected compared to the non-directional filters (Laplacian filters) due to the capability of better enhancing specific linear trends from the satellite imagery and identify linear features of almost any orientation of the satellite imagery, especially for the HV band of an ALOS PALSAR.

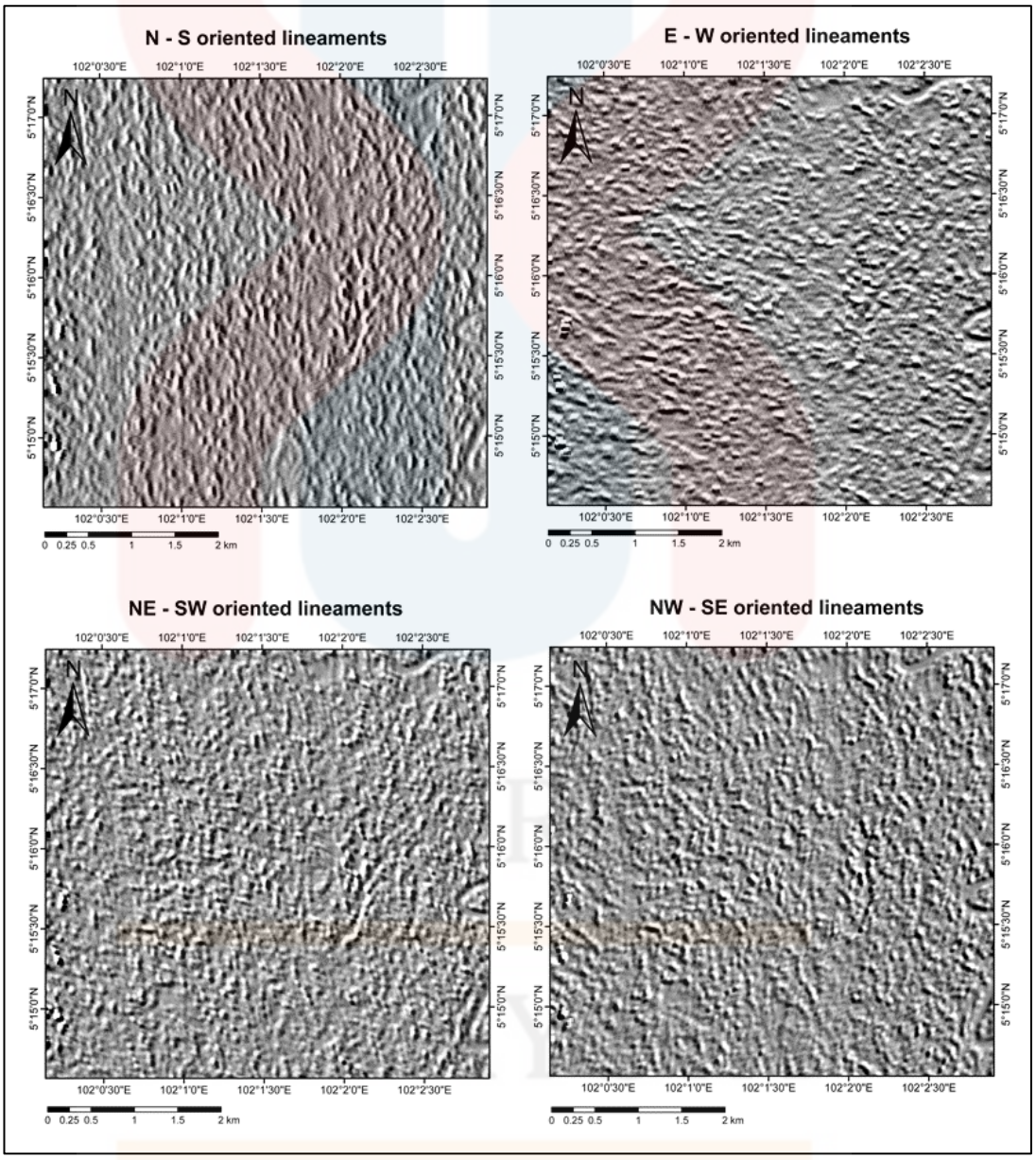

Figure 4.10: Four subset filtered images derived from HV band of ALOS PALSAR

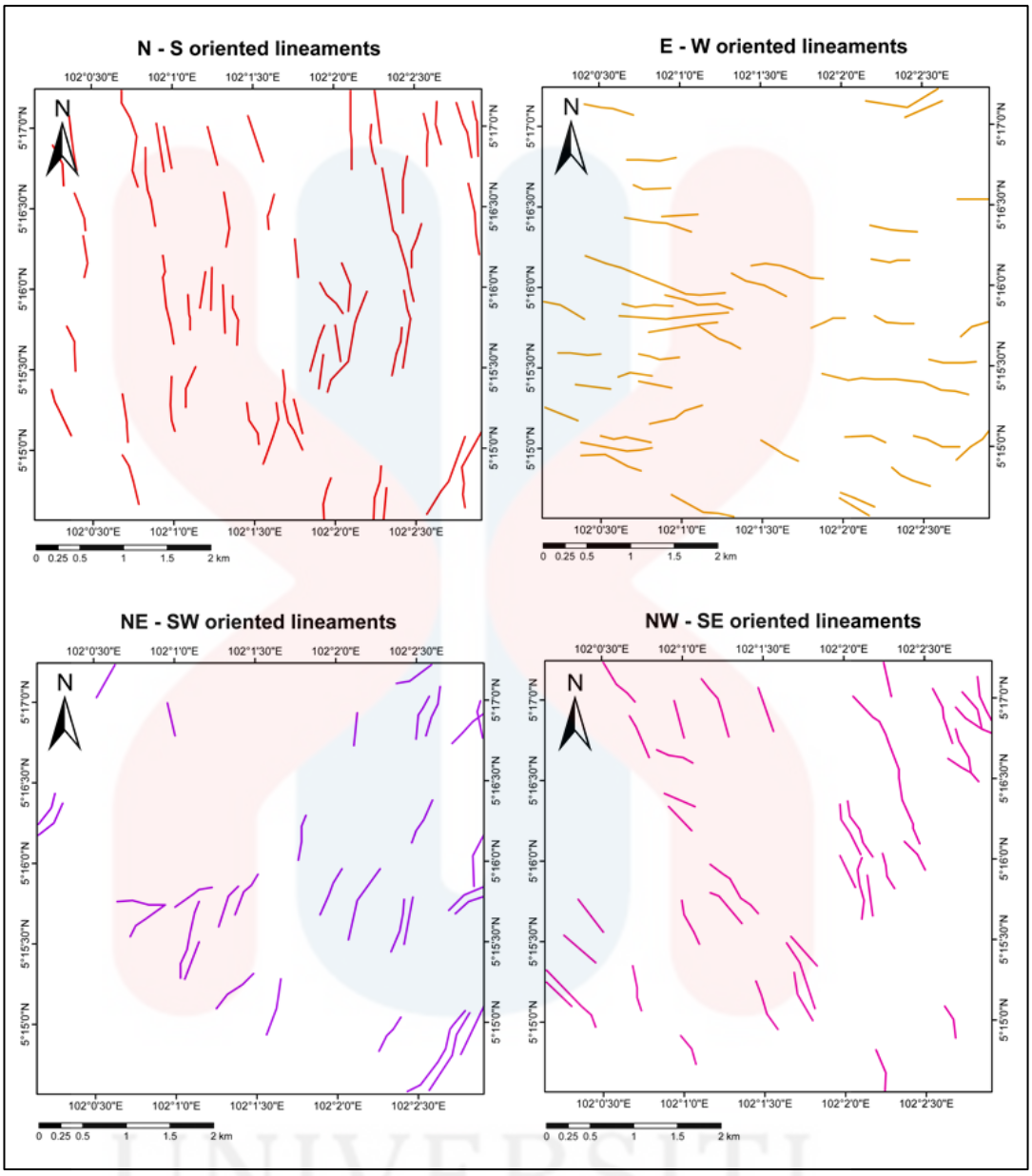

Figure 4.11: Four subset linear features images oriented in a specific direction by automatic extraction of PCI Geomatics software.

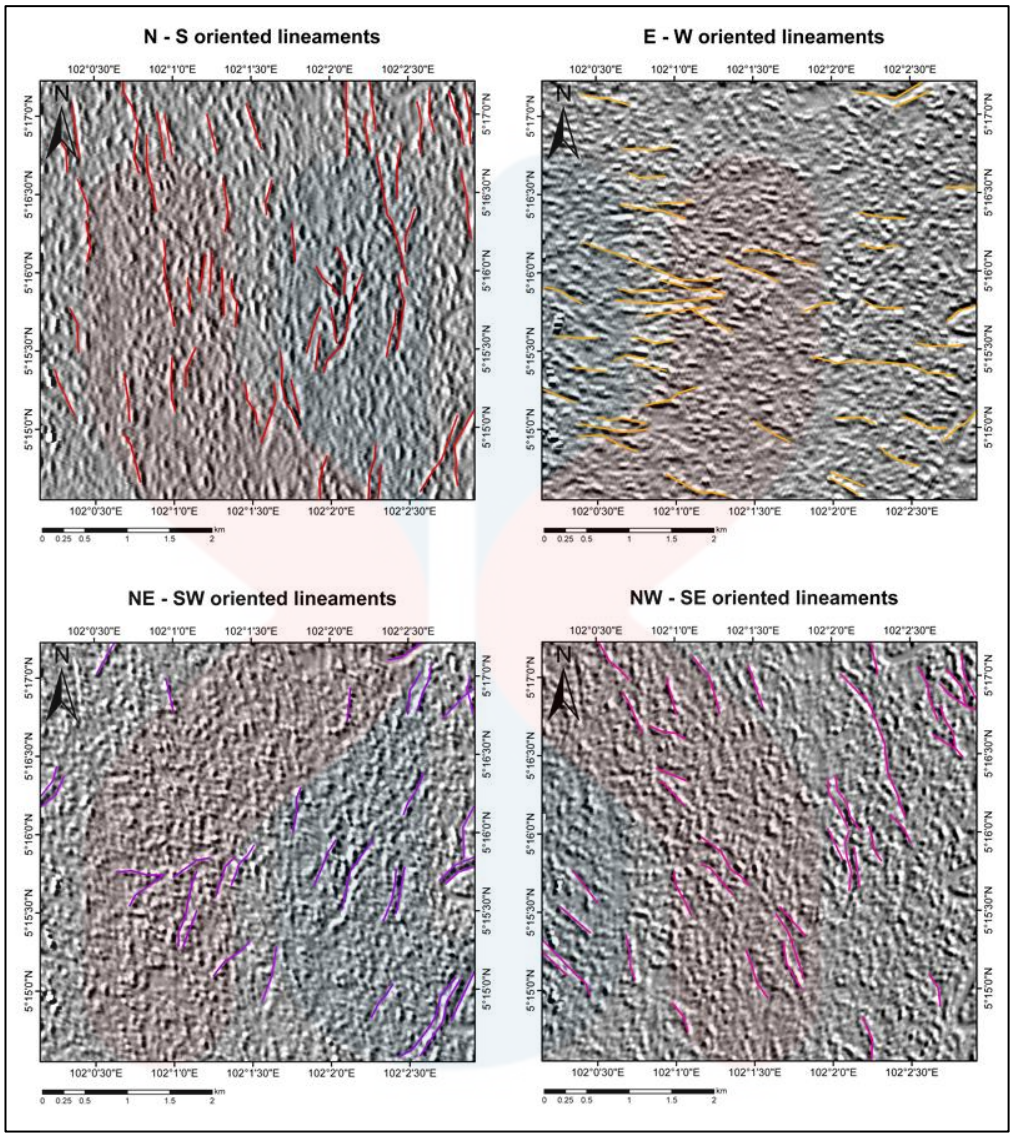

Figure 4.12: The amalgamation of four subset linear features with four subsets filtered for HV band of ALOS Palsar

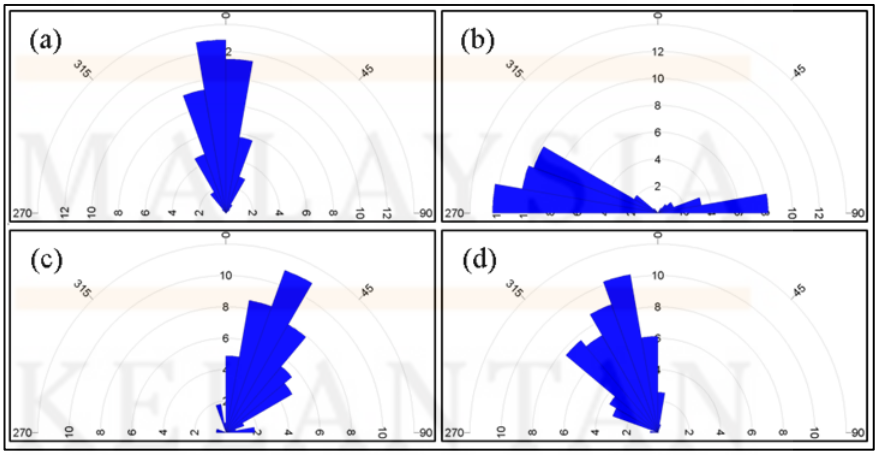

Figure 4.13: Rose diagram for (a) N–S: 0°, (b) E–W: 90°, (c) NE–SW: 45° and (c) NW–SE: 135° of a different direction

4.5 Historical Geology

Previously, Peninsular Malaysia was regarded as upon the NNW-SSE longitudinal belts due to the tectonic evolution, mineralization, stratigraphy, geological history, and geological structure. There are many theories in classifying Malaysia's Peninsular (Scrivenor, 1928; Khoo & Tan, 1983). There is a threefold section of Peninsula: Western Belt, Central Belt, and Eastern Belt due to the different interests, for Scrivenor (1928) the minerals interest while for Khoo and Tan (1983) the differences in stratigraphy and geological history within Peninsular Malaysia interest. Meanwhile, Hutchison (1977) argues that there are four major tectonic of Peninsula; Western Stable Shelf, Main Range Belt, Central graben, and Eastern Belt based on the distinction of tectonic histories.

According to Khoo and Tan (1983), the Central Belt is underlain transcendently by Permian-Triassic clastic, volcanic, and limestones. Moreover, it also consists of low-grade metasediments, deep to shallow marine clastic sediments, and limestone with abundant intermediate to acid volcanics and volcaniclastics, deposited in paleo-arc basin volcanic (Kamar Shah Ariffin & Hewson, 2007).

CHAPTER 5

LANDSLIDE SUSCEPTIBILITY ANALYSIS

5.1 Introduction

The primary data required for landslide susceptibility and risk assessment in this study were collected from various and constructed of a spatial database. For each of these thematic maps, the incidence of landslides in their classes was evaluated. The thematic layers of the selected factors governing landslides, including slope value, slope aspect, elevation, lithology, land use/cover, distance to roads, distance to drainage network, distance to lineaments, were developed. All produced layers were then combined using weights of factors and sub-factors determined by the AHP method to generate the landslide susceptibility map. All thematic layers were integrated into the GIS environment by the combination of AHP results.

The thematic layers of distance to drainage network, to faults and roads, were calculated by Euclidean distance tool in spatial analyst tools of ArcGIS 10.7. Sentinel-2 image with 10 x 10 m spatial resolution acquired also used to generate the land use/cover map after radiometric and atmospheric corrections. The land use/cover map was produced by Support Vector Machine (SVM) of satellite data using ENVI 5.0 software. Topographic related factors such as slope degree, slope aspect and elevation were derived from a 10m Digital Elevation Model from ALOS PALSAR data of the study area. The digital layer drainage network was also produced from 10m DEM by hydrology tools in ArcGIS 10.7 software. All thematic layers were converted to raster

format with 12.5 m × 12.5 m cell resolution, and each raster was classified into several classes to calculate the numbers of landslide and non-landslide pixels. The preparation procedure for each thematic layer is summarized below.

5.2 Parameter of Landslide Susceptibility Map

5.2.1 Precipitation

Rainfall is one of the climate elements that play a significant role in landslides. Infiltration of rainwater into the soil layer will fill the soil and weaken the slope forming material, thus triggering landslides. Rain with high precipitation and intensity will provide a greater threat of mass wasting.

Several landslides occur yearly in the Kelantan River basin during heavy monsoon rainfall. In particular, several major flooding events (in 2005, 2006, 2007, 2008, 2009, 2014 and 2015) have occurred in recent years, leading to considerable damage to livestock, agricultural development, homes and businesses in the Kelantan River basin (Pradhan, 2009).

According to Figure 5.2, the climate chart indicates the temperature average (26.4 ^{o}c) and precipitation average (27344.4mm) within the year 2014 until 2019. The spatial distribution of rainfall can be seen in Figure 5.3; it can be explained that the research area comprises average annual precipitation from 2377.03mm to 2336.32mm in 2019.

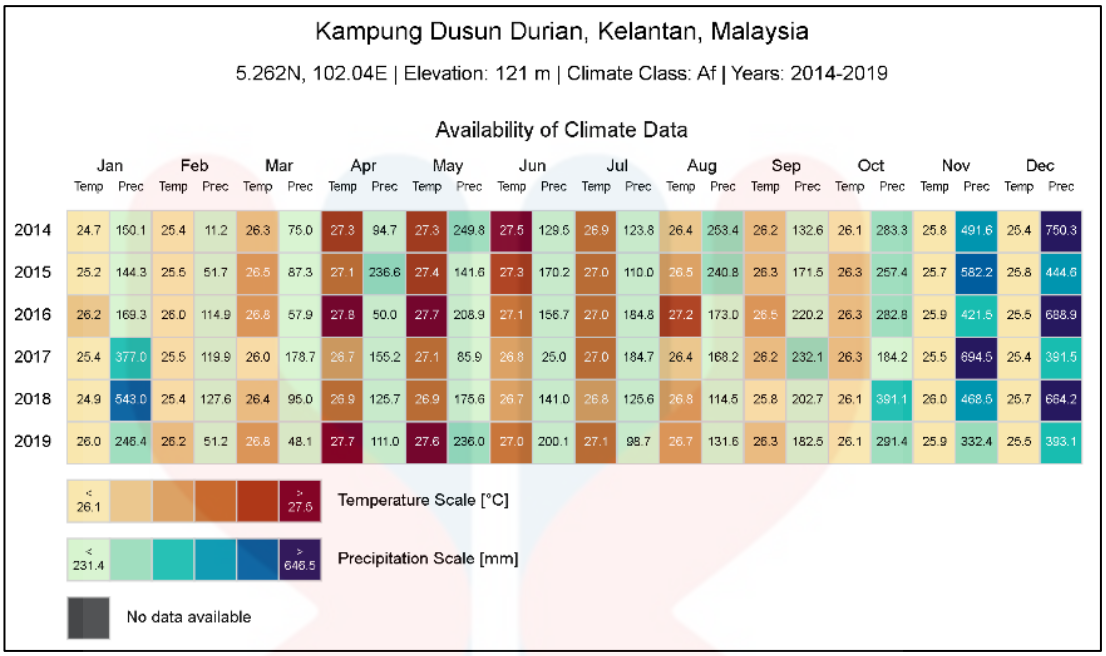

Figure 5.1: Availability of Climate Data (https://climatecharts.net/, 2019)

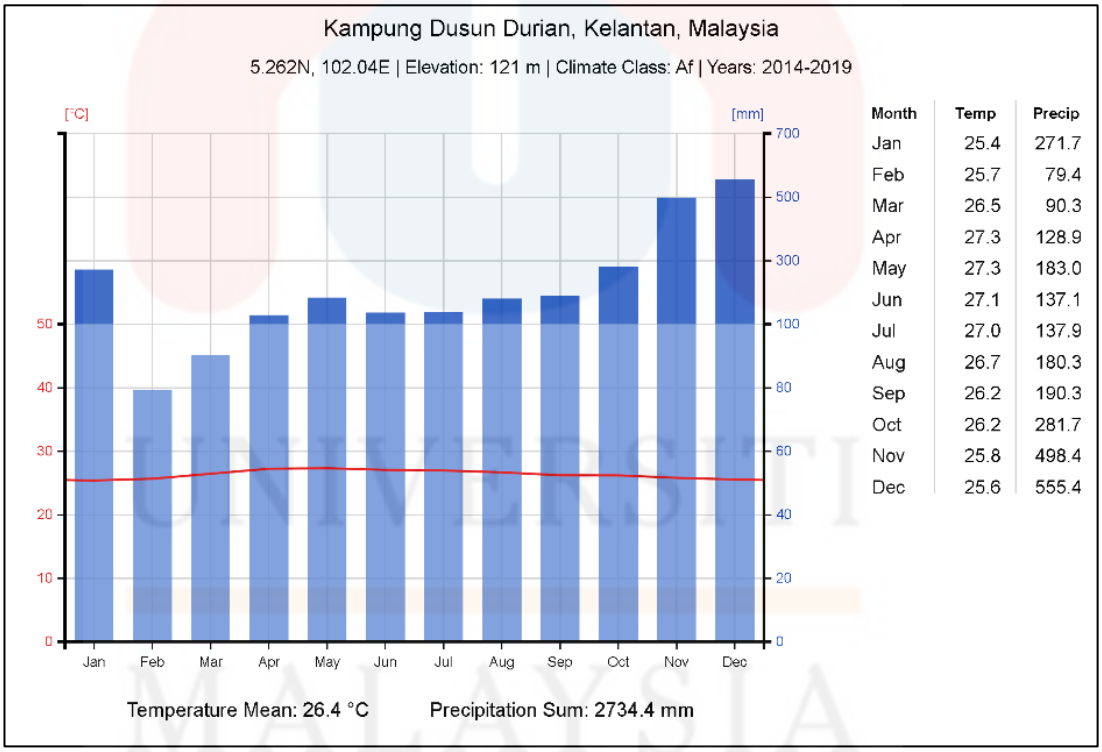

Figure 5.2: Climate Chart (https://climatecharts.net/, 2019)

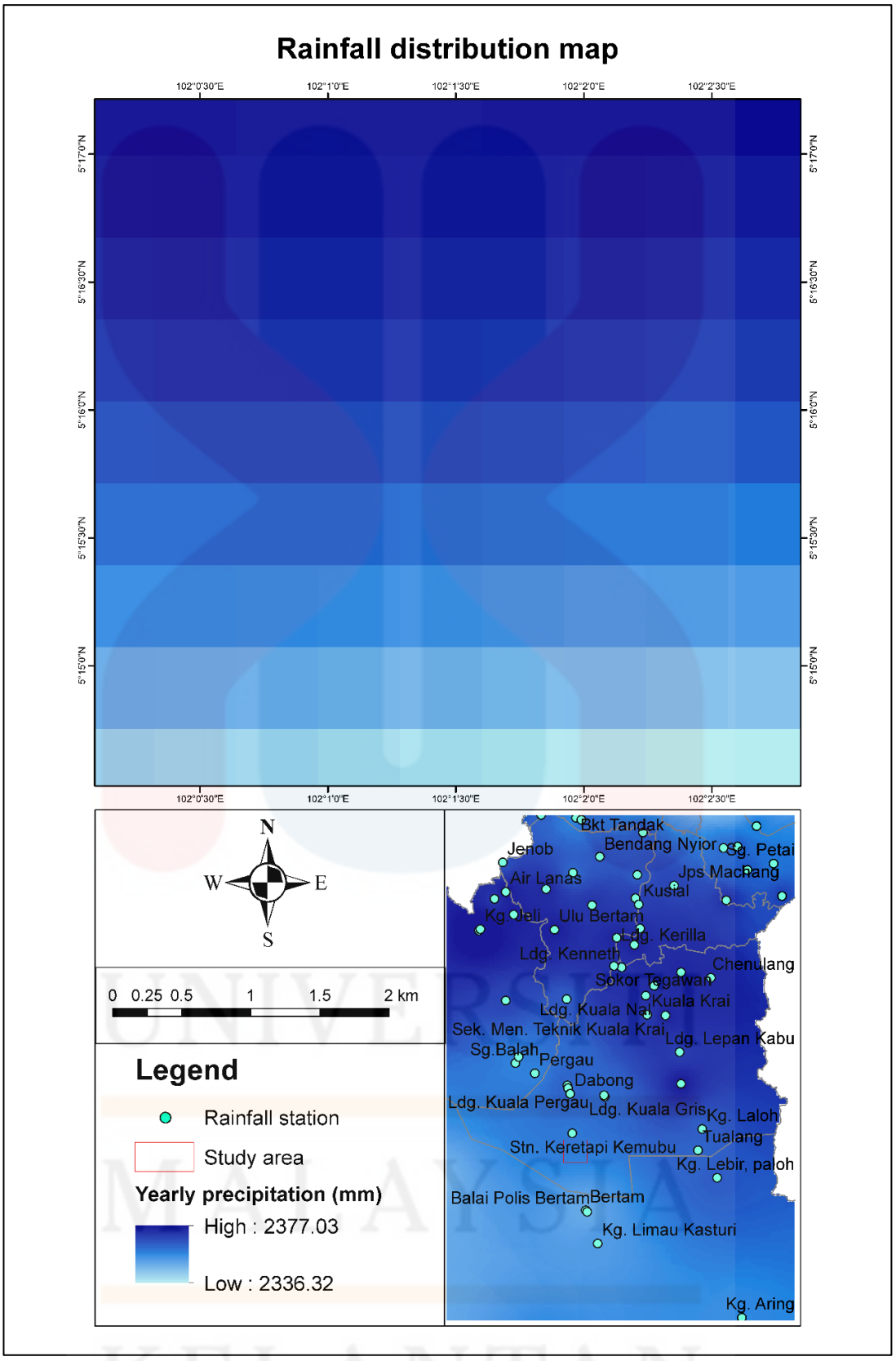

Figure 5.3: Rainfall distribution map for 2019 (https://chrsdata.eng.uci.edu/, 2020)

5.2.2 Slope

The topography element that has the greatest influence on landslides is the slope. The steeper the slope, the bigger and faster the landslides will occur. On slopes > 40%, landslides often occur, mainly due to the influence of gravity. However, in reality, not all sloping land/areas have the potential for landslides, but it depends on the slopes' character and their constituent materials for the trigger force's response, especially the slope's response toward rainfall. Besides, the potential for landslides to occur depends on vegetation's presence on the slope because the slopes can withstand conditions of limited vegetation stability. Based on the results of processing the contour map of the study area into a slope class map using DEM (Digital Elevation Model) of ALOS PALSAR analysis, the research area is classified into five classes of the slope, namely flat to almost flat slope class with slope angles ranging from (0 - 2%), very sloping slope class (2 - 7%), sloping slope class (7 - 15%), a rather steep slope class (15 - 20%) and steep slope class (20 - 30%). The complete spatial distribution of the slopes of the study area can be seen in Figure 5.4. Based on the following table, the distribution of slope and landform quantitatively through calculations grouped by the number of percentages and slope angle to determine the amount of slope percentage through the calculation of the comparison between the height differences with the formed flat distance.

Table 5.1: The division of the slope based on USSSM and USLE

Slope (°)	Slope (%)	Description	USSSM (%)	USLE (%)
< 1	0 – 2	Flat – Almost Flat	0 – 2	1 – 2
1 – 3	3 – 7	Very Sloping	2 – 6	2 – 7
3 – 6	8 – 13	Sloping	6 – 13	7 – 12
6 – 9	14 – 20	Rather Steep	13 – 25	12 – 18
9 – 25	21 – 55	Steep	25 – 55	18 – 24
25 – 26	56 – 140	Very Steep	> 55	> 24
> 65	> 140	Rugged		
USSSM = United Stated Soil System Management				
USLE = Universal Soil Loss Equation				

(Van Zuidam, 1985)

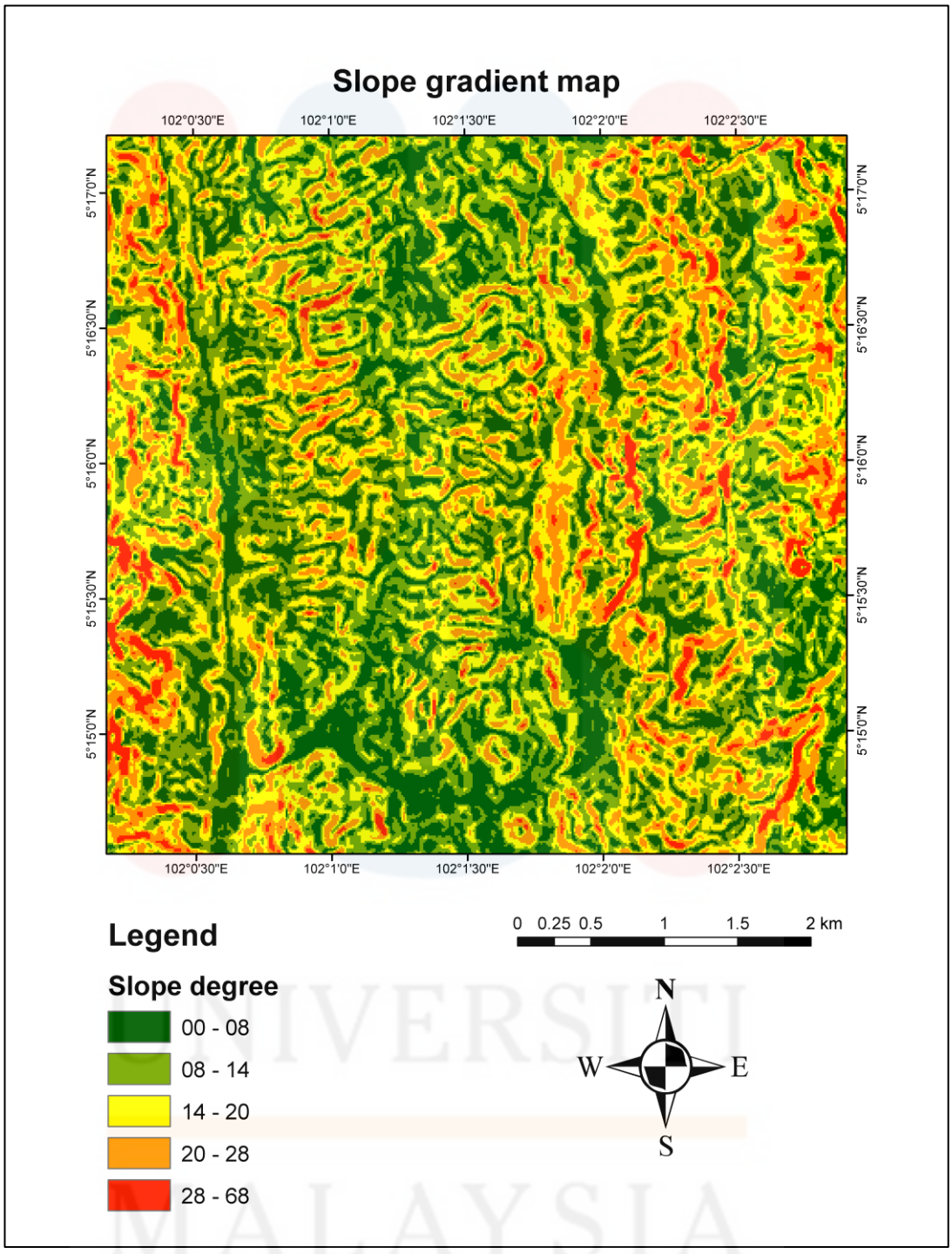

Figure 5.4: Slope map of the study area

5.2.3 Soil moisture

Soil moisture is the amount of water stored between soil pores. Soil moisture is very dynamic, caused by evaporation through the soil surface, transpiration, and percolation. Soil moisture information from remote sensing data is essential to support

agricultural activities, floods, drought, and soil erosion because each soil type's moisture content varies in terms of the water content and the infiltration rate. Based on soil pores' texture and distribution, each soil type displays differences in soil moisture characteristics. The soil's physical characteristics play a part in its ability to store water; e.g., in sandy soils, the water holding potential is minimal, meaning that plants can easily deplete the water supply and dry out more quickly plants growing on loam soils. The scale of the soil's capacity to retain water would also determine the soil's moisture content. Remote Sensing Technology that is processed using a transformation (algorithm) can provide new information about surface soil moisture. Soil moisture detected by remote sensing is soil moisture with a depth of several cm (less than 5 cm) from the soil surface.

From the study area, the data of soil moisture extracted from "SMAP/Sentinel-1 L2 Radiometer/Radar 30-Second Scene 3 km EASE-Grid Soil Moisture, Version 3" depicted that the highest value ($0.327 – 0.346 cm^3$) as well as lowest value ($0.155 – 0.190 cm^3$). Information on the spectral value can be obtained by extracting the study area's image, such as vegetation coverage and surface temperature, with the satellite imagery recorded in a year not too far from the research time. Besides, the best soil moisture information is achievable from L-band microwaves because it comes out from deeper soils. Soil moisture is one essential factor in hydrogeological hazards for flood forecasting and prevention in Kelantan. Remote sensing has advantages in several ways in measuring such as data can be in the form of digital data, information can reach areas that are difficult to reach as well as areas where the availability and quality of hydrology is limited, the measurement includes a distributed area which means that the coverage of the study area becomes broad and suitable for large regional

scales, and has the potential to measure several variables (surface temperature, soil moisture, and vegetation coverage)

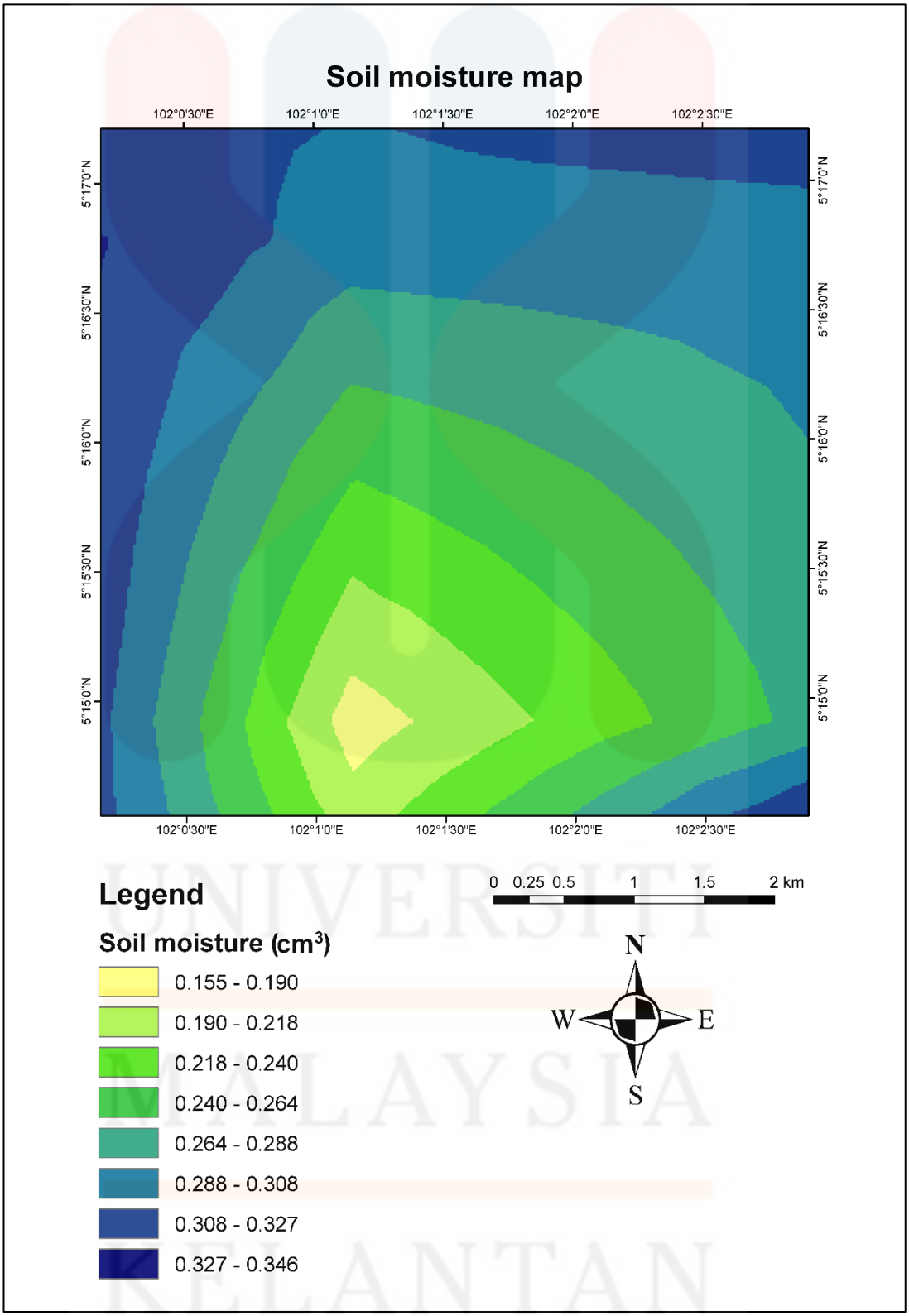

Figure 5.5: Soil moisture map of the study area (https://nsidc.org/data/SPL2SMAP_S/versions/3)

Table 5.2: Description of soil moisture

No	Soil moisture (cm^3)	Area (km^2)	Area (%)
0	0.155 - 0.190	0.204	0.008
1	0.190 - 0.218	1.552	0.061
2	0.218 - 0.240	2.775	0.110
3	0.240 - 0.264	4.357	0.172
4	0.264 - 0.288	6.094	0.241
5	0.288 - 0.308	6.607	0.261
6	0.308 - 0.327	3.709	0.146
7	0.327 - 0.346	0.024	0.001

5.2.3 Aspect

Aspect (degree) was produced through raster data of digital elevation model (DEM) of the study area with the scale of 1:25,000 using digital processing software of GIS, ArcMap 10.7

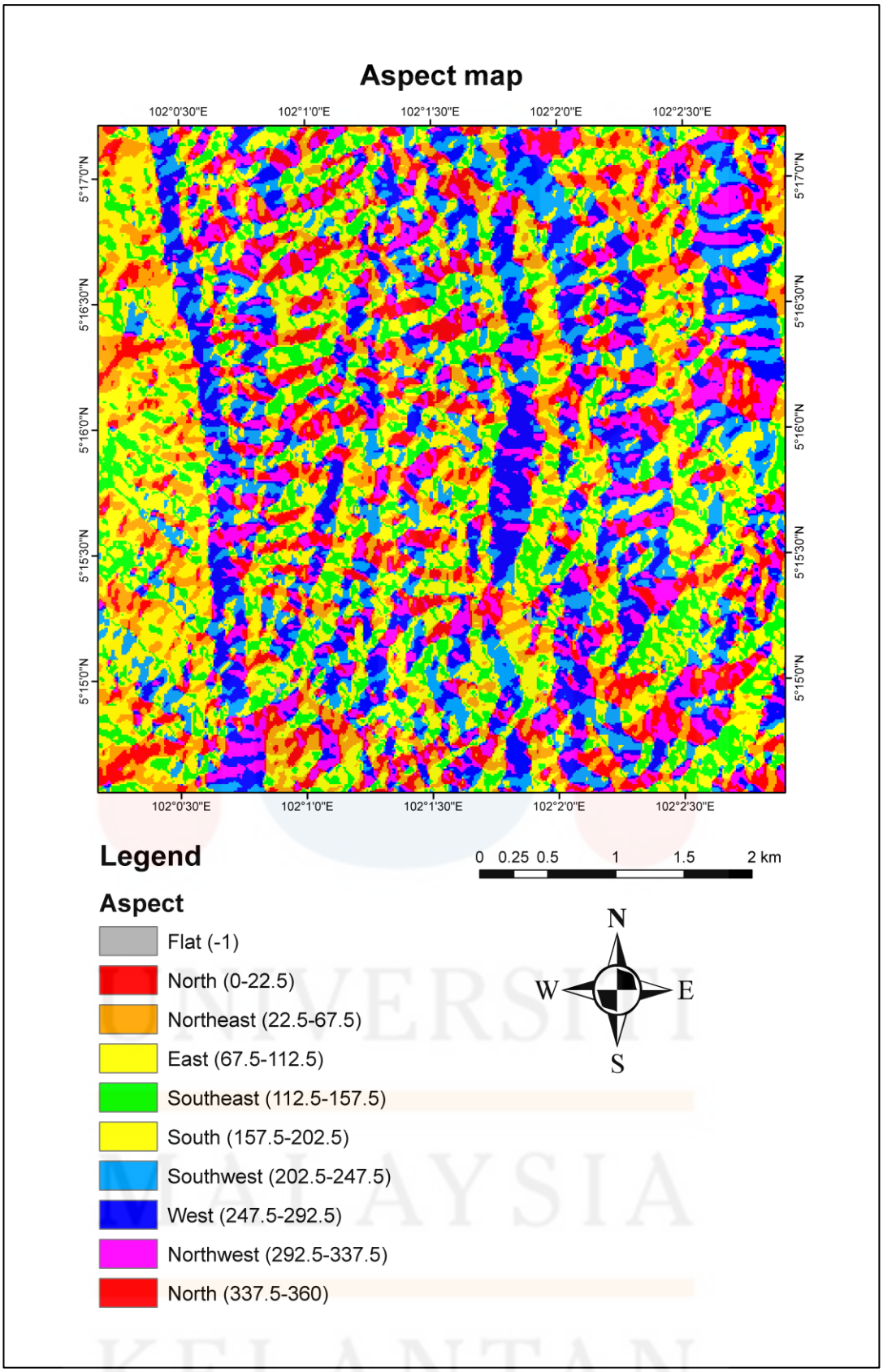

Figure 5.6: Aspect map of the study area

5.2.4 Lithology

Research area lithology can also play a significant role in assessing the vulnerability of area landslide occurrences. It is because lithology variations can still affect whether the region is vulnerable to landslides or the hazard's low susceptibility. The rock type in the study area falls within the period of Permian in the Paleozoic era, Triassic in the Mesozoic era and Tertiary in the Cenozoic era. Geologically, the lithologies of the study area were divided in accordance to the three eras that is the Paleozoic (limestone, acid to intermediate volcanic (pyroclastic, rhyolitic to dacitic composition), phyllite and shale), Mesozoic (interbedded sandstone, siltstone and shale) and Cenozoic (granite). Table 5.3 and Figure 5.7 depicted the weightage and score of the type of lithology and the lithological map respectively

The lithology map of the study area for Kampung Dusun Durian, Dabong was derived from the Geologic map of the Kelantan state (scale 1:250,000) that modified from Department of Minerals and Geoscience Malaysia in 2003 and lithology map of Batu Ban Chuan (scale 1:25,000) from the previous researcher namely Zakiah Ainul Kamal in 2013.

Table 5.3: Lithology area of Kampung Dusun Durian, Dabong, Kuala Krai.

No	Lithology	Area (km^2)	Area (%)
1	Alluvium	0.26	1.04%
2	Phyllite and Slate	2.31	9.09%
3	Limestone	1.54	6.06%
4	Granite	3.92	15.45%
5	Interbedded sandstone, siltstone and shale	14.21	55.97%
6	Acid to intermediate volcanic (pyroclastic, rhyolitic to dacitic composition)	3.15	12.40%

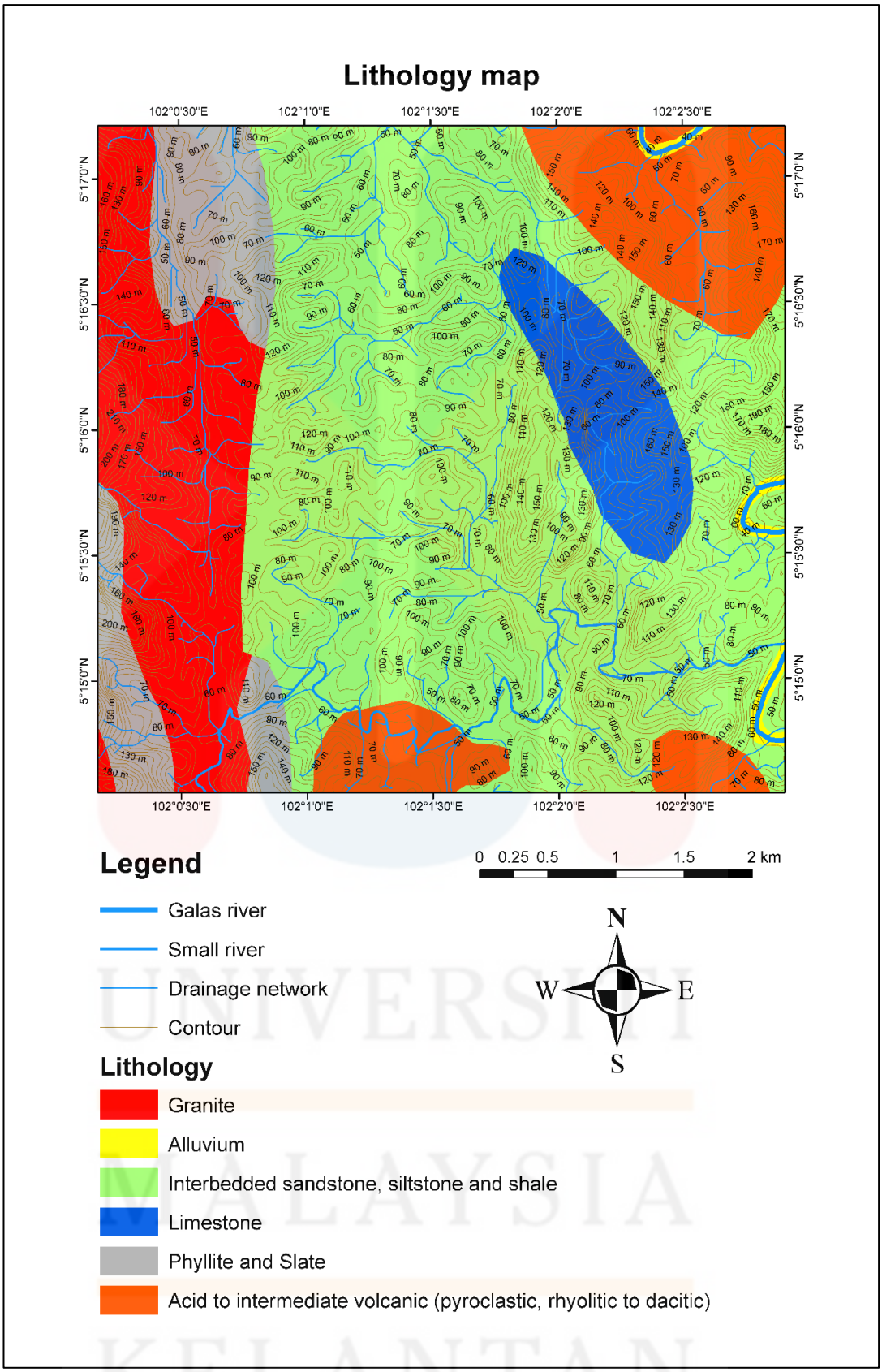

Figure 5.7: Lithology of the study area

5.2.5 Land Use Land Cover (LULC)

The number of vegetation changes (as land cover) from forest stands or dense vegetation to mixed gardens, shrubs, settlements, or into empty land will greatly affect the slope's stability, especially in forest areas that are converted into agricultural land. In observations, landslides also occurred in areas with land cover in the form of high-density tree stands. In certain cases, plants that live on slopes with a certain slope increase slope loads that encourage landslides. Based on the results of the updating map of land cover in 2019, it is known that the types and percentages of land cover in the study area are mostly dominated by forest and mixed rubber/agriculture (Table 5.4). The complete spatial distribution of land cover is presented in Figure 5.7.

Table 5.4: Land use land cover map classification

Land use and land cover	Area (km^2)	Area (%)
Bareland	0.91	3.52%
Forest	14.78	57.38%
River	0.21	0.82%
Road connection	0.53	2.07%
Rubber/ Agriculture	9.23	35.85%
Urban/ Built-up	0.09	0.36%

Based on Table 5.4, it can be seen that mixed forest is the largest land cover found in the study area, which is 14.78km^2 or about 51.4% of the total area of the study area. The forest has a high frequency of vegetation; it includes a deep and strong root system that can bind soil aggregates and reduce landslides' potential. However, in rubber/ agriculture regions that have become shrubs, it will increase the potential for landslides because shrubs generally do not have a strong and deep root system that can bind soil aggregates, especially if there is heavy rainfall.

The landform where the area is not overgrown by vegetation or has not been used by the community is called an empty land area. If it rains with a high enough intensity, it will be immediately absorbed by the soil to become saturated quickly with water, resulting in the increasing of soil's weight and more unstable. Under these conditions, bare land areas are at risk of landslides, so it is necessary to make conservation efforts through rehabilitation or reforestation of bare land by residents and the local government. The settlement is a type of land cover used to meet the population's housing needs around the study area. These residential areas are evenly distributed throughout the study area with an area of 0.09km^2 or about 0.36%. Settlements located on a rather steep to very steep slope are very vulnerable to the risk of landslide hazards, causing major negative impacts.

The land cover type in the river region in the study area has an area of 0.21km^2 or about 0.82%. The water body source will be very influential as a trigger for landslides if located in a rather steep or sloping area. In that situation, the slopes are saturated with water, which results in increasing mass wasting so that it often becomes unstable.

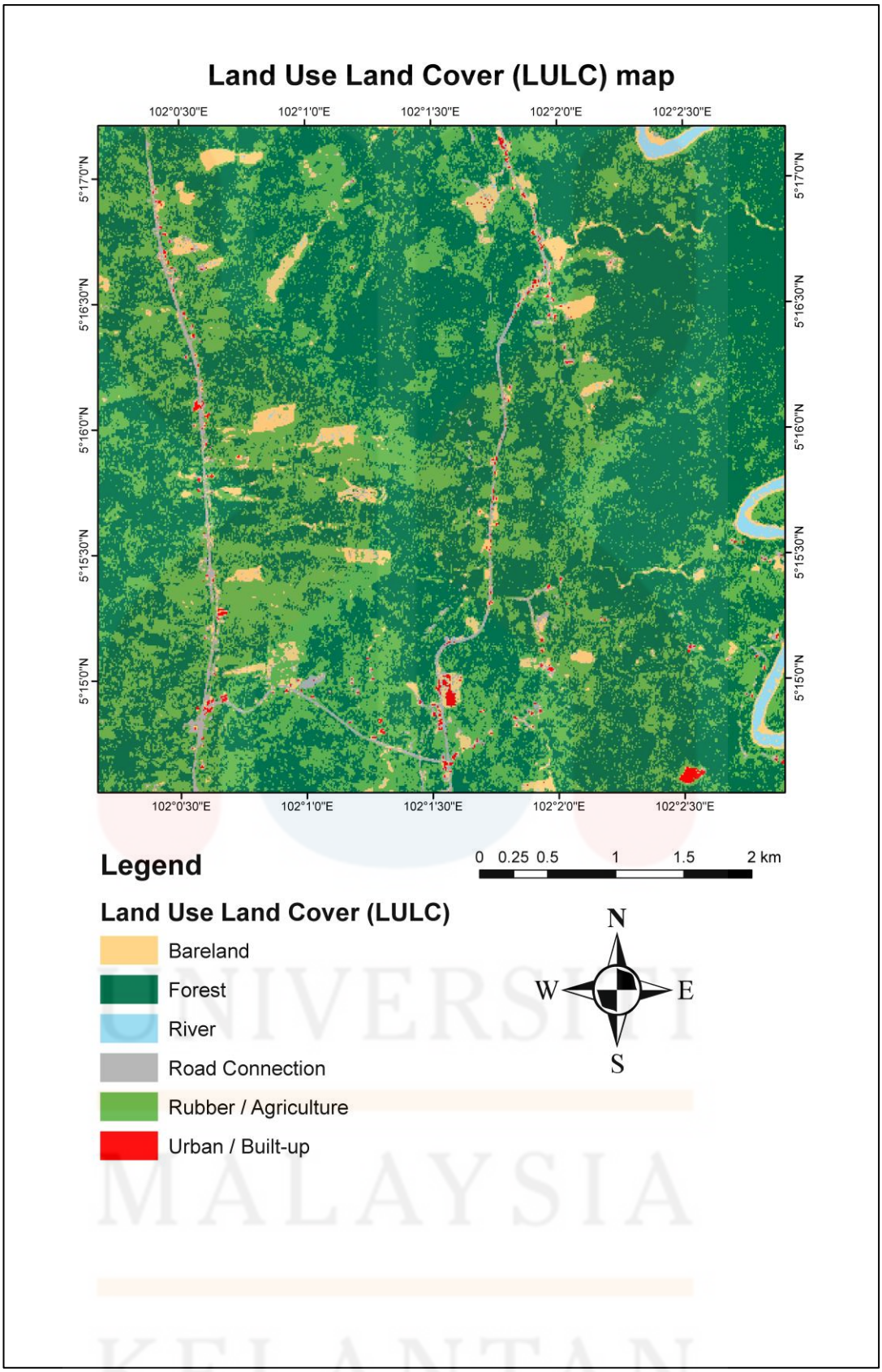

Figure 5.8: Land Use Land Cover (LULC) map of the study area

The SVM methods able to determine the accuracy of each LULC classification, confusion matrix assessment was performed. For this purpose, firstly, a reference data set, including 12,777 points based on Table 5.5, was created. These points were selected over different locations representing different land cover/use classes. Same reference data were used for the accuracy assessment of Sentinel-2 images and different classification algorithms. The error matrix of each classification was created, and the user's and producer's accuracy values of each class were analyzed to evaluate classification accuracy. The SVM method's overall accuracy for Sentinel-2 data is about 84.9965%, with a kappa value of 0.8028.

Classification results illustrated that the water body could be successfully identified using SVM upon the satellite images besides, the best accuracy from the research area depicted by river areas with 94.32%. The least accuracy from SVM results obtained from urban /built-up area with 59.68% is among the six different classifications.

Table 5.5: accuracy assessment for Sentinel-2 LULC using SVM

Confusion Matrix: SENTINEL 2 LULC\SVM Method\2019\SVM classify\2019_class					
Overall Accuracy = (10860/12777) 84.9965%					
Kappa Coefficient = 0.8028					
Ground Truth (Pixels)					
Class	**Bareland**	**Forest**	**River**	**Road Connection**	**Rubber / Agriculture**
Unclassified	0	0	0	0	0
Bareland	2217	1	15	189	83
Forest	9	3455	0	2	372
River	70	0	249	2	0
Road Connection	151	1	0	1183	14
Rubber / Agriculture	215	266	0	117	3312
Urban / Built-up	21	0	0	89	0
Total	2683	3723	264	1582	3781
Ground Truth (Pixels)					
Class	**Urban / Built-up**			**Total**	
Unclassified	0			**0**	

Bareland	117	**2622**
Forest	0	**3838**
River	3	**324**
Road Connection	169	**1518**
Rubber / Agriculture	11	**3921**
Urban / Built-up	444	**554**
Total	**744**	**12777**

Ground Truth (Percent)

Class	Bareland	Forest	River	Road Connection	Rubber / Agriculture
Unclassified	0	0	0	0	0
Bareland	82.63	0.03	5.68	11.95	2.2
Forest	0.34	92.8	0	0.13	9.84
River	2.61	0	94.32	0.13	0
Road Connection	5.63	0.03	0	74.78	0.37
Rubber / Agriculture	8.01	7.14	0	7.4	87.6
Urban / Built-up	0.78	0	0	5.63	0
Total	**100**	**100**	**100**	**100**	**100**

Ground Truth (Percent)

Class	Urban / Built-up	Total
Unclassified	0	0
Bareland	15.73	20.52
Forest	0	30.04
River	0.4	2.54
Road Connection	22.72	11.88
Rubber / Agriculture	1.48	30.69
Urban / Built-up	59.68	4.34
Total	**100**	**100**

Class	Commission (%)	Omission (%)	Commission (Pixels)	Omission (Pixels)
Bareland	15.45	17.37	405/2622	466/2683
Forest	9.98	7.2	383/3838	268/3723
River	23.15	5.68	75/324	15/264
Road Connection	22.07	25.22	335/1518	399/1582
Rubber / Agriculture	15.53	12.4	609/3921	469/3781
Urban / Built-up	19.86	40.32	110/554	300/744
Class	**Producer Accuracy (%)**	**User Accuracy (%)**	**Producer Accuracy (Pixels)**	**User Accuracy (Pixels)**
Bareland	82.63	84.55	2217/2683	2217/2622
Forest	92.8	90.02	3455/3723	3455/3838
River	94.32	76.85	249/264	249/324
Road Connection	74.78	77.93	1183/1582	1183/1518
Rubber / Agriculture	87.6	84.47	3312/3781	3312/3921
Urban / Built-up	59.68	80.14	444/744	444/554

5.2.6 Distance to roads

Distance to roads (Figure 5.9) is one of the major anthropogenic factors influencing landslide occurrences. By definition, anthropogenic describes those objects and phenomena that have their origins in the activities of humans. Based on the research region, the distance to roads is generated by using the Euclidean tools. The function of Euclidean tools as stated from the Table 3.3.

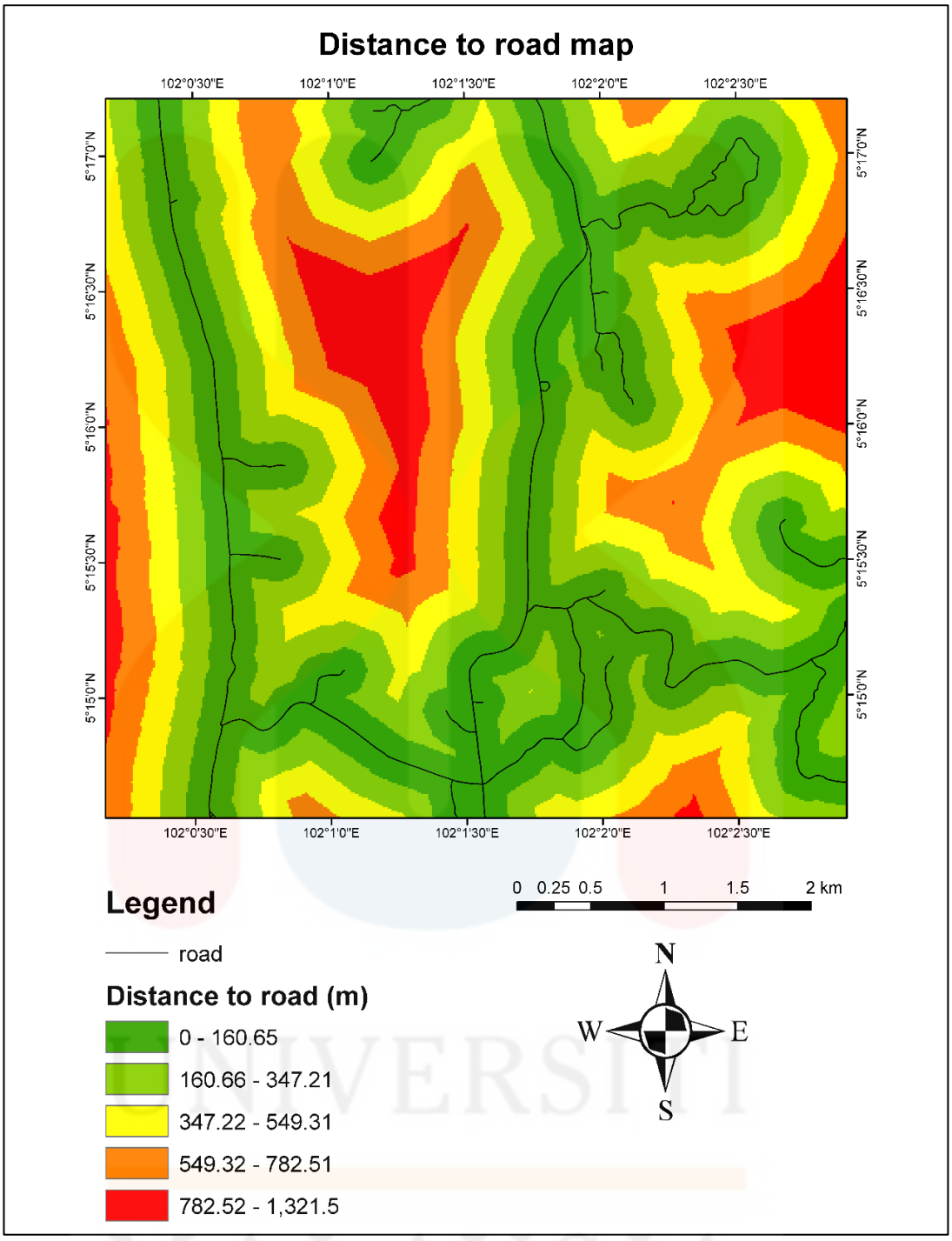

Figure 5.9: Distance to roads map

5.2.7 Distance to drainage

Rivers play a major role in landslide development (Park et al., 2013). They can lead to banks' failure because of the sub-quotation of slopes, and the modification of the ground caused by gully erosion may also influence landslide initiation. In the present study, the drainage network was produced from 12.5m DEM of ALOS

PALSAR by hydrology tools in ArcGIS 10.7. Four different buffers were generated using the Euclidean distance method to determine the degree to which the streams could affect the bank slopes (Figure 5.10).

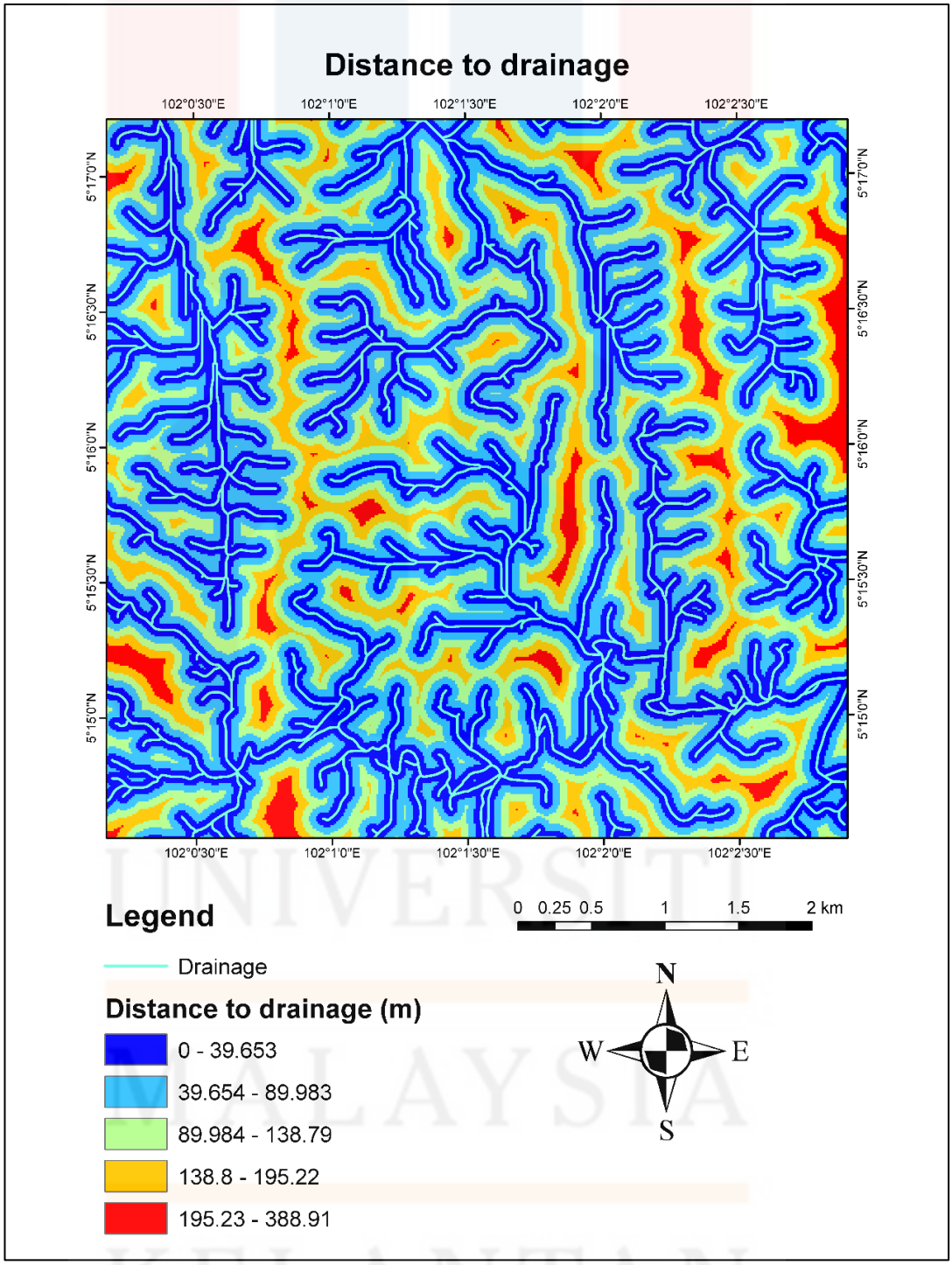

Figure 5.10: Distance to drainage map

5.2.8 NDVI

NDVI map results from processing remotely sensed data using appropriate visible bands (Red and Near Infrared), which only focuses on the vegetated area. The index ranged from -1 (most unhealthy vegetation area) to +1 (most healthy vegetation area).

Normalized Vegetation Index (NDVI) quantifies vegetation by calculating the difference between near-infrared (which highly reflects vegetation) and red light (which vegetation absorbs). For example, if you have negative values, it is highly likely water. On the other hand, if you have an NDVI value similar to +1, there is a good probability of thick green leaves. However, when NDVI is near zero, there are no green leaves, and it may be an urbanized area.

The NDVI value was calculated using the NDVI = (IR − R)/ (IR + R) formula, where IR is near-infrared band image, and R is the red band image of Sentinel-2.

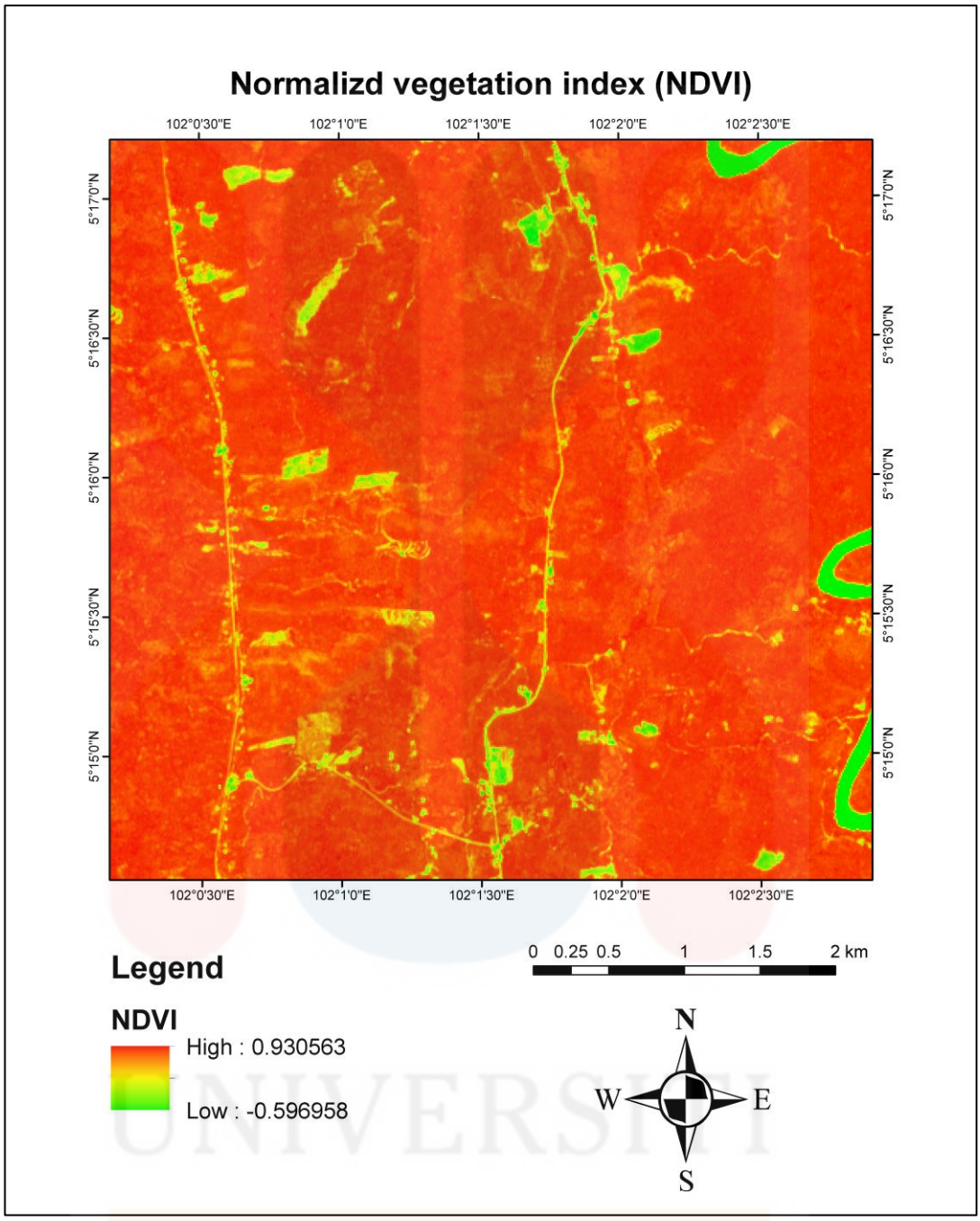

Figure 5.11: NDVI map of the study area

5.2.9 Distance to lineaments

Distance to lineament (m) was measured using the Euclidean distance operational function in ArcMap, where the distance between the fault line and lineament able to be identified. Figure 5.12 shows the combination of lineaments as a result of directional filters from Envi software. The lineaments feature are classes based on four categories of diverse orientation: N–S: 0°, E–W: 90°, NE–SW: 45° and

NW–SE: 135° with 7 x 7 kernel size. Then automatically extracted the lineaments through LINE module inside PCI Geomatics.

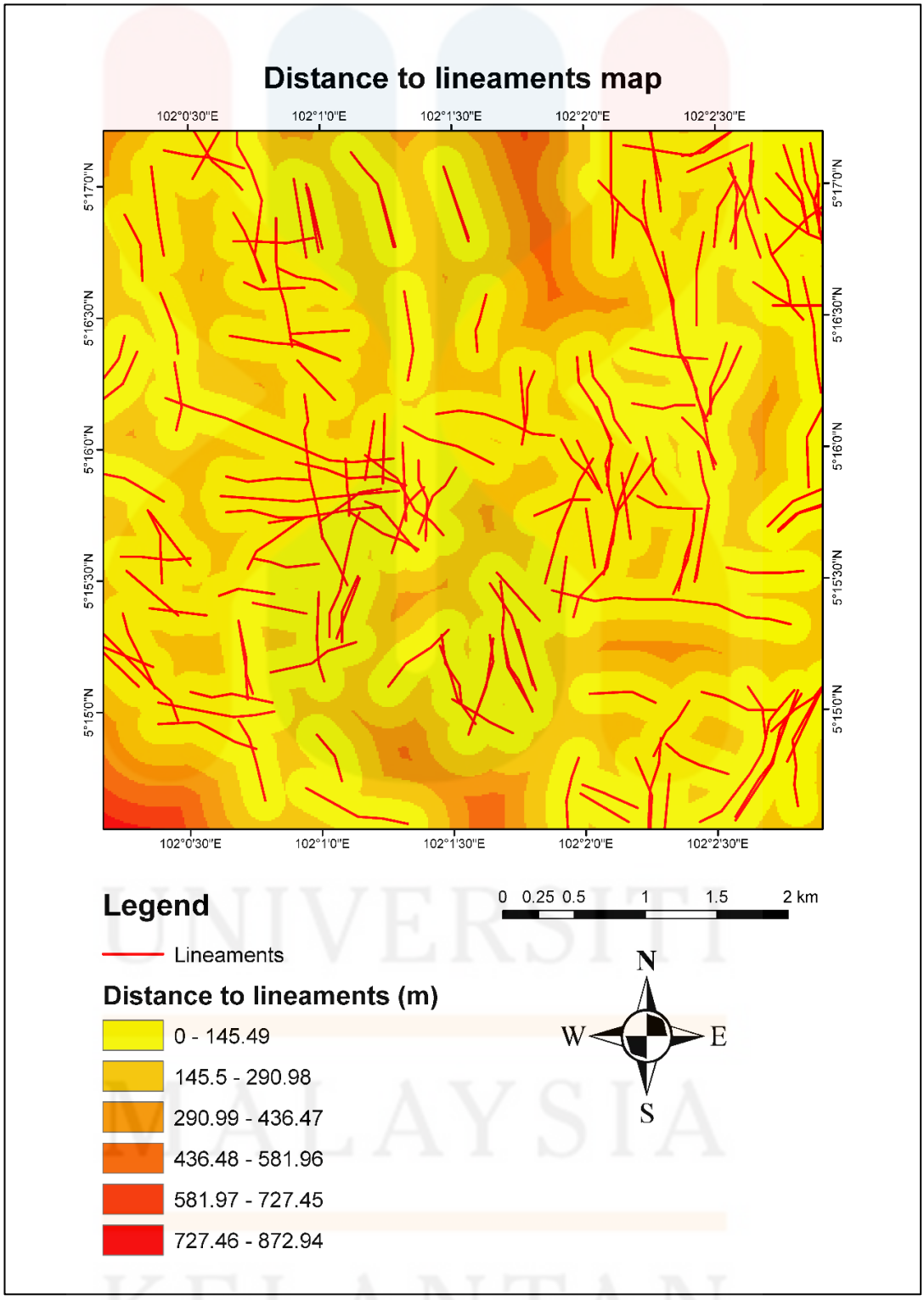

Figure 5.12: Distance to lineaments map of the study area

5.3 Landslide Susceptibility Analysis

The estimation of landslide susceptibility areas was carried out using an AHP method, thus coming up with landslide susceptibility map based on Kampung Dusun Durian's research within 2014 until 2019. The parameters used to estimate landslide susceptibility map include precipitation, slope, soil moisture, aspect, lithology, land use land cover (LULC), distance to roads, distance to drainage, and normalized vegetation index (NDVI) and distance to lineaments. AHP method introduced by Saaty (1990) and the rating method are used in this study to determine the weight for each criterion. The AHP extension 2.0 tool, namely "extAhp20" retrieved from the ArcGIS website, was later installed inside the ArcGIS software.

Each criterion's value is determined from the literature review, expert opinion, previous study, and existing guidelines. The entire parameters are classified based on the preference matrix from equal (1) to strong (9) preference, then rearrange according to their respective contributions, and then the data is processed. Based on the results of the analysis of 10 landslide susceptibility parameters using the AHP method, five criteria for landslide susceptibility map were obtained, namely very low, low, moderate, high and very high (Figure 5.16) as well as the suitability analysis with the AHP (Table 5.6). In the Landslide susceptibility evaluation, each of the parameters obtained a diverse value of criteria weights where slope (23.69%), soil moisture (20.16%), lithology (14.68%), NDVI (10.05%), LULC (10.88%), precipitation (5.90%), distance to lineaments (5.77%), distance to roads (3.50%), aspect (2.72%), and distance to drainage (2.67%).

Table 5.6: Suitability analysis with the AHP extension 2.0 tool from ArcGIS

Criteria and source layers	
Slope	A1
soil moisture	A2
Lithology	A3

Normalized vegetation index (NDVI)	A4
Land use land cover (LULC)	A5
Precipitation	A6
Distance to lineaments	A7
Distance to road	A8
Aspect	A9
Distance to drainage	A10
Number of the criteria	**10**

AHP preference matrices and results

	A1	A2	A3	A4	A5	A6	A7	A8	A9	A10
A1	1	2	2	5	3	3	5	6	7	5
A2	0.5	1	2	5	5	3	3	2	6	4
A3	0.5	0.5	1	3	2	3	4	5	6	3
A4	0.2	0.2	0.333	1	4	2	2	3	3	3
A5	0.333	0.2	0.5	0.25	1	3	4	6	7	5
A6	0.333	0.333	0.333	0.5	0.333	1	2	2	4	2
A7	0.2	0.333	0.25	0.5	0.25	0.5	1	4	6	2
A8	0.167	0.5	0.2	0.333	0.167	0.5	0.25	1	2	2
A9	0.143	0.167	0.167	0.333	0.143	0.25	0.167	0.5	1	4
A10	0.2	0.25	0.333	0.333	0.2	0.5	0.5	0.5	0.25	1

Eigenvalues	**Eigenvector of largest Eigenvalue**
11.6581	1
0.379	0.8509
0.379	0.6196
-0.4341	0.4244
-0.4341	0.4591
-0.0966	0.2491
-0.0966	0.2434
-0.837	0.1477
-0.2588	0.1147
-0.2588	0.1127

Criteria weights (%)	
slope	23.6866
soil moisture	20.1557
Lithology	14.6751
Normalized vegetation index (NDVI)	10.0538
Land use land cover (LULC)	10.8752
Precipitation	5.9013
Distance to lineaments	5.7664
Distance to road	3.4988
Aspect	2.7171
Distance to drainage	2.67
count, n	10.00
lambda max, λ_{max}	11.273
Concentration Index, CI	0.141
Concentration Ratio, CR	0.09
constant	1.49

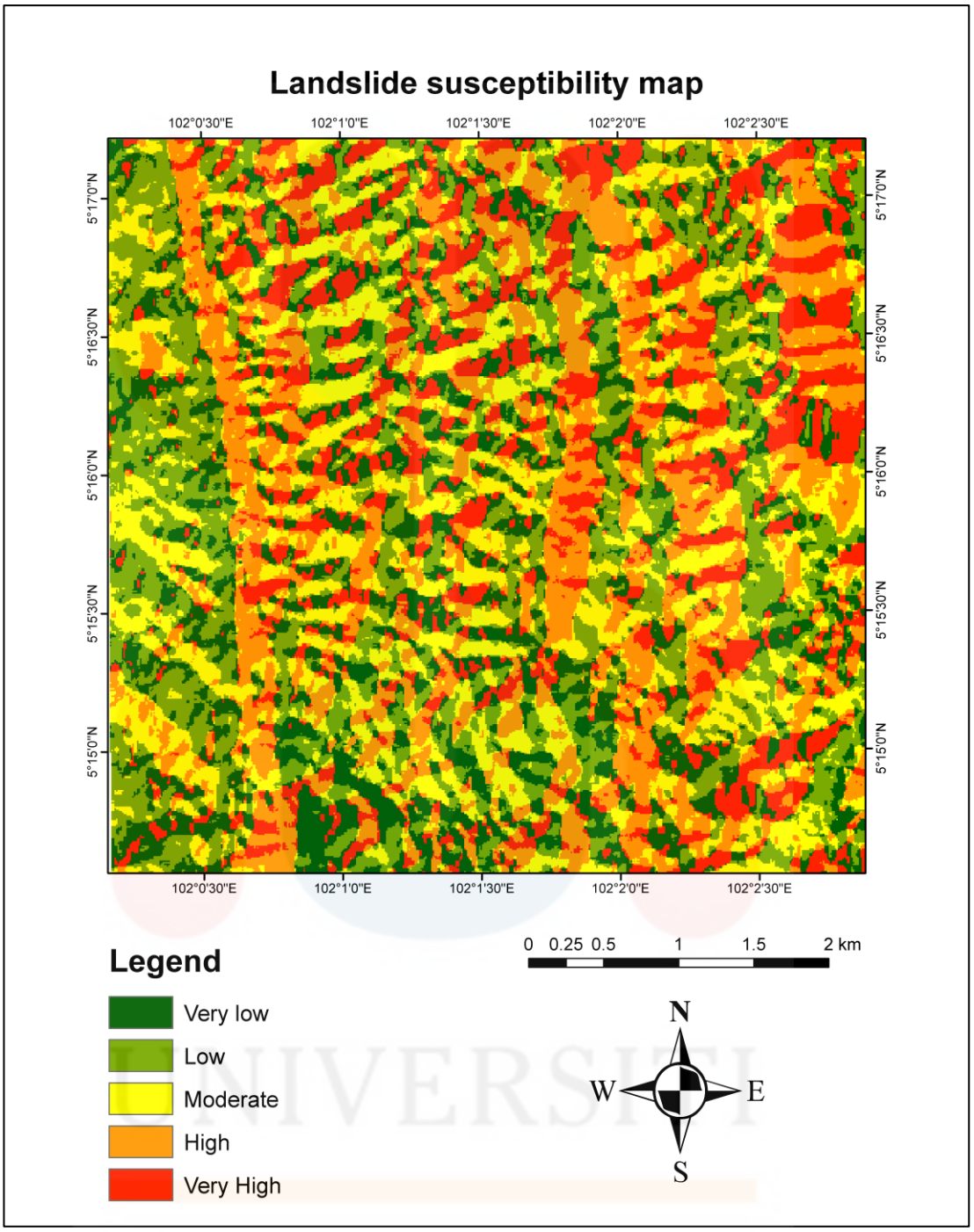

Figure 5.13: Landslide susceptibility map of the study area

Table 5.7: Percentage area in accordance with levels of landslide susceptibility

No	Levels	area (km^2)	Percentage
1	Very low	4.301372	17.30%
2	Low	5.749775	23.12%
3	Moderate	4.980375	20.03%
4	High	5.531734	22.24%
5	Very high	4.304365	17.31%

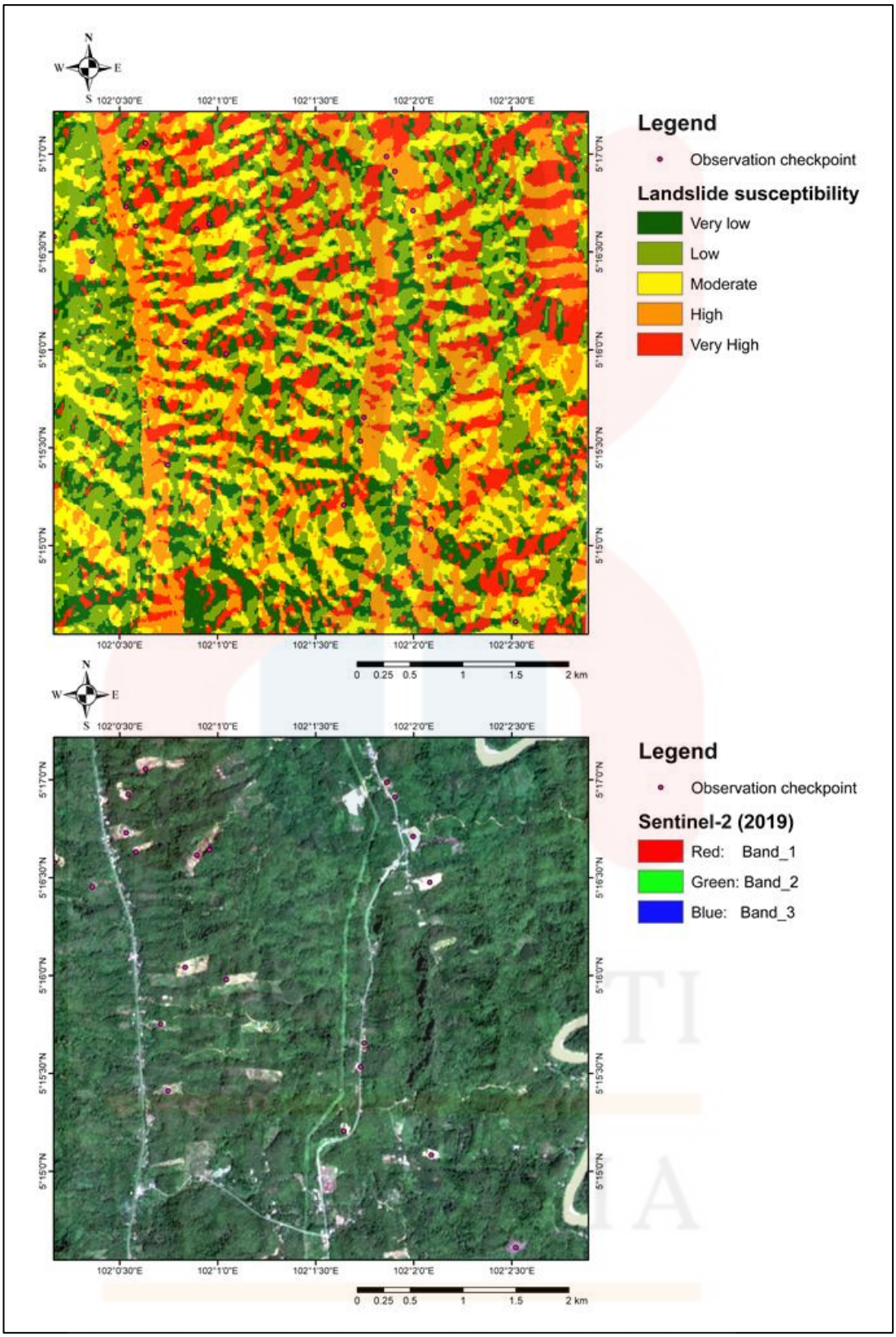

Figure 5.14: Depiction of observation checkpoint from Sentinel-2 satellite image and landslide susceptibility map.

In other to verify the precision rate of the landslide susceptibility model in the study area, the Success rate and prediction rate curves were generated based on the observation checkpoint derived from the Sentinel-2 results and the validation data of the landslide susceptibility map.

Thus, twenty-one landslide position points were obtained using point function by examine Sentinel-2 within 2016 to 2019 and Google Earth satellite image, and then, compared with five stages of landslide susceptibility map as a result from ten parameters used. The ROC curve was developed by the use of a combined percentage of LSI along with a False Positive Rate (FPR) on X-axis and True Positive Rate (TPR) on Y-axis (Figure 5.18).

The accuracy curve of the AUC value was calculated, and it was found to be 0.684 equal to 68.4%. The results showed that the landslide susceptibility map's success rate was 68.4% (Figure 5.18). AUC of the conditioning factors must surpass the minimum AUC value of 0.6, which means the performance is substantially higher. The AUC is a graph that shows varying index numbers normally between a maximum value of 1 that equal to 100% and a value of 0.5 that equal to 50%.

AUC is one type of accuracy statistics for prediction models (probabilities) in assessing or analyzing natural disasters (Pimiento, 2010). According to Silalahi et al. (2019), from the AUC analysis, it concluded that a score of 0.9 is a very good classification, a score of 0.8-0.9 is a good classification, a score of 0.7-0.8 is a moderate/ reasonable classification, and a score of less than 0.6 is a poor classification. It is known as the area under the curve (AUC) parameters, suggested with a minimum limit of 0.6. The greater the population's AUC value of a specific parameter, the greater the influence of that landslide event.

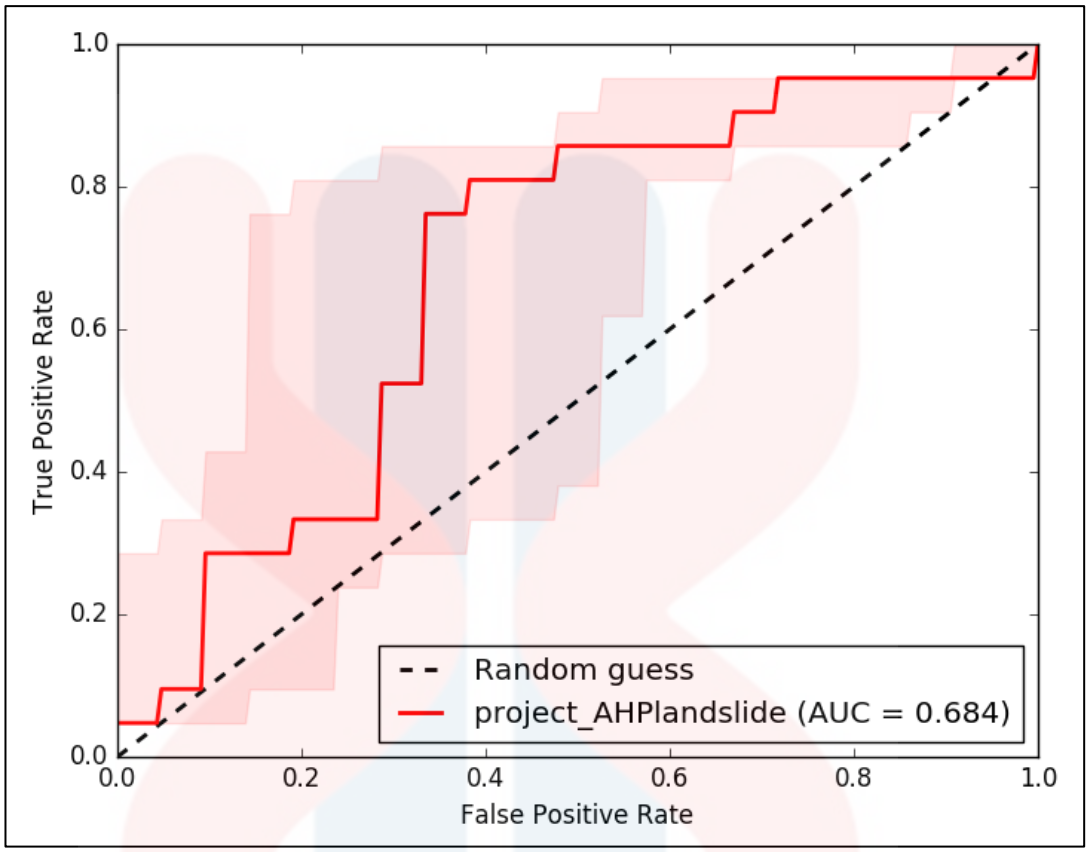

Figure 5.15: Receiver operating characteristic (ROC) curve and in accordance to landslide susceptibility assessment of value area under curve (AUC) data by ArcSDM tools in ArcGIS.

CHAPTER 6

CONCLUSION AND RECOMMENDATION

6.1 Conclusion

To conclude, ten selected component were gathered and processed into GIS and remote sensing program. The component consists of a slope, aspect, lithology, soil moisture, LULC, NDVI, distance to roads, distance to drainage, distance to lineaments, and annual precipitation over six years from 2014 until 2019 then evaluated utilizing the AHP method. The data were confirmed by correlating each component with the landslide observation checkpoint collection and justified by determining the forecast AUC curve. In AHP, the consistency applied to establish a matrix is verified by a consistency ratio (CR), which depends on the number of criteria. According to Rahamana (2014), for a 10 x 10 matrix, the CR must be less than 0.1 to acknowledge the computed values and the models with a CR greater than 0.1 were immediately dismissed, while a CR less than 0.1 were usually acceptable. In this study, the CR is 0.09. The scale implies an acceptable standard of consistency in the pair-wise comparison, which is great enough to notice the component weights. However, according to Saaty, he declares that an adequate consistency ratio should be less than 0.l0, although a ratio of less than 0.20 is considered tolerable. The calculated success percentage of AUC curve for prediction AHP model is 68.4%. The result from AHP illustrated that slope plays the most significant control for landslide-causing factors in the study area. The second dominant control is soil moisture, and the next factor that

also influences is lithology. The LULC and NDVI also affect, although it is less dominant. The research area is dominated by low to moderate susceptibility zones. Meanwhile, the high to a very high susceptibility level can cause landslides that are quite dangerous in the study area. These areas are generally located in medium vegetated areas close to residential areas. The landslide vulnerability map produced can provide initial attention and information for local governments, communities, researchers, or other interested parties. However, the susceptibility maps made are only limited to preliminary information regarding the spread of landslide hazards that may occur in the study area. This map does not have comprehensive information about the landslide area that occurred regarding its use in regional development and environmental spatial planning.

6.2 Recommendation

From the research conducted and specification part, various types of parameters, such as the form of vegetation, the previous landslide inventory from authorities, and the more in-depth geomorphology study of the research area, are recommended for use next study. The explanation is that the different parameters used can provide diverse outcomes, where the outcome afterwards can be compared to know which parameters most affected the landslide vulnerability to the research field.

More attention should be taken in terrain units with a high level of landslide vulnerability to prevent severe disasters or cause casualties and property. Besides, the community needs to be exposed by attending training and counselling to understand knowledge related to landslides, as well as increase the knowledge and awareness of the importance of taking disaster management measures before, during and after a landslide disaster occurs.

REFERENCE

Avanzi, G. D. A., Giannecchini, R., & Puccinelli, A. (2004). The influence of the geological and geomorphological settings on shallow landslides. An example in a temperate climate environment: the June 19, 1996 event in northwestern Tuscany (Italy). *Engineering Geology*, *73*(3-4), 215-228.

Aditya, T. (2010). Visualisasi Risiko Bencana di Atas Peta (Visualization of Hazard Risk in a Map), Department of Geodetic Engineering. *Gadjah Mada University. Yogyakarta. Indonesia.*

Amani Dahaman. (2016). PENYELIDIKAN PENDIDIKAN: TINJAUAN LITERATUR / SOROTAN KAJIAN. Retrieved May 10, 2020 from http://amaniresearch.blogspot.com/2011/04/tinjauan-literatur-sorotan-kajian.html

Standard, B. (1981). Code of practice for site investigations. *British Standards Institution, London (5930, 1981).*

Bujang, B. K. H., Faisal, H. A., David, H. B., Harwant, S., & Husaini, O. (2008). Landslides in Malaysia: Occurrences, Assessment, Analysis and Remediation. *Penerbitan Universiti Putra Malaysia*, 406-421.

Cruden, D. M. (1991). A simple definition of a landslide. Bulletin of the *International Association of Engineering Geology-Bulletin de l'Association Internationale de Géologie de l'Ingénieur*, 43(1), 27-29.

Cruden, D. M., & Varnes, D. J. (1996). Landslides: investigation and mitigation. Chapter 3-Landslide types and processes. *Transportation research board special report*, (247).

Department of Minerals and Geoscience Malaysia. (2003). Quarry Resource Planning for the State of Kelantan. *Osborne & Chappel Sdn. Bhd.*

Dahal, R. K., Hasegawa, S., Nonomura, A., Yamanaka, M., Masuda, T., & Nishino, K. (2008). GIS-based weights-of-evidence modelling of rainfall-induced landslides in small catchments for landslide susceptibility mapping. *Environmental Geology*, *54*(2), 311-324.

Department of Town and Country Planning Peninsular Malaysia. (2011). Rancangan Tempatan Jajahan Kuala Krai 2020 Jilid I. Retrieved March 5, 2020 from https://www.yumpu.com/id/document/read/40035764/jilid-i-pernyataan-bertulis-epublisiti-jpbd

Das, N. N., Entekhabi, D., Dunbar, R. S., Chaubell, M. J., Colliander, A., Yueh, S., ... & Walker, J. P. (2019). The SMAP and Copernicus Sentinel 1A/B microwave active-passive high resolution surface soil moisture product. *Remote Sensing of Environment*, 233, 111380. Retrieved May 2, 2020 https://doi.org/10.1016/j.rse.2019.111380

Earth Observing System. (2015). SENTINEL-2: SENTINEL-2 BANDS. Retrieved April 22, 2020 from https://eos.com/sentinel-2/

Esri. (2016). Understanding Euclidean distance analysis - Help | ArcGIS for Desktop. Retrieved April 28, 2020 from https://desktop.arcgis.com/en/arcmap/10.3/tools/spatial-analyst-toolbox/understanding-euclidean-distance-analysis.htm

Hutchison, C. S. (1977). Granite emplacement and tectonic subdivision of Peninsular Malaysia. *Bulletin of the Geological Society of Malaysia, 9, 187–207*. Retrieved April 21, 2020 from https://doi.org/10.7186/bgsm09197714

Heng, C. L., & Potisat, M. S. (2003). This report together with its accompanying geological map on the scale 1: 250,000 is the result of close cooperation between the Minerals and Geoscience Department Malaysia, and the Department of Mineral Resources, Thailand in resolving problems related to cross border geological correlation between Malaysia and Thailand. Fieldwork was carried out separately (July–August 2001) in the Batu Melintang and Sungai Kolok areas and then jointly checked.

Heng, G. S., Hoe, T. G., & Hassan, W. F. W. (2006). Gold mineralization and zonation in the state of Kelantan.

Highland, L., & Bobrowsky, P. T. (2008). The landslide handbook: a guide to understanding landslides (p. 129). *Reston: US Geological Survey.*

Hutchison, C. S., & Tan, D. N. K. (Eds.). (2009). *Geology of peninsular Malaysia.* Published jointly by the University of Malaya [and] the Geological Society of Malaysia.

Hungr, O., Leroueil, S., & Picarelli, L. (2014). The Varnes classification of landslide types, an update. *Landslides*, 11(2), 167-194

Hamzah Hussin, Abdul Ghani, S. A., Tajul Anuar Jamaluddin, & Abdul Razab, M. K. A. (2015). Tanah runtuh di Malaysia: "Geobencana" atau "geobahaya." *Jurnal Teknologi*, *77*(1), 229–235.

Humboldt State University. (2017). Raster to Vector. Conversion Between Data Models. Retrieved from http://gsp.humboldt.edu/OLM_2017/Lessons/GIS/08%20Rasters/RasterToVector.html

Hashim, Mazlan & Misbari, Syarifuddin. (2017). Landslide Mapping and Assessment by Integrating Landsat-8, PALSAR-2 and GIS Techniques: A Case Study from Kelantan State, Peninsular Malaysia. *Journal of the Indian Society of Remote Sensing.* 46. 10.1007/s12524-017-0675-9.

Ibrahim Komoo. 1985. Pengelasan kegagalan cerun di Malaysia. *Ilmu Alam 14 & 15: 47-58.*

Ichikawa, K. (1966). Discovery of early Triassic bivalves from Kelantan, Malaya. Journal of Geosciences, Osaka City University, 9, 101-106.

Ibbitt, R., Takara, K., & Pawitan H., Mohd. Nor bin Mohd. Desa and Pawitan, H., (2002). CATALOGUE OF RIVERS FOR SOUTHEAST ASIA AND THE PACIFIC-Volume IV. 6. Malaysia: 3. Kelantan. *The UNESCO-IHP Regional Steering Committee for Southeast Asia and The Pacific*. Retrieved April 30, 2020 from http://hywr.kuciv.kyoto-u.ac.jp/ihp/riverCatalogue/Vol_04/index.Html

JAXA. (2006). ALOS-2 Project. About ALOS-PALSAR: PALSAR Phased Array type L-band Synthetic Aperture Radar. Retrieved May 20, 2020 from ww.eorc.jaxa.jp/ALOS/en/about/palsar.htm

JPS JAJAHAN KUALA KRAI (n.d.). PETA LEMBANGAN DALAM JAJAHAN KUALA KRAI. Retrieved May 1, 2020, http://apps.water.gov.my /jpskomuniti/dokumen/JPS%20Komuniti%20(Intro).pdf

Khoo, T. T., & Tan, B. K. (1983). GEOLOGICAL EVOLUTION OF PENINSULAR MALAYSIA. *Department of Geology, University of Malaya, Kuala Lumpur*, 253-290. Retrieved April 23, 2020 from https://gsm.org.my/file/SCTM_15.pdf

Kamar Shah Ariffin & Hewson, N. J. (2007). Gold-related sulphide mineralization and ore genesis of the Penjom gold deposit, Pahang, Malaysia. *Resource geology*, *57*(2), 149-169.

Khanh, N. Q. (2009). Landslide hazard assessment in muonglay, Vietnam applying GIS and remote sensing. *Dr. rer. nat. at the Faculty of Mathematics and Natural Sciences Ernst-Moritz-Arndt-University Greifswald*.

Macdonald, S. (1967). The geology and mineral resources of North Kelantan and North Terengganu (No. 10). Geological Survey Headquarters.

Mustaffa Kamal Shuib (2000). Syndepositional deformations in the Permo-triassic and latest triassic to cretaceous central basins of Peninsular Malaysia.

Mezughi, T. H., Akhir, J. M., Rafek, A. G., & Abdullah, I. (2012). Analytical hierarchy process method for mapping landslide susceptibility to an area along the EW highway (Gerik-Jeli), Malaysia. *Asian Journal of Earth Sciences*, 5(1), 13.

Metcalfe, I. (2013). Tectonic evolution of the Malay Peninsula. *Journal of Asian Earth Sciences*, 76, 195-213.

Nelson, S. A. (2013). Slope stability, triggering events, mass movement hazards. *Nat. Disasters.*

Novotný, J. (2013). Varnes Landslide Classification (1978). *Charles University in Prague, Faculty of Science, Czech Republic (Issue November).* Retrieved April 22, 2020 from http://www.geology.cz/projekt681900/vyukove-materialy /2_Varnes_landslide_classification.pdf

Nazaruddin, D. A., Mansor, H. E., & Khan, M. M. A. (2017). Some unique and imaginative geological features (mimetoliths) in selected limestone sites in Malaysia: study on their formational processes and geotourism potentials.

Pradhan, B., Shafiee, M., & Pirasteh, S. (2009). Maximum flood prone area mapping using RADARSAT images and GIS: Kelantan river basin. *International Journal of Geoinformatics*, 5(2).

Pimiento Chamorro, E. (2010). Shallow landslide susceptibility: modelling and validation. *LUMA-GIS Thesis*.

Richardson, J. A. (1939). The geology and mineral resources of the neighbourhood of Raub, Pahang, Federated Malay States, with an account of the geology of the Raub Australian gold mine.

Richardson, J. A. (1950). The Geology and Mineral Resources of the Neighbourhood of Chegar Perah and Merapoh, Pahang, Federated Malay States. Geological Survey Department Federation of Malaya, Ipoh.

Rahamana, S. A., Aruchamy, S., & Jegankumar, R. (2014). Geospatial approach on landslide hazard zonation mapping using multicriteria decision analysis: A study on Coonoor and Ooty, part of Kallar watershed, the Nilgiris, Tamil Nadu. *The International Archives of Photogrammetry, Remote Sensing and Spatial*

Information Sciences, 40(8), https://doi.org/10.5194/isprsarchives-XL-8-1417-2014

Scrivenor, J. B. (1928). The Geology of Malayan Ore-Deposits. *The Geographical Journal, 72 (*4). 378. Retrieved May 2, 2020 from https://doi.org/10.2307/1782390

.Sharpe, C. F. S. (1938). Landslides and Related Phenomena: A Study of Mass-Movements of Soil and Rock. *The Geographical Journal*, 92(3), 276. Retrieved May 2, 2020 from https://doi.org/10.2307/1788849

Saaty, T. L. (1977). A scaling method for priorities in hierarchical structures. *Journal of mathematical psychology, 15(3),* 234-281.

Saaty, T. L. (1980). The Analytic Hierarchy Process Mcgraw Hill, *New York. Agricultural Economics Review*, *70.*

Suryadi, K., & Ramdhani, M. A. (1998). Sistem Pendukung Keputusan. *PT Remaja Rosdakarya, Bandung.*

Sarp, G. (2005). Lineament analysis from satellite images, north-west of Ankara (Master's thesis). Retrieved May 20, 2020 from https://etd.lib.metu.edu.tr/upload/12606520/index.pdf

Salui, C. L. (2018). Methodological validation for automated lineament extraction by LINE method in PCI Geomatica and MATLAB based Hough transformation. *Journal of the Geological Society of India*, *92*(3), 321-328.

Silalahi, F. E. S., Arifianti, Y., & Hidayat, F. (2019). Landslide susceptibility assessment using frequency ratio model in Bogor, West Java, Indonesia. *Geoscience Letters*, 6(1), 10.

Tajul Anuar Jamaluddin. (1990). *Geologi kejuruteraan Lebuh raya Timur–Barat penekanan kepada kestabilan cerun.* Tesis Sarjana Sains

Tajul Anuar Jamaluddin (2006). Faktor Manusia dan Kegagalan Cerun di Malaysia (HUMAN FACTORS AND SLOPE FAILURES IN MALAYSIA). *Geological Society of Malaysia Bulletin, 52,* 75-84. Retrieved April 20, 2020 from http://www.gsm.org.my/products/702001-100519-PDF.pdf

Tajul Anuar Jamaluddin, Norasiah Sulaiman, & Nazer, N. S. M. (2020). Penilaian geomorfologi tanah runtuh lama di tanah tinggi tropika-Kajian kes Cameron Highlands dan Kundasang, Malaysia. *Bulletin of the Geological Society of Malaysia, 69.*

Unjah, T., Ibrahim Komoo, Hamzah Mohamad (2001). Pengenalpastian sumber warisan geologi di negeri Kelantan. *Geological Heritage of Malaysia (Geoheritage Mapping and Geosite Characterization),* LESTARI UMK, Bangi, 111–126.

Varnes, D. J. (1978). Slope movement types and processes. *Special report*, 176, 11-33. Retrieved April 21, 2020 from http://onlinepubs.trb.org/Onlinepubs/sr/sr176/176-002.pdf

Van Zuidam, R. A. (1979). Terrain analysis and classification using aerial photographs: *a geomorphological approach* (No. 526.982 V3).

Van Zuidam, R. A. (1985). Aerial photo-interpretation in terrain analysis and geomorphic mapping. *International Institute for Aerospace Survey and Earth Science (ITC)*.

Zaiton Harun (2002). Late Mesozoic-Early Tertiary Faults of Peninsular Malaysia. *Geological Society of Malaysia Annual Geological Conference 2002*. Retrieved April 22, 2020 from https://gsm.org.my/products/702001-100734-PDF.pdf

Zakiah Ainul Kamal, (2013) General geology and microfacies analysis of Batu Ban Chuan, Dabong, Kelantan. [Undergraduate Final Year Project Report] (Submitted)

APPENDICES

Appendix A

Table of rainfall station located in Kelantan state

No	Station name	Coordinate		Mean Precipitation (mm)						IDW 2014 to 2019
		Y	X	2014	2015	2016	2017	2018	2019	
1	Brook	4.6764	101.4847	2798	1913	3370	3463	2509	2084	2689.5
2	Lojing	4.6000	101.4	2544	1872	3014	3455	2512	2117	2585.8
3	Blau	4.7667	101.7569	2932	2022	3381	3476	2612	2144	2761.2
4	Ldg. Mentara	4.7556	102.0167	3166	2035	3480	3551	2502	2222	2826.1
5	Upper Chiku	4.7653	102.1736	3208	1927	3476	3455	2618	2308	2832.1
6	Gunung Gagau	4.7569	102.6556	3987	2013	3984	4078	3345	2256	3277.1
7	Hau (Replace with REDIP))	4.8111	101.5667	3031	2078	3416	3518	2668	2119	2805.0
8	Redip	4.8111	101.5667	3031	2078	3416	3518	2668	2119	2805.0
9	Redip	4.8167	101.9833	3074	1967	3516	3560	2704	2353	2862.3
10	Gua Musang	4.8792	101.9694	3159	1944	3485	3404	2684	2345	2836.9
11	Chabai	5.0000	101.5792	3199	1956	3317	3300	2514	2085	2728.5
12	Kg. Lebir, paloh	5.2125	102.3042	3957	2133	3573	3854	2940	2470	3154.1
13	Kg. Aring	4.9375	102.3528	3827	2044	3625	3773	2921	2291	3080.1
14	Gemala	5.0986	101.7625	3164	1784	3359	3305	2400	2198	2701.7
15	Kg. Limau Kasturi	5.0833	102.0694	3432	2000	3514	3524	2615	2246	2888.6
16	Bertam	5.1486	102.0458	3463	2022	3502	3537	2558	2188	2878.4
17	Balai Polis Bertam	5.1458	102.0486	3463	2022	3502	3537	2558	2188	2878.5
18	Gob	5.2514	101.6625	3274	1949	3243	3394	2441	2222	2753.9
19	Pasik	5.2139	101.7597	3240	1925	3227	3321	2318	2137	2695.1
20	Stn. Keretapi Kemubu	5.3000	102.0194	3578	2036	3486	3691	2796	2376	2993.7
21	Tualang	5.2667	102.2667	3838	2068	3503	3770	2794	2439	3069.0
22	Stn. Pertanian Dabong	5.3944	102.0097	3502	1908	3445	3742	2812	2441	2974.9
23	Stn. Keretapi Bukit Abu	5.3722	102.0833	3612	1932	3394	3773	2723	2420	2975.7
24	Ldg. Kuala Pergau	5.3889	102.0111	3502	1908	3445	3742	2812	2441	2974.9

25	Dabong	5.3778	102.0153	3502	1908	3445	3742	2812	2441	2975.0
26	Ldg. Kuala Gris	5.3750	102.0819	3612	1932	3394	3773	2723	2420	2975.7
27	Kg. Laloh	5.3083	102.275	3901	2043	3519	3837	2820	2460	3096.7
28	Stn. Keretapi Manek Urai	5.3972	102.2333	3762	1996	3652	4195	2976	2696	3212.7
29	Pergau	5.4181	101.9458	3527	1922	3378	3583	2693	2335	2906.7
30	Sg.Balah	5.4380	101.9077	3398	1866	3416	3673	2758	2327	2908.8
31	Ldg. Kuala Balah (Kg. Tg. Ab. Rahman)	5.4500	101.9139	3520	1934	3421	3681	2738	2381	2944.8
32	Ldg. Lepan Kabu	5.4597	102.2306	3688	1932	3558	4172	2834	2579	3127.3
33	Sek.Keb.Lubok Bungor	5.5611	101.8889	3660	2045	3461	3857	2824	2550	3066.3
34	Ulu Sekor (Ulu Sokor)	5.5639	102.0083	3546	1916	3392	3922	2728	2476	2996.7
35	Kuala Krai	5.5333	102.1667	3656	1925	3506	4284	2794	2583	3124.9
36	Stn. Keretapi Sg. Nal	5.5903	102.1806	3707	1938	3441	4388	2841	2633	3158.0
37	Ldg. Kuala Nal	5.5708	102.1639	3707	1938	3441	4388	2841	2633	3157.9
38	Sek. Men. Teknik Kuala Krai	5.5319	102.2028	3606	1845	3378	4379	2803	2667	3113.5
39	Stn. Pemereksaan Hutan, Jeli	5.6986	101.8361	3669	2287	3803	4476	3175	2765	3362.2
40	Ldg. Kenneth	5.6264	102.1167	3559	1969	3399	4348	2966	2617	3143.3
41	Ldg. Kerilla	5.6847	102.1069	3620	1979	3601	4618	3159	2669	3272.8
42	Stn. Janakuasa Temangan	5.6708	102.1417	3515	1840	3482	4550	3062	2681	3188.4
43	Sokor Tegawan	5.6292	102.1014	3559	1969	3399	4348	2966	2617	3143.7
44	Bt.13. Jeli	5.6041	101.7101	3710	2249	3535	3999	3127	2612	3205.4
45	Ldg. Kuala Pertang	5.6167	102.2333	3650	1912	3529	4559	2977	2658	3214.1
46	Chenulang	5.6061	102.2919	3525	1801	3549	4776	2999	2645	3215.8
47	Kem Lln. Batu Melintang	5.7014	101.7306	3622	2242	3780	4284	3125	2641	3282.3
48	Kg. Gemang Bahru (Sek. Men. Teknik Jeli)	5.7611	101.8667	3587	2173	3693	4502	3244	2600	3300.5
49	Air Lanas	5.7750	101.8889	3583	2208	3680	4698	3257	2703	3353.9
50	Kg. Jeli	5.7014	101.8389	3669	2287	3803	4476	3175	2765	3362.3
51	Kg. Durian Daun (Lawang)	5.7806	101.9681	3477	2028	3823	4744	3323	2653	3340.3
52	Ulu Bertam	5.7006	101.9846	3513	2011	3631	4485	3177	2684	3250.2
53	Gual Ipoh, Ulu Kusial	5.7486	102.0583	3548	2048	3540	4527	3077	2610	3225.2

54	Majlis Tempatan Temangan	5.7028	102.1528	3534	1873	3549	4603	3108	2633	3216.7
55	Ldg Tebing Tinggi	5.7625	102.1436	3457	1973	3697	4788	3205	2573	3281.2
56	Kusial	5.7500	102.15	3571	1981	3644	4728	3157	2567	3274.4
57	Stn. Keretapi Temangan	5.7028	102.1528	3534	1873	3549	4603	3108	2633	3216.7
58	Stn. Keretapi Tanah Merah	5.8083	102.1472	3254	1952	3596	4799	3097	2454	3192.1
59	Jps Machang	5.7875	102.2194	3401	1939	3659	4844	3172	2549	3260.5
60	Telusan (Rumah Pam Telusan)	5.7583	102.3222	3211	1882	3669	4857	3087	2614	3219.5
61	Kg. Wakaf Raja (Ibu Bekalan Bkt. Yong)	5.7667	102.4319	3019	1900	3589	4699	3013	2521	3123.3
62	Balai Polis Bukit Yong	5.7303	101.9042	3610	2192	3674	4476	3168	2687	3301.3
63	Jenob	5.8328	101.8831	3428	2049	3642	4611	3202	2496	3238.9
64	Pej. Pertanian Batang Merbau	5.8125	102.0208	3416	2051	3486	4673	3111	2429	3194.9
65	Bendang Nyior	5.8444	102.0736	3202	1932	3678	4994	3193	2485	3247.2
66	Stn. Keretapi Bkt. Panau (Sek. Keb. Bkt.Panau)	5.8917	102.1583	3099	1865	3685	5007	3262	2442	3226.1
67	Ibu Bekalan Tiga Daerah	5.8639	102.3444	2888	1868	3606	4674	3136	2441	3102.2
68	Rumah Pengawas Bkt. Abal	5.8611	102.3167	2949	1886	3681	4884	3260	2414	3178.6
69	Ldg. Cherang Tuli (LTN Pdg. Pak Amat)	5.8181	102.3639	2835	1830	3525	4687	3064	2442	3064.1
70	Sg. Petai	5.8306	102.4153	2852	1843	3528	4546	3000	2357	3021.2
71	Sek. Men. Cherang Ruku	5.8597	102.4944	2737	1926	3560	4626	3038	2322	3034.9
72	Sg. Petai Pasir Puteh	5.8306	102.4153	2852	1843	3528	4546	3000	2357	3021.2
73	Bkt. Kwong (Ampangan Bkt. Kwong)	5.9264	101.9583	3221	1856	3710	5001	3196	2458	3240.2
74	Kg. Batu Karang	5.9568	102.0821	2914	1789	3764	5007	3238	2426	3189.3
75	Bkt Tandak	5.9204	102.027	3042	1798	3672	4948	3188	2295	3162.2
76	Kg. Tandak (Kg. Bkt. Pak Junus)	5.9167	102.0375	3179	1843	3714	5050	3215	2412	3232.0
77	Ibu Bekalan To' Uban	5.9694	102.1375	2839	1751	3596	4781	3064	2203	3039.2
78	Stn. Pertanian Melor	5.9639	102.2917	2780	1731	3575	4695	3175	2070	3004.3
79	Pej. Pertanian Melor Pengawas	5.9667	102.2986	2780	1731	3575	4695	3175	2070	3003.7

80	Serdang, Gunong Barat Bachok	5.9417	102.3417	2813	1781	3597	4530	3132	2144	2999.5
81	Tok Ajam (Bkt. Gedombak P. Puteh)	5.9042	102.3819	2749	1782	3556	4608	3161	2333	3031.5
82	Rumah Kastam Rantau Panjang	6.0236	101.9792	2895	1698	3550	4630	2947	2218	2990.1
83	Stn. Keretapi Gual Periok	6.0292	102.3819	2622	1793	3467	4561	3032	2020	2915.7
84	Lemal Pasir Mas	6.0251	102.1466	2758	1703	3580	4742	2966	2091	2973.8
85	Rumah Pam Repek (Kg. Pdg. Ragut Repek)	6.0125	102.1028	2838	1752	3672	4757	3010	2147	3029.4
86	Rumah Kerajaan Jps, Meranti	6.1000	102.1083	2717	1693	3436	4517	2841	2081	2880.8
87	Rumah Pam Salor di Pengkalan Kubor	6.0181	102.1778	2795	1732	3632	4813	3008	2125	3017.3
88	Kg. Peringat	6.0208	102.2875	2669	1726	3463	4612	3030	2010	2918.7
89	Chabang Tiga Pendek (Kg. Lubuk Jambu)	6.0403	102.2194	2669	1625	3608	4763	3039	2025	2954.7
90	Kg. Binjai	6.0750	102.3014	2581	1719	3453	4660	3106	1978	2916.2
91	Balai Polis Binjai	6.0764	102.3014	2581	1719	3453	4660	3106	1978	2916.2
92	Teratak Pulai	6.0056	102.3583	2657	1787	3402	4459	3004	2024	2889.4
93	Kg. Tangkok	6.0139	102.3917	2622	1793	3467	4561	3032	2020	2915.7
94	Pejabat JPS Bachok	6.0556	102.4014	2458	1723	3365	4470	2984	1967	2828.6
95	Kuala Jambu	6.1500	102.0958	2700	1674	3342	4460	2796	2000	2828.9
96	Kg. Kebakat	6.1500	102.2056	2520	1694	3447	4572	2879	1976	2848.0
97	Chabang Ampat	6.1556	102.1569	2634	1602	3346	4587	2843	1957	2828.2
98	Balai Polis Wakaf Bharu	6.1194	102.1958	2618	1711	3386	4557	2869	1991	2855.2
99	Stn. Keretapi Kg. Berangan	6.1681	102.1986	2573	1617	3253	4541	2740	1900	2773.0
100	Stn. Keretapi Tumpat (Pengkalan Nangka Tumpat)	6.1986	102.1694	2573	1617	3253	4541	2740	1900	2770.9
101	Jeti Kastam	6.1333	102.2333	2520	1694	3447	4572	2879	1976	2847.9
102	Stor JPS Kota Bharu	6.1083	102.2569	2514	1737	3357	4510	2899	1949	2828.1
103	Stn. Keretapi Pelekbang	6.1486	102.2278	2520	1694	3447	4572	2879	1976	2847.7
104	Stn. Kajicuaca Pengkalan Chepa	6.1681	102.2944	2410	1765	3348	4645	2832	1883	2814.1

Appendix B

Graph of mean precipitation from 2014 to 2019 in Kelantan state

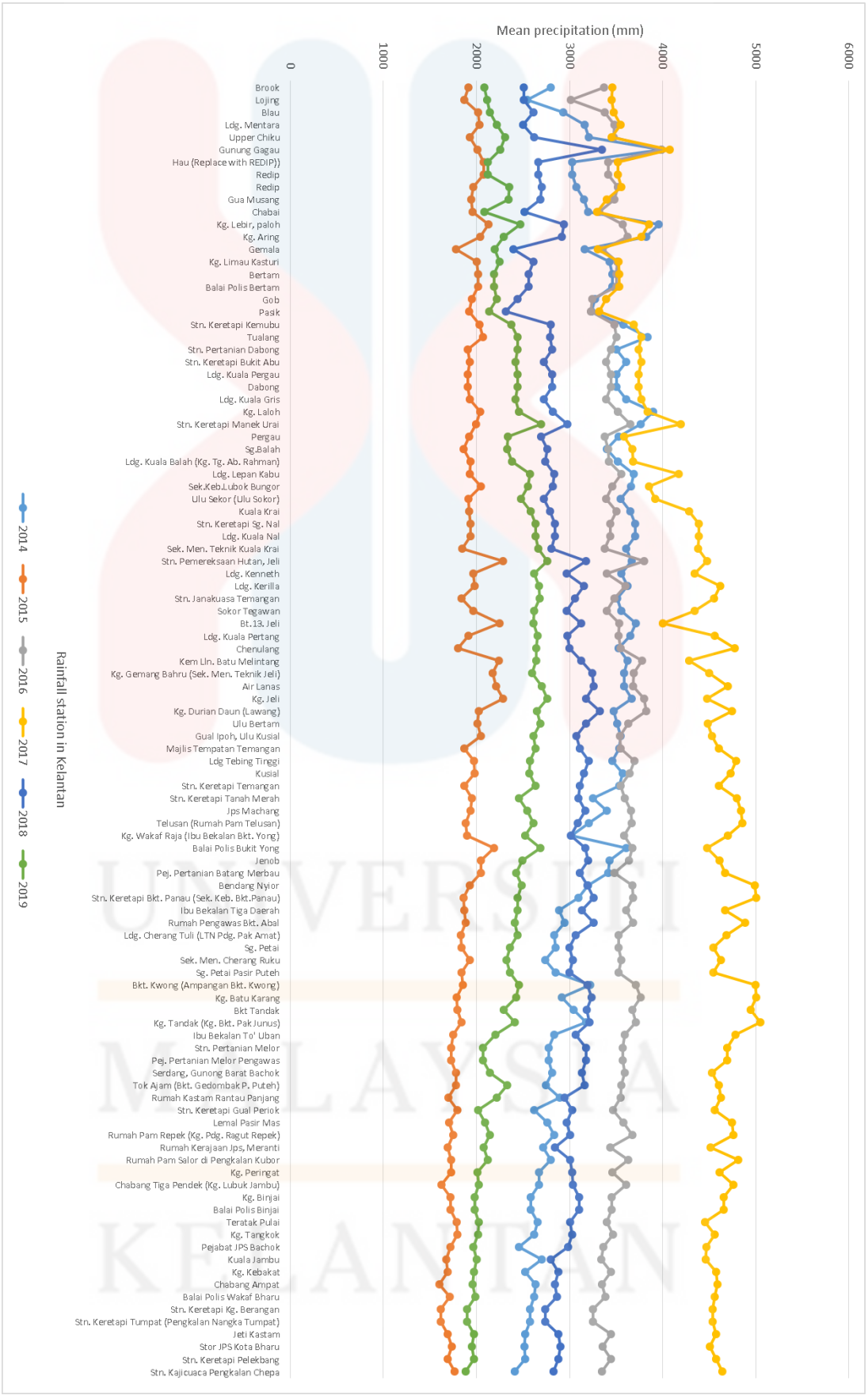

Appendix C

Percentage mean of soil moisture of study from year 2014 – 2020 graph

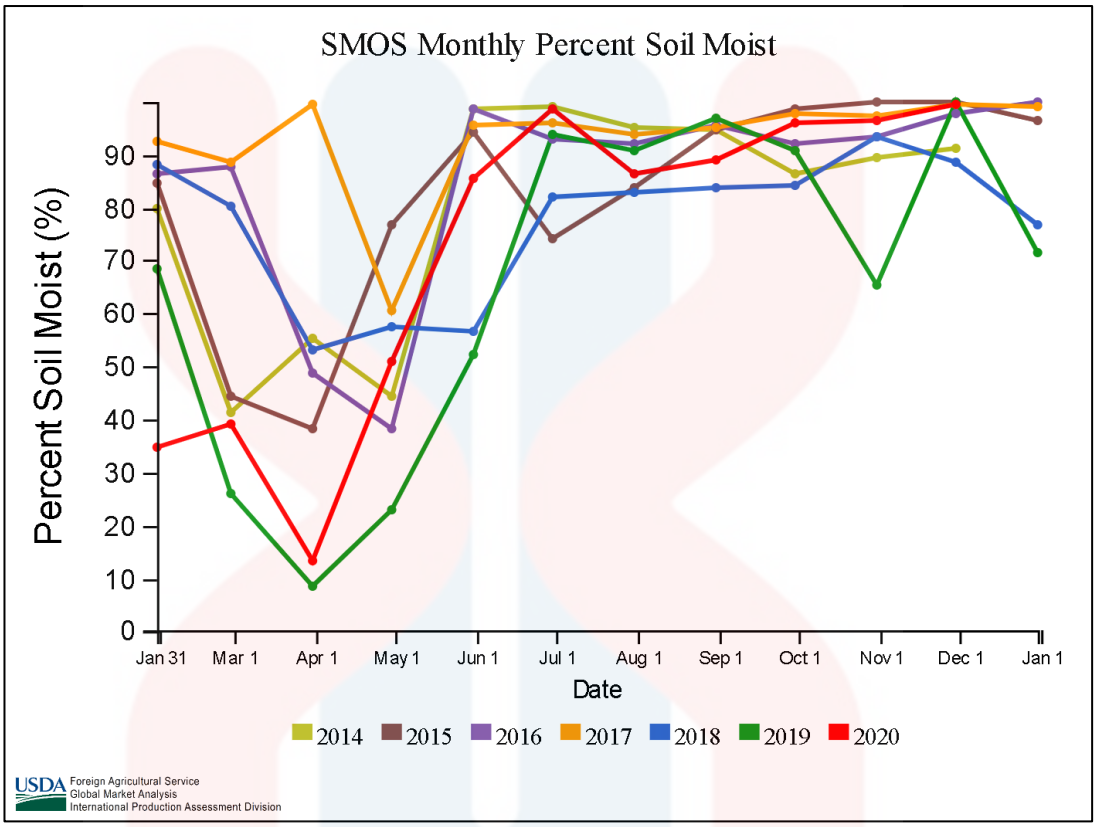

Appendix D

Percentage mean of soil moisture of study area from year 2014 – 2020 table

		Date						
	Jan	**2014**	**2015**	**2016**	**2017**	**2018**	**2019**	**2020**
SMOS Monthly Percent Soil Moist (%)	**Mar**	79.92	84.69	86.54	92.61	88.28	68.5	34.75
	Apr	41.34	44.5	87.48	88.53	80.08	25.98	39.3
	May	55.34	38.32	48.72	99.38	53.05	8.65	13.48
	Jun	44.27	76.62	38.05	60.72	57.61	22.96	51.1
	Jul	98.57	94.45	98.48	95.67	56.7	52.28	85.5
	Aug	99.14	74.06	92.91	96.02	81.96	93.61	98.64
	Sep	95.02	83.75	92.27	93.63	82.86	90.85	86.46
	Oct	94.59	94.87	95.41	95.25	83.81	96.75	88.86
	No	86.37	98.56	92.1	97.56	84.11	90.54	96.17
	Dec	89.62	99.76	93.53	97.44	93.42	65.48	96.53
	Jan	91.15	99.73	97.69	99.65	88.56	99.84	99.63